Energy-Efficient Pilot-Data Power Control in MU-MIMO Communication Systems

Ye Zhang

A Thesis
In the Department
of
Electrical and Computer Engineering

Presented in Partial Fulfillment of the Requirements
For the Degree of
Doctor of Philosophy (Electrical and Computer Engineering) at
Concordia University
Montreal, Quebec, Canada

July 2018

© Ye Zhang, 2018

CONCORDIA UNIVERSITY

SCHOOL OF GRADUATE STUDIES

This is to certify that the thesis prepared

By: Ye Zhang

Entitled: Energy Efficient Pilot Data Power Control in MU-MIMO Communication Systems

and submitted in partial fulfillment of the requirements for the degree of

Doctor of Philosophy (Electrical & Computer Engineering)

complies with the regulations of the University and meets the accepted standards with respect to originality and quality.

Signed by the final examining committee:

_____ Chair
Dr. Yuhong Yan

_____ External Examiner
Dr. Yu-Dong Yao

_____ External to Program
Dr. Wen Fang Xie

_____ Examiner
Dr. M. Omair Ahmad

_____ Examiner
Dr. Yousef R. Shayan

_____ Thesis Supervisor
Dr. Wei-Ping Zhu

Approved by _____
Dr. Mustafa Mehet Ali, Graduate Program Director

Wednesday, September 5, 2018

_____
Dr. Amir Asif, Dean
Faculty of Engineering and Computer Science

Abstract

Energy-Efficient Pilot-Data Power Control in MU-MIMO Communication Systems

Ye Zhang, Ph.D.

Concordia University, 2018

Multiple-input multiple-output (MIMO) antenna system is considered as a core technology for wireless communication. To reap the benefits of MIMO at a greater scale, massive MIMO with very large antenna arrays deployed at base station (BS) has recently become the forefront in wireless communication research. Till present, the design and analysis of large-scale MIMO systems is a fairly new subject. On the other hand, excessive power usage in MIMO networks is a crucial issue for mobile operators and the explosive growth of wireless services contributes largely to the worldwide carbon footprint. As such, significant efforts have been devoted to improve the spectral efficiency (SE) as well as energy efficiency (EE) of MIMO communication systems over the past decade, resulting in many energy efficient techniques such as power allocation. This thesis investigates novel energy-efficient pilot-data power control strategies which can be used in both conventional MIMO and massive MIMO communication systems. The new pilot-data power control algorithms are developed based ontwo optimization frameworks: one aims to minimize the total transmit power while satisfying per-user signal-interference-plus-noise ratio (SINR) and power constraints; the other aims to maximize the total EE, which is defined as the ratio of the total SE to the transmit power, under individual user power constraints. The proposed novel pilot-data power allocation schemes also take into account the maximum-ratio combining (MRC) and zero-forcing (ZF) detectors in the uplink together with maximum-ratio transmission (MRT) and ZF precoder in the downlink.

Considering that a direct use of such SINR expressions in the power control schemeswould lead to a very difficult optimization problem which is not mathematically tractable, we first investigatethe statistical SINR lower bounds for multi-cell multi-user MIMO (MU-MIMO)communication systemsunder minimum mean square error (MMSE) channel estimation. These lower bounds of the per-user average SINRs are used to replace the true SINRs to simplify the power allocation optimization problems. Such relaxation of the original average SINR yields a simplified problem and leads to a suboptimal solution.

Then, based on the derived average SINR lower bounds, two novel energy efficient pilot-data power control problems are formulatedwithin the first optimization framework,aiming to minimize the total transmit power budget subject to the per-user SINR requirement and power consumption constraint in multi-cell MU-MIMO systems. For the EE-optimal power allocation problems with MRT precoder and MRC detector, it is revealed that such minimization problems can be converted to a standard geometric programming (GP) procedure which can be further converted to a convex optimization problem. For the pilot-data power control scheme with ZF precoder and ZF detector, geometric inequality is used to approximate the original non-convex optimization to GP problem. The very large number of BS station situation is also discussed by assuming infinite antennas at BS. Numerical results validate the tightness of the derived SINR lower bounds and the advantages of the proposed energy efficient power allocation schemes.

Next, two pilot and data power control schemes are developed based on the second power allocation optimization framework to jointly maximize the total EE for both uplink and downlink transmissions in multi-cell MU-MIMO systems under per-user and BS power constraints. The original power control problems are simplified to equivalent convex problems based on the derived SINR lower bounds along with the Dinkelbach's method and the FrankWolfe (FW) iteration. By assuming infinite antennas at BS, the pilot-data power control in massive MIMO case is also discussed. The performance of the proposed pilot-data power allocation schemes based on the two frameworks, namely total transmit power minimization and total EE maximization, are evaluated and compared with the SE maximization scheme.

Furthermore, we investigate the pilot-data power allocation for EE communications in single-cell MU-MIMO systems with circuit power consumption in consideration. The pilot and data power allocation schemes are proposed to minimize the total weighted uplink and downlink transmit

power as well as processing circuit power consumption while meeting the per-user SINR and BS power consumption constraints. In our proposed schemes, both fixed and flexible numbers of BS antennas are investigated. For the fixed number of BS antennas case, the non-convex optimization problems are converted to a general GP problem to facilitate the solution. An iterative algorithm is proposed to solve the EE-optimal power control problems in the flexible number of BS antennas casebased on the partial convexity of both the cost function and the constraints. It is shown that the convergence of the proposed iterative algorithm is guaranteed due to the fact that each iteration follows convex optimization.

Acknowledgements

My sincerest thanks go to my supervisor Prof. Wei-Ping Zhu, for his guidance, patience, and encouragement throughout my research at Concordia University. It was his advices and critiques that allowed me to convey my ideas through this thesis as well as the publications we completed together, led to timely accomplishment of this work.

I want to thank the members of my Ph.D. supervisory committee at Concordia University: Dr. M. Omair Ahmad, Dr. Yousef Shayan and Dr. Wen-Fang Xie for their time and efforts on reading my doctoral proposal, seminal report and thesis and providing comments on my research are greatly appreciated. I would also like to thank the external examiner Dr. Yu-Dong Yao from Stevens Institute of Technology for his careful review of my thesis and his participation in my defence.

My thanks also go to my friends and colleagues in Concordia University. They gave me great help and encouragement.

Finally, I would like to say thanks to my parents for always believing in me and encouraging me to achieve my goals. This thesis would not have been possible without my husband, Dr. Ran Zhu who provided emotional support and boundless love.

Table of Contents

List of Figures

List of Symbols

$\boldsymbol{X}^T$	Transpose of $\boldsymbol{X}$
$\boldsymbol{X}^H$	Complex conjugate transpose of $\boldsymbol{X}$
$\boldsymbol{X}^*$	Conjugate transpose of $\boldsymbol{X}$
$\boldsymbol{X}^{-1}$	Inverse of $\boldsymbol{X}$
$Tr(\boldsymbol{X})$	Trace of $\boldsymbol{X}$
$\|\boldsymbol{x}\|$	Vector norm of $\boldsymbol{x}$
$diag(\boldsymbol{x})$	Diagonal matrix with its diagonal elements denoted by $\boldsymbol{x}$
δ	Dirac delta function
$E[x]$	Expected value of x
$\boldsymbol{I}_n$	Identity matrix or unit matrix of size n
$\boldsymbol{x}(a:b)$	From a-th to b-th elements of $\boldsymbol{x}$
$arg(x)$	Argument or phase of x
$det(\boldsymbol{X})$	Determinant of $\boldsymbol{X}$
$[\boldsymbol{X}]_{a,b}$	a-th row and b-th column element of $\boldsymbol{X}$
$\|x\|$	Absolute value of x

List of Abbreviations

5G	Fifth Generation
AWGN	Additive White Gaussian Noise
BS	Base Station
CSI	Channel State Information
EE	Energy Efficiency
FDD	Frequency Division Duplex
FW	FrankWolfe
i.i.d.	Independently Identically Distributed
GP	geometric programming
GGP	General geometric programming
LS	Least Square
LTE	Long-Term Evolution
MIMO	Multiple-Input Multiple-Output
MISO	Multiple-Input Single-Output
ML	Maximum Likelihood
MMSE	Minimum Mean Square Error
MRC	Maximum Ratio Combining
MRT	Maximum Ratio Transmission

MU-MIMO	Multi-user Multiple-Input Multiple-output
OFDM	Orthogonal Frequency Division Multiplexing
PPP	Poisson Point Process
QoS	Quality of Service
RF	Radio Frequency
RV	Random Variable
SE	Spectral Efficiency
SNR	Signal-to-Noise-Ratio
SINR	Signal-to-Interference-plus-Noise-Ratio
TDD	Time Division Duplex
TDMA	Time Division Multiple Access
TS	Training Sequence
ZF	Zero Forcing

Chapter 1

Introduction

1.1 Background and Motivation

Over the past decades, multiple-input multiple-output (MIMO) technology has received a great deal of attention in wireless communication research community. It is considered as a strong candidate for future wireless communication systems due to its exploiting the spatial multiplexing gain, spatial diversity and array gain [1]-[4]. With the development of nowadays MIMO networks, more and more antennas are employed on transmitter and/or receiver in order to reduce intra-cell interference and serve more users at the same time, thus leading to a new technology called massive MIMO system [5]-[10]. Typically, massive MIMO is a multi-user MIMO (MU-MIMO) technology in which a base station (BS) equipped with a very large antenna array services several users simultaneously. It has been proved that in massive MU-MIMO systems, the effect of small-scale fading and additive white Gaussian noise (AWGN) can be averaged out with simple signal processing. The research in [11]-[12] based on random matrix theory has demonstrated that linear receivers with infinite number of BS antennas and perfect channel state information (CSI) can completely eliminate the intra-cell interference and noise, resulting in the "favourable propagation". The design and analysis of large scale MIMO systems is a new subject which is attracting more and more interests.

Because of the explosive growth of user demands on high-data-rate multimedia traffic, energy consumption of MIMO communication has been dramatically increasing in recent years. Such huge energy consumption results in a large amount of carbon dioxide emission and high capital and operating expenditures [13]-[15]. Moreover, the mobile terminals also desire high energy efficiency for the reason that the development of battery technology has not kept up with the demand of broad band mobile communications [16]-[18]. Therefore, green communication design has become a significant trend for the development of future wireless communication technologies and has been considered as a promising research direction in both the academic and industrial areas [19]–[20].

One main topic of green communication focuses on the energy efficient resource allocation [21]-[25]. Because of the environment changing and users' mobility, the CSI of wireless links varies randomly with time. In almost all communication scenarios, the system performance highly depends on the accuracy of CSI at transmit and/or receive ends. To learn the channel, one popular method is to let the transmitter send known training signal, which is known as pilot signal, to the receiver during a certain transmission time interval. A proper training signal is very important for MIMO communication systems, especially for massive MIMO systems. Little training power leads to a heavy noise caused by the channel estimation error, which directly affects the transmission performance, i.e. a very low signal-to-interference-plus-noise ratio (SINR) [26]-[28]. On the contrary, if a longer training sequence or more training power is used, it means less remaining energy for the useful data transmission for a given energy budget spent in a coherence interval, causing a waste of resource in MIMO

communication systems, such as power, time and bandwidth [29]-[32]. Therefore, the power allocation between training and data signal is a major problem that has a large impact on the performance of MIMO systems. As a result, it is crucial to study the resource allocation strategy for MIMO communication systems in order to save the energy consumption on BS and/or user terminals. Therefore, this thesis focuses on the trade-off between system performance and energy consumption by developing the power allocation schemes for both training and data signal to achieve the green communication requirement. Moreover, it is generally believed that the massive MU-MIMO as a results of using tremendous antennas at BS can save the energy cost without sacrificing system performance as compared to traditional MU-MIMO systems [11] [33]-[36]. We will also discuss the power saving and system performance improvement of the energy efficient power allocation versus the number of antennas used in massive MU-MIMO networks.

1.2 Literature Review

1.2.1 Power Allocation Based on Perfect CSI

Wireless communication usage has gained a huge growth recently and will continue to grow rapidly in the following years. The power consumption of the mobile devices has become a major concern because battery technologies have not been able to scale up with the increasingly higher communication speed. Moreover, the large amount of carbon dioxide emission gives rise to significant environmental problem, which has made power consumption a crucial performance metric that is highly concerned in wireless communication systems. As a result, energy efficient optimal resource allocation, aiming at increasing the energy efficiency (EE)

as well as saving power cost of the whole system, has emerged as a significant research topic in MIMO communication systems.

In the past decades, many researchers have studied the energy efficient resource allocation in MIMO communication systems based on perfect CSI. For example, an energy efficient power allocation algorithm for MIMO wireless systems was formulated as a convex optimization problem with quality of service (QoS) constraints in [37]. The bit energy of training-based single-input single-output (SISO) and MIMO system was investigated in [48], where the works were based on optimization of SNR for single user MIMO systems. In [39], an energy efficient optimal power control based on water-filling algorithm for the downlink MU-MIMO system was developed. In [40], an optimal power allocation that maximizes the EE performance in the downlink of a MU-MIMO was studied with zero-forcing (ZF) precoder used at BS. The optimal number of active users and their power allocation in uplink MU-MIMO systems was discussed in [41] based on the maximization of total EE. The authors of [11] studied the trade-off between uplink energy and spectral efficiency in large-scale MU-MIMO systems under both perfect and imperfect CSI. It is shown that by employing very large antenna arrays at BS, both spectral and energy efficiency can be improved greatly with a simple power allocation scheme in which all users are assumed to have the same pilot power and data power.

However, in practice we can never have perfect CSI because of channel estimation error [42]-[44]. Usually, the CSI in MU-MIMO system is estimated based on training signal, which is called training-based channel estimation. For a massive MU-MIMO system as a large number of antennas are employed at BS, it is extremely difficult to estimate CSI at user side [30] [45]. As such, the channel estimation is performed at BS through uplink training

under the assumption of time-division duplexing (TDD) in large-scale MU-MIMO systems. In this thesis, we will focus on the study of EE techniques in both conventional and massive MU-MIMO communication systems based on the imperfect CSI, which is a more practical situation.

1.2.2 Power Allocation Based on Imperfect CSI

Generally speaking, there are two main energy efficient power allocation frameworks for MIMO communication systems based on imperfect CSI: one aims to minimize the total transmit power under certain constraints, i.e. QoS constraint, per-user power constraint, etc.; the other is to maximize total EE defined as the spectral efficiency (sum-rate in bit/channel) divided by the transmit power (in Joules/channel) [11] [46]-[48]. It is straightforward to understand the first framework which is to use minimum power to satisfy the required system performance. Typically, increasing the SE is associated with increasing the power and the achievable transmission rate. On the contrary, the energy saving optimization aims to save power in the whole system and sometimes decreases the system performance, such as spectral efficiency (SE), signal to interference-plus-noise ratio (SINR), system reliability, etc. There is a fundamental trade-off between the power consumption and the SE. The idea of the second framework is to jointly optimize the power cost and the SE in one operating regime. Even though the main goal is to save energy cost in MIMO communication systems, these two frameworks are based on different purpose of system design. The first framework aims to minimize power cost over a given system performance target while the second aims to find a balance between spectral efficiency and power cost.

Under the first framework, the power allocation work in [49] aims to minimize the downlink transmission energy of the time-division multiple-access (TDMA) MIMO systems while meeting the individual users' effective capacity constraints, which is defined as the maximum achievable source rate under a given delay bound. The authors of [50] proposed a resource allocation scheme to minimize the overall transmit power subject to given user target rates in a downlink MIMO orthogonal frequency division multiplexing (OFDM) system. The authors of [51] investigated the energy-efficient uplink power control in multi-cell massive MU-MIMO systems with the linear minimum mean-square-error (MMSE) receiver based on the lower bound of statistic uplink SINR. Paper [52] exploited the interdependency between pilot and data transmission and achieved total power saving is achieved subject to the per-user SINR constraint. The work in [53] considered a linear downlink transceiver design for the sum power minimization problem with per-user rate constraints in a multi-cell MU-MIMO system. The works in [54] and [55] aimed to minimize radiated power in MIMO systems under sum rate constraint with channel correlation and partial CSI at the transmitter in consideration. The work in [56] studied an optimization problem to minimize the overall energy consumption while ensuring users' QoS requirement by considering both perfect CSI and statistical CSI from users to the primary receiver in a single cell time-division multiple access (TDMA) MIMO cognitive radio (CR) network.

Under the second energy-efficient optimization framework, the work in [57] discussed the pilot-data power allocation to maximize the total EE for training-based single user MIMO with and without feedback, by taking circuit power consumption into consideration. The works in [58] studied the SE and EE optimal power allocation between reverse training,

forward training and data transmission in two-way training based multiple-input single-output (MISO) systems. The work in [59] studies the energy-efficient downlink resource allocation for frequency-division duplexing (FDD) MIMO system under a correlated Rayleigh fading channel. The authors in [60] proposed a power control algorithm to maximize the downlink energy efficiency by assuming equal data power allocation among all users. The work in [61] addresses optimal energy-efficient design of uplink MU-MIMO in a single cell environment with radio frequency (RF) transmission power and device electronic circuit power considered. The works in [62]-[65] are essentially targeted to analyse the maximal achievable EE in MIMO systems under the statistical QoS constraint. The authors in [66] studied the transmit power control for multi-tier MIMO heterogeneous cellular networks (HetNets), where each tier operates in closed-access policy and base stations (BSs) in each tier are distributed as a stationary Poisson point process (PPP).

It should be noted that the schemes in [48]-[66], as mentioned above, considered the energy efficient power control for the uplink and downlink transmissions separately by ignoring the relation between uplink and downlink transmit powers, which limit their use in practical MIMO systems. Moreover, some of these works on energy efficiency in MIMO systems as described in [46]-[49], [54], [58] and [67] are based on the assumption that all users are allocated the same pilot power or data power. Such equal power allocation strategies may cause squaring effect in low power regime [67].

1.2.3 Power Control Schemes in Massive MIMO systems

Massive MIMO is a promising technique to increase the EE of cellular networks by deploying antenna arrays with a very large number of active antennas at the BSs. This technique allows

for very efficient spatial multiplexing, and has a significant gain in reliability due to flattening out unrelated noise, deep fades, hardening of the channel and array gain. In massive MIMO systems, power control among users should be considered as a necessary and essential tool to take full advantage of massive antenna arrays. However, since the design and analysis of very large scale MIMO systems is a fairly new subject, limited research has been done on the power allocation for massive MIMO, especially for multi-cell massive MIMO systems. As mentioned in the previous subsection, the work in [48], [51] and [59] discussed the power control schemes in massive MIMO systems by assuming no more than two hundreds of antennas employed at BSs. In [68], a power control strategy among different users has been proposed to maximize the SE in single-cell massive MIMO systems. In [69] and [70], power control among different users is applied as an effective way to minimize the uplink power consumption with maximum sum SE in multi-cell massive MIMO systems. It should be noted that all the above power control algorithms only take into consideration the transmit power consumption, and tend to achieve higher SE and better EE performance with more BS antennas. However, in practical massive MIMO systems, since the effect of circuit power consumption would be gradually aggravated by the number of BS antennas as the size of hardware systems increases, it would bring nonnegligible negative impacts on massive MIMO systems.

It is generally believed that circuit power consumption is fundamentally the limit in massive MIMO systems in the high-power regime [71]-[72]. However, there are only a few publications found so far discussed such behaviour in the large number of antenna regime. In [73], the lower bounds on the achievable uplink sum rate in massive single-cell systems with phase noise from free-running oscillators were derived. The authors in [74] used the

excess degrees of freedom offered by massive MIMO to optimize the downlink precoding for low peak-to-average power ratio (PAPR), while the work in [75] designed a constant envelope precoding scheme for very low PAPR. The authors in [71] analysed the capacity and estimation accuracy of massive MIMO systems with non-ideal transceiver hardware based on a new system model that considers the hardware impairment at each antenna by an additive distortion noise proportional to the signal power at this antenna.

Note that the power control algorithms in [48], [51], [59], [69] and [70] only considered the transmit power consumption while the work in [73]–[75] only considered the single type of hardware impairments. In contrast to these power allocation works, by using the power consumption model of different hardware impairments as discussed in [71]-[75] along with large antenna arrays, we will investigate a more practical power control scheme in this thesis that takes into account circuit power consumption.

1.3 Organization and Contributions

The organization of the thesis along with the main contributions of each chapter is presented as follows.

Chapter 2 describes the system model, including the time-division duplex (TDD) multi-cell MU-MIMO channel model, minimum mean square error (MMSE) channel estimation as well as the uplink and downlink SINRs. Both small-scale fading and large-scale fading in the proposed TDD multi-cell MU-MIMO system, which incorporate path-loss and shadowing effect, are also considered in the channel model.

In chapter 3, two optimization frameworks are established to meet the goal of this thesis: to develop energy efficient algorithms for pilot and data power allocation in the proposed

TDD multi-cell MU-MIMO system. As the original optimization problems using true SINR expressions are very difficult to solve, we investigate the average SINR lower bounds in order to simplify the power allocation optimization problems. In particular, close-form average SINR lower bounds are derived under MMSE channel estimation for both uplink and downlink transmissions of MU-MIMO systems, by considering the conventional linear maximum-ratio combining (MRC) and zero-forcing (ZF) detectors in the uplink and the maximum-ratio transmission (MRT) and ZF precoder in the downlink. These lower bounds of the per-user average SINR will be used to replace the true SINR in the optimization frameworks to facilitate the solution in later chapters. Such relaxation of the original average SINR yields a simplified problem and leads to a suboptimal solution.

In chapter 4, based on the first EE power allocation framework, two schemes for power control between pilot and data symbols in the TDD multi-cell MU-MIMO system are developed to minimize the total weighted uplink and downlink transmit power while meeting the per-user SINR and BS power constraints. In order to simplify the power allocation optimization problem, the derived lower bounds of the per-user average SINR in chapter 2 are used to establish the SINR QoS constraints for the proposed problem. Then, the non-convex optimization problems are converted to a standard geometric programming (GP) problem to facilitate their solution. The performance of the power control algorithms in massive MU-MIMO situation with infinite number of antennas employed at BS is also discussed. Numerical simulation results have confirmed the tightness of the derived per-user average SINR lower bounds and the advantage of the proposed power allocation schemes.

Chapter 5 proposes and investigates two pilot and data power control schemes based on the second EE power allocation framework to jointly maximize the total EE for both

uplink and downlink transmissions under per-user and BS power constraints for multi-cell TDD MU-MIMO systems. The non-convex problems formulated with the derived SINR lower bounds are simplified to equivalent convex problems based on Dinkelbach's method and FrankWolfe (FW) iteration. Simulation results and discussions are given to validate our proposed schemes, including the tightness analysis of the derived SINR lower bounds, the total transmit power and EE for large-scale MU-MIMO, and the comparison of our proposed power allocation schemes with the existing SE maximization scheme.

Chapter 6 addresses the energy efficient power allocation issue in single-cell TDD massive MU-MIMO communication systems for both uplink and downlink transmission with circuit power consumption taken into account. Firstly based on the discussion in chapters 2 and 3, we modify the system model and SINR lower bounds from multi-cell to single-cell MU-MIMO, and accommodate the model of circuit power consumption for the new optimization problem. Then, pilot and data power allocation schemes are proposed to minimize the total weighted uplink and downlink transmit power while meeting the per-user SINR and BS power consumption constraints with circuit power in consideration. In our proposed power control schemes, both fixed and variable numbers of BS antennas are investigated. For the fixed number of BS antennas case, the non-convex optimization problems are converted to a general GP problem to facilitate their solution. For the variable number of BS antennas case, we present an iterative algorithm to solve the optimization problem. Simulation results are provided to demonstrate the effectiveness of the proposed methods.

Chapter 7 gives a summary of the thesis work and provides suggestions for future investigation.

Chapter 2

Multi-Cell MU-MIMO Systems with Channel Estimation

2.1 Introduction

Currently, we are in the era of 4G and 4.5G networks, which are referred to as Long Term Evolution (LTE). MIMO technology has been under active research over the last decade and been considered in 3GPP standard for LTE and LTE-Advanced networks. In the near future, we expect an explosive increase in the number of connected devices, such as smart phones, tablets, sensors, connected vehicles and so on, leading to the 5th-generation (5G) communication. Massive MIMO is considered as one of the enabling and promising technologies for 5G wireless communications and has already attracted considerable interest in communication and signal processing fields.

The availability of accurate CSI at transmitter and/or receiver is vital to achieve the desired performance in almost all communication scenarios. Acquiring accurate CSI is very important in both conventional and massive MU-MIMO systems because the performance of several BS operations, such as linear detection on the uplink and linear precoding on the downlink, is subject to the availability of accurate CSI at the BS. The ideal situation is that the perfect CSI is available at BS. As discussed in [11], with perfect CSI, "favourable propagation" can be achieved in massive MU-MIMO systems where the wireless channels

become near-deterministic because the channel vectors between BS and users become near-orthogonal to each other. This is because the effects of small-scale fading tend to disappear when the number of antennas at the BS increases unboundedly. However, from the practical point of view, having access to perfect CSI is not possible since this compromises the intrinsic capabilities of communication systems. Therefore, it is essential to estimate and evaluate the CSI in MIMO systems.

Generally speaking, there are three kinds of channel estimation approaches in MIMO channel estimation. The first one is called the training-based channel estimation methods which employ known pilot signals to render an accurate channel estimation [76]-[78], such as the least squares (LS), maximum likelihood (ML) and MMSE algorithms. The second one is blind channel estimation algorithms which exploit the second-order cyclo-stationary statistics, correlative coding and other properties [79]-[82]. Thirdly, by combining the idea of both the training-based and blind methods, with a small number of training symbols, semi-blind channel estimation problems based on the second-order statistics of a long vector can be solved [82]-[86]. Among these three channel estimation methods, the most popular one is training-based channel estimation which always requires less complicated processing circuits.

Moreover, in conventional MIMO systems, a duplex communication link can either be established under TDD or FDD. In TDD, there is one frequency band for both uplink and downlink transmission. And in FDD operation mode, two frequency bands are used, one for the uplink and one for the downlink. In general, the number of licenses for the FDD mode is much more than that for TDD, since when compared to TDD systems, FDD operating systems facilitate better hardware re-use, easier software upgrades, and a smoother

transition. However, most research works on massive MIMO have focused on the TDD mode of operation. This is because, in the FDD mode, the uplink and downlink channels use different frequency bands and are not reciprocal, and thus the CSI corresponding to the uplink and downlink is different. The uplink channel estimation is done at the BS with the uplink pilot sequences sent by users. The time required for uplink pilots is independent of the number of BS antennas. However, to get downlink CSI under FDD protocol, the BS needs to transmit pilot symbols to all users. The number of required downlink pilot symbols is proportional to the number of BS antennas. As the number of BS antennas grows very large for massive MIMO, the traditional downlink channel estimation strategy for FDD systems becomes infeasible [10]. On the other hand, in TDD systems based on the assumption of channel reciprocity, only the CSI for the uplink needs to be estimated, avoiding the channel estimation at mobile users for the downlink. Therefore, TDD mode is more efficient and realistic, and is widely utilized in massive MIMO systems.

In this chapter, we explain the structure of a multi-cell MU-MIMO communication system. First, we briefly address the channel model and the frame structure of TDD operation mode. Then, we present the training-based MMSE channel estimation method. Finally, we derive the uplink and downlink SINRs.

2.2 Channel Model

We consider a TDD multi-cell MU-MIMO system with L cells as shown in Fig. 2.1, in which each cell has one BS equipped with M antennas serving K $(K<M)$ single-antenna mobile users and all cells share the same frequency band. When M comes to a large value, say a hundred or a few hundreds, we call this system a large-scale MU-MIMO system.

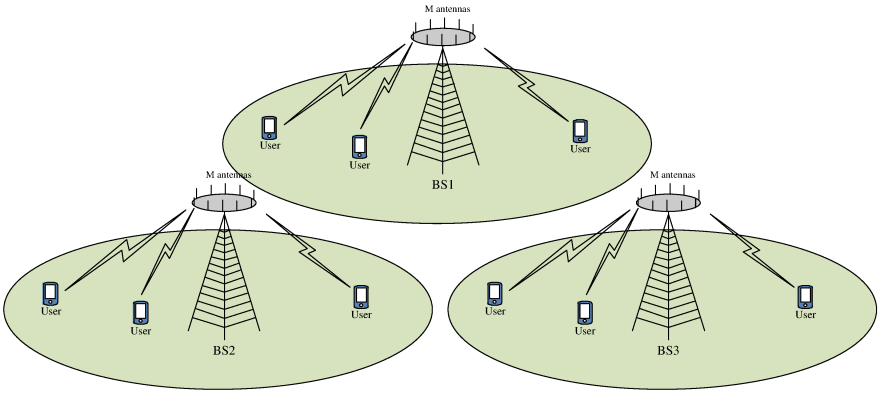

Figure 2.1: Structure of a multi-cell MU-MIMO system

The signal received at the l-th BS can be represented by an $M \times 1$ vector as given below

$$\boldsymbol{y}_l = \sum_{i=1}^{L} \boldsymbol{G}_{li} \boldsymbol{P}_{d,i}^{1/2} \boldsymbol{s}_i + \boldsymbol{n}_l, \ (l = 1, 2, ..., L), \tag{2.1}$$

where the m-th element of $\boldsymbol{y}_l$ represents the signal received by the m-th antenna of the BS, $(m = 1, 2, ..., M)$, the $K \times 1$ vector $\boldsymbol{s}_i$ represents the data symbols transmitted by the K users in cell i, and the $M \times 1$ vector $\mathbf{n}_l$ denotes the additive independent and identically distributed (i.i.d.) white complex Gaussian noise with zero-mean and unit variance. The $M \times K$ matrix $\boldsymbol{G}_{li}$ denotes the channel matrix between the K users in cell i and the BS in cell l, and the diagonal matrix $\boldsymbol{P}_{d,i} = diag\{[p_{d,i1}, p_{d,i2}, \ldots, p_{d,iK}]\}$ represents the transmit data power of each user in the i-th cell. By assuming flat fading channel, $\boldsymbol{G}_{li}$ can be represented as

$$\boldsymbol{G}_{li} = \boldsymbol{H}_{li} \boldsymbol{D}_{li}^{1/2} \tag{2.2}$$

where $\boldsymbol{H}_{li}$ denotes the $M \times K$ fast fading channel matrix from the K users in cell i to the BS in cell l whose elements are i.i.d. complex Gaussian RVs with zero-mean and unit variance.

The diagonal matrix $\boldsymbol{D}_{li}^{1/2} = diag\{[\beta_{li1}, \beta_{li2}, \ldots, \beta_{liK}]\}$ denotes the large-scale channel fading coefficients which incorporate the path-loss and shadowing effect and are assumed to be constant and known as a priori.

We assume a block fading structure where the channel gains remain constant in each coherence time period. In pilot-assisted channel estimation as discussed in [10], [67] and [73], when large antenna arrays are employed at BS, it is difficult to estimate the downlink CSI at users, since in this case the number of pilot symbols must be larger than or equal to the number of BS antennas. On the contrary, the uplink CSI is easier to estimate at BS as the number of uplink pilot symbols depends on the number of active users rather than the number of BS antennas. Under the assumption of ideal channel reciprocity, however, we can estimate the uplink CSI at BS and then use such estimated uplink CSI for both uplink and downlink data transmission.

Based on the discussion above, we assume that the multi-cell MU-MIMO system, all users and BSs in all cells synchronously transmit and receive data by following the TDD block fading structure as in Fig. 2.2. Namely, in the first τ ($\tau \geq K$) slots of a coherent time interval, all users from all cells synchronously transmit uplink pilot signal to all BSs for CSI estimation. Based on the assumption of channel reciprocity, such estimated uplink CSI can be used to detect the uplink data and generate pre-coding matrix for downlink data transmission. After the transmission of training sequences, T_1 symbols are used for uplink data transmission followed by T_2 symbols for downlink data transmission. Note that the silent slots used for BS processing as discussed in [10] [73] are not included in Fig. 2.2.

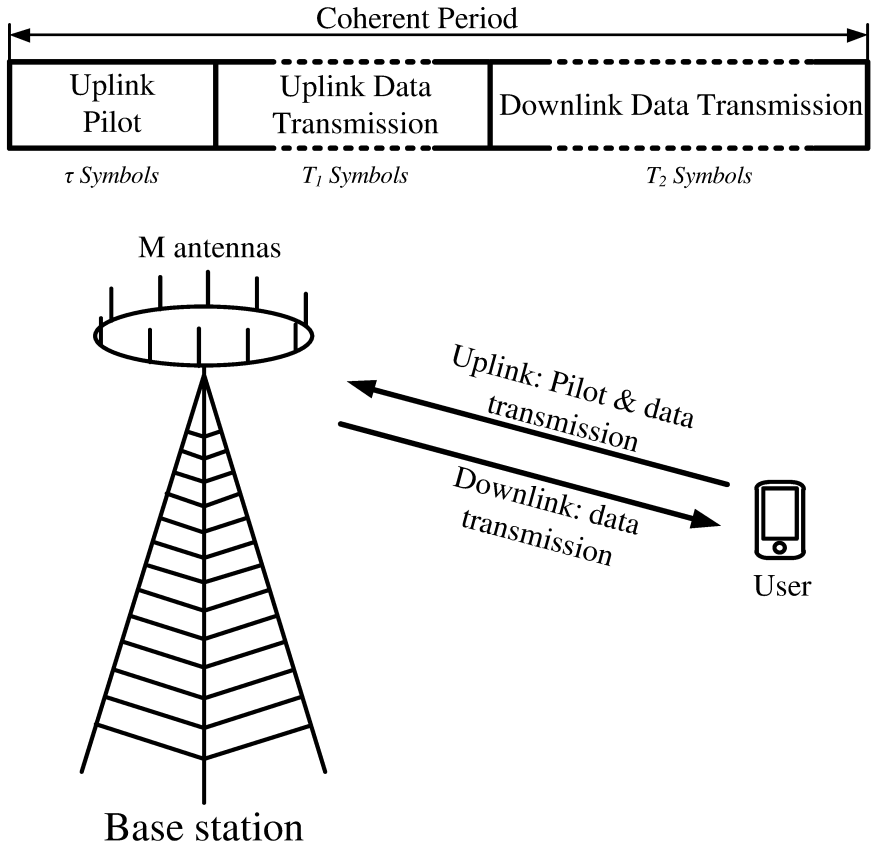

Figure 2.2: Frame structure of TDD system, where the BS acquires CSI via uplink training

2.3 Channel Estimation

By using the MMSE channel estimation during the training phase as discussed in [87], we have

$$\boldsymbol{Y}_{p,l} = \sum_{i=1}^{L} \boldsymbol{G}_{li} \boldsymbol{P}_{p,i}^{1/2} \boldsymbol{\Phi} + \boldsymbol{N}_l \tag{2.3}$$

where $\boldsymbol{Y}_{p,l}$ denotes the $M \times \tau$ received pilot signal matrix at the l-th BS and $\boldsymbol{N}_l$ is an $M \times \tau$ complex noise matrix whose entries are i.i.d. Gaussian RVs with zero-mean and unit variance. The diagonal matrix $\boldsymbol{P}_{p,i} = diag\{[\tau p_{p,i1}, \tau p_{p,i2}, \ldots, \tau p_{p,iK}]\}$ denotes the pilot power of the K users in cell i. We assume that the same set of pilots is used by different cells and the pilots satisfy the orthogonality, i.e., $\boldsymbol{\Phi}^H \boldsymbol{\Phi} = \boldsymbol{I}_K$. Then, the estimated channel matrix can be expressed as

$$\hat{\boldsymbol{G}}_{li} = \boldsymbol{Y}_{p,l} \boldsymbol{\Phi}^H (\boldsymbol{I}_K + \sum_{j=1}^{L} \boldsymbol{D}_{lj} \boldsymbol{P}_{p,j})^{-1} \boldsymbol{D}_{li} \boldsymbol{P}_{p,i}^{1/2} \tag{2.4}$$

Since the same set of pilots is reused among different cells, the CSI estimated at BS is simply a scaled version of the same term which can be expressed as

$$\boldsymbol{Y}_{p,l} \boldsymbol{\Phi}^H (\boldsymbol{I}_K + \sum_{j=1}^{L} \boldsymbol{D}_{lj} \boldsymbol{P}_{p,j})^{-1}. \tag{2.5}$$

The detailed discussion with respect to the pilot contamination can be found in [51]. Then, from (2.5) we have the relation below

$$\hat{\boldsymbol{G}}_{li} = \frac{\boldsymbol{D}_{li} \boldsymbol{P}_{p,i}^{1/2}}{\boldsymbol{D}_{lj} \boldsymbol{P}_{p,j}^{1/2}} \hat{\boldsymbol{G}}_{lj} \tag{2.6}$$

Similar to the single-cell MU-MINO situation [88] [89], the estimation error matrix can

be defined as $\Delta \boldsymbol{G}_{li} = \boldsymbol{G}_{li} - \hat{\boldsymbol{G}}_{li}$. From the properties of MMSE channel estimation [69] [77], $\hat{\boldsymbol{G}}_{li}$ and $\Delta \boldsymbol{G}_{li}$ have i.i.d. Gaussian RVs with zero mean. Let $M \times 1$ vectors $\hat{\boldsymbol{g}}_{lik}$ and $\Delta \boldsymbol{g}_{lik}$ denote the k-th column of matrix $\hat{\boldsymbol{G}}_{li}$ and $\Delta \boldsymbol{G}_{li}$ respectively. The elements of $\hat{\boldsymbol{g}}_{lik}$ are independent of that of $\Delta \boldsymbol{g}_{lik}$ and the variance of the elements of $\hat{\boldsymbol{g}}_{lik}$ and $\Delta \boldsymbol{g}_{lik}$ can be expressed as follows

$$\sigma_{lik}^2 \triangleq \frac{\tau p_{p,ik} \beta_{lik}^2}{1 + \sum_{j=1}^{L} \tau p_{p,jk} \beta_{ljk}} \tag{2.7}$$

$$\varepsilon_{lik}^2 \triangleq \frac{\beta_{lik}(1 + \sum_{j \neq i}^{L} \tau p_{p,jk} \beta_{ljk})}{1 + \sum_{j=1}^{L} \tau p_{p,jk} \beta_{ljk}} \tag{2.8}$$

From (2.7) and (2.8), we have the following relations,

$$\hat{\boldsymbol{g}}_{lik} = \frac{\beta_{lik} p_{p,ik}^{1/2}}{\beta_{llk} p_{p,lk}^{1/2}} \hat{\boldsymbol{g}}_{llk} = \frac{\sigma_{lik}}{\sigma_{llk}} \hat{\boldsymbol{g}}_{llk} \tag{2.9}$$

$$\hat{\boldsymbol{g}}_{ilk} = \frac{\beta_{ilk} p_{p,lk}^{1/2}}{\beta_{iik} p_{p,ik}^{1/2}} \hat{\boldsymbol{g}}_{iik} = \frac{\sigma_{ilk}}{\sigma_{iik}} \hat{\boldsymbol{g}}_{iik} \tag{2.10}$$

Based on the MMSE channel estimation results, in the next section, we will present a discussion on the linear multi-user detectors and precoders for MU-MIMO systems, namely MRC and ZF detectors, and MRT and ZF precoders. We will also derive the SINR expression of these linear detectors and precoders.

2.4 Uplink Data Transmission

After applying the $M \times K$ receive beamforming matrix $\boldsymbol{W}_l$, the data or user signal received at BS l can be represented by the following $M \times 1$ vector,

$$\boldsymbol{r}_l = \boldsymbol{W}_l^H \boldsymbol{y}_l = \boldsymbol{W}_l^H \sum_{i=1}^{L} \boldsymbol{G}_{li} \boldsymbol{P}_{d,i}^{1/2} \boldsymbol{s}_i + \boldsymbol{W}_l^H \boldsymbol{n}_l \tag{2.11}$$

where $K \times 1$ vector $\boldsymbol{s}_i$ denotes the data symbols transmitted by the K users in cell i and $M \times 1$ vector $\boldsymbol{n}_l$ represents the white complex Gaussian noise with zero-mean and unit variance. Let r_{lk} and s_{lk} denote the k-th element of the $M \times 1$ vector $\boldsymbol{r}_l$ and that of $\boldsymbol{s}_l$, respectively. The uplink received signal associated to the k-th user at BS l can be expressed as

$$\begin{aligned} r_{lk} = \hat{\boldsymbol{w}}_{lk}^H \boldsymbol{y}_l = p_{d,lk}^{1/2} \hat{\boldsymbol{w}}_{lk}^H \hat{\boldsymbol{g}}_{llk} s_{lk} + \hat{\boldsymbol{w}}_{lk}^H \sum_{\kappa \neq k}^{K} p_{d,l\kappa}^{1/2} \hat{\boldsymbol{g}}_{ll\kappa} s_{l\kappa} \\ + \hat{\boldsymbol{w}}_{lk}^H \boldsymbol{n}_l - \hat{\boldsymbol{w}}_{lk}^H \sum_{i=1}^{L} \Delta \boldsymbol{G}_{li} \boldsymbol{P}_{d,i}^{1/2} \boldsymbol{s}_i + \hat{\boldsymbol{w}}_{lk}^H \sum_{i \neq l}^{L} \hat{\boldsymbol{G}}_{li} \boldsymbol{P}_{d,i}^{1/2} \boldsymbol{s}_i \end{aligned} \tag{2.12}$$

where $\hat{\boldsymbol{w}}_{lk}$ denotes the k-th column of matrix $\boldsymbol{W}_l$. From (2.12), it can be seen that the first term represents the desired signal and the second term is the intra-cell interference. The third term means the white Gaussian noise which is independent of any transmit signal. The fourth term can be considered as the additive noise caused by channel estimation error and the last term represents the inter-cell interference.

When linear multi-user detection techniques are used, the BS multiplies the received signal with a linear detection matrix so as to decode the data streams transmitted by the K users on the uplink. By employing the MRC receiver at BS with detection matrix $\boldsymbol{W}_l = \hat{\boldsymbol{G}}_{ll}$, we have $\boldsymbol{w}_{lk}^H = \hat{\boldsymbol{g}}_{llk}^H$. From (2.12), the received SINR of user k in cell l, which is defined as the

power ratio of the desired signal to the sum of noise, intra-cell and inter-cell interferences, can be derived as given by (2.13).

$$\gamma_{lk}^{MRC} = \\ p_{d,lk}\|\hat{\boldsymbol{g}}_{llk}\|^4 \Big/ \Big(\sum_{\kappa=1,\kappa\neq k}^{K} p_{u,l\kappa}\left|\hat{\boldsymbol{g}}_{llk}^H \hat{\boldsymbol{g}}_{ll\kappa}\right|^2 + \left\|\hat{\boldsymbol{g}}_{llk}^H\right\|^2 + \sum_{i=1}^{L}\sum_{\kappa=1}^{K} p_{u,i\kappa}\left|\hat{\boldsymbol{g}}_{llk}^H \Delta\boldsymbol{g}_{li\kappa}\right|^2 \\ + \sum_{i=1,i\neq l}^{L}\sum_{\kappa=1,\kappa\neq k}^{K} p_{u,i\kappa}\left|\hat{\boldsymbol{g}}_{llk}^H \hat{\boldsymbol{g}}_{ll\kappa}\right|^2 \frac{\beta_{li\kappa}^2 p_{p,i\kappa}}{\beta_{ll\kappa}^2 p_{p,l\kappa}} + \sum_{i=1,i\neq l}^{L} p_{u,ik}\|\hat{\boldsymbol{g}}_{llk}\|^4 \frac{\beta_{lik}^2 p_{p,ik}}{\beta_{llk}^2 p_{p,lk}} \Big) \tag{2.13}$$

When ZF receiver is used at BS with receiving matrix $\boldsymbol{W}_l = \hat{\boldsymbol{G}}_{ll}(\hat{\boldsymbol{G}}_{ll}^H \hat{\boldsymbol{G}}_{ll})^{-1}$ [11], we have $\hat{\boldsymbol{w}}_{lk}^H \hat{\boldsymbol{g}}_{llk} = 1$ and $\hat{\boldsymbol{w}}_{lk}^H \hat{\boldsymbol{g}}_{ll\kappa} = 0$ $(k \neq \kappa)$. Then, the received uplink SINR of user k can be obtained by using (2.12), as given by

$$\gamma_{lk}^{ZF} = \frac{p_{u,lk}}{\sum_{i=1}^{L}\sum_{\kappa=1}^{K} p_{u,i\kappa}|\hat{\boldsymbol{w}}_{lk}^H \Delta\hat{\boldsymbol{g}}_{li\kappa}|^2 + \sum_{i=1,i\neq l}^{L} p_{u,ik}\frac{\beta_{lik}^2 p_{p,ik}}{\beta_{llk}^2 p_{p,lk}} + \|\hat{\boldsymbol{w}}_{lk}^H\|^2} \tag{2.14}$$

2.5 Downlink Data Transmission

When linear multi-user precoding techniques are used, the BS multiplies the transmit signal with a linear precoding matrix to precode the data streams on the downlink. Based on the assumption of channel reciprocity as discussed in section 2.2, the estimated uplink CSI is used to generate the precoding matrix for downlink data transmission.

When a normalized precoding vector $\boldsymbol{a}_{lk}/\|\boldsymbol{a}_{lk}\|$ is employed at BS, the signal received at the k-th user $\tilde{r}_{lk}$ in cell l can be expressed as

$$\tilde{r}_{lk} = p_{d,lk}^{1/2}\frac{\hat{\boldsymbol{g}}_{llk}^H \boldsymbol{a}_{lk}}{\|\boldsymbol{a}_{lk}\|}s_{lk} + \sum_{\kappa\neq k}^{K} p_{d,l\kappa}^{1/2}\frac{\hat{\boldsymbol{g}}_{llk}^H \boldsymbol{a}_{l\kappa}}{\|\boldsymbol{a}_{l\kappa}\|}s_{l\kappa} + \boldsymbol{n}_l - \sum_{i=1}^{L}\sum_{\kappa=1}^{K} p_{d,i\kappa}^{1/2}\frac{\Delta\boldsymbol{g}_{ilk}^H \boldsymbol{a}_{i\kappa}}{\|\boldsymbol{a}_{i\kappa}\|} + \sum_{i\neq l}^{L}\sum_{\kappa=1}^{K} p_{d,i\kappa}^{1/2}\frac{\hat{\boldsymbol{g}}_{ilk}^H \boldsymbol{a}_{i\kappa}}{\|\boldsymbol{a}_{i\kappa}\|} \tag{2.15}$$

where $p_{d,k}$ represents the downlink data power for the k-th user in cell l and $\tilde{s}_{lk}$ denotes the data signal of user k in cell l. Similar to the uplink transmission, only the first term in (2.15) is the desired signal, and other four terms represent the intra-cell interference, white Gaussian noise, channel estimation error and inter-cell interference, respectively.

When MRT precoder is employed at BS, we have $\boldsymbol{v}_{lk} = \hat{\boldsymbol{g}}_{llk}$ (or $\boldsymbol{v}_{ik} = \hat{\boldsymbol{g}}_{iik}$) [11]. The received SINR of user k in cell l can then be obtained as

$$\tilde{\gamma}_{lk}^{MRT} = \frac{p_{d,lk}\|\hat{\boldsymbol{g}}_{llk}\|^2}{\sum\limits_{\kappa=1,\kappa\neq k}^{K} p_{d,l\kappa}\frac{\left|\hat{\boldsymbol{g}}_{llk}^H\hat{\boldsymbol{g}}_{ll\kappa}\right|^2}{\|\hat{\boldsymbol{g}}_{ll\kappa}\|^2} + \sum\limits_{i=1}^{L}\sum\limits_{\kappa=1}^{K} p_{d,i\kappa}\frac{\left|\Delta\boldsymbol{g}_{ilk}^H\hat{\boldsymbol{g}}_{ii\kappa}\right|^2}{\|\hat{\boldsymbol{g}}_{ii\kappa}\|^2} + \sum\limits_{i\neq l}^{L}\sum\limits_{\kappa=1}^{K} p_{d,i\kappa}\frac{\left|\hat{\boldsymbol{g}}_{iik}^H\hat{\boldsymbol{g}}_{ii\kappa}\right|^2}{\|\hat{\boldsymbol{g}}_{ii\kappa}\|^2}\frac{\beta_{ilk}^2 p_{p,lk}}{\beta_{iik}^2 p_{p,ik}} + 1} \tag{2.16}$$

When ZF precoder [10] is used at BS with precoding matrix $\boldsymbol{A}_l = \hat{\boldsymbol{G}}_{ll}(\hat{\boldsymbol{G}}_{ll}^H\hat{\boldsymbol{G}}_{ll})^{-1}$, we have $\hat{\boldsymbol{g}}_{llk}\hat{\boldsymbol{a}}_{lk}^H = 1$ and $\hat{\boldsymbol{g}}_{llk}\hat{\boldsymbol{a}}_{l\kappa}^H = 0$ $(k \neq \kappa)$. Then, by using (2.15), the downlink SINR of user k can be obtained as

$$\tilde{\gamma}_{lk}^{ZF} = \frac{\frac{p_{d,lk}}{\|\boldsymbol{a}_{lk}\|^2}}{\sum\limits_{i=1}^{L}\sum\limits_{\kappa=1}^{K} p_{d,i\kappa}\frac{\left|\Delta\hat{\boldsymbol{g}}_{ilk}^H\boldsymbol{a}_{i\kappa}\right|^2}{\|\boldsymbol{a}_{i\kappa}\|^2} + \sum\limits_{i=1,i\neq l}^{L}\frac{1}{\|\boldsymbol{a}_{ik}\|^2}\frac{p_{d,ik}\beta_{ilk}^2 p_{p,lk}}{\beta_{iik}^2 p_{p,ik}} + 1} \tag{2.17}$$

It is obvious that the SINRs of these precoders and detectors are very complicated. In the next chapter, we will derive their lower bounds to be used in the development of power allocation algorithms.

2.6 Conclusion

At the beginning of this chapter, we presented a brief introduction about conventional MU-MIMO and large-scale MU-MIMO systems and discussed different channel estimation methods. Then, we introduced multi-cell MU-MIMO model including TDD operating mode frame structure and MMSE channel estimation with pilot contamination. In the proposed TDD multi-cell MU-MIMO system, both small-scale fading and large-scale fading, which incorporate path-loss and shadowing effect, were considered in the channel model. Finally, based on the assumption of channel reciprocity, the uplink and downlink data transmission and SINRs were discussed by considering the conventional linear MRC and ZF detectors in the uplink and the MRT and ZF precoder in the downlink.

Chapter 3

Lower Bounds of SINR

3.1 Introduction

The increasing popularity of mobile devices and the success of wireless communication networking over the past few decades have brought an exponential growth of data traffic. The ubiquity of energy-consuming wireless applications has raised a serious energy efficiency concern, which triggered an immense interest in the development of energy-efficient and eco-friendly wireless communication technology. For this reason, future 5G communication networks are required to provide both high data rate and low power consumption services[90]-[92], necessitating the design of green communication systems with energy efficiency as a primary goal.

Green communication aims to find innovative solutions to improve EE, and to relieve/reduce the energy consumption and carbon footprint of wireless industry, while maintaining/improving system performance and/or users' quality of service. Power allocation focused on suppressing the interferences, improving the quality of the signal reception and increasing the coverage and/or capacity of overall network, is one main topic of green communication. Generally speaking, there are two frameworks of power allocation in conventional MIMO systems to improve the EE. The first framework aims to minimize the total transmit power under certain constraints, such as QoS requirement and per-user power constraint. In other words,

this framework aims to transmit minimum power to satisfy the desired system performance. The second framework is to maximize the total EE which is defined as the spectral efficiency (sum-rate in bit/channel) divided by the transmit power (in Joules/channel) under certain power constraints. Typically, increasing SE is associated with increasing the power and the achievable transmission rate. On the contrary, the energy saving optimization aims to save power in the whole system and sometimes decreases the system performance, such as SE, SINR, system reliability, etc. Hence, there is a fundamental trade-off between the power consumption and the SE. The idea of the second framework is to jointly optimize the power cost and SE in one operating regime.

The objective of this thesis is to develop energy efficient power control methods for both conventional and massive MU-MIMO systems by following the two frameworks mentioned above. Under the first framework, we would like to formulate an optimization problem to minimize the total transmit power while satisfying the per-user SINR requirements and power consumption constraints [93] [94]. In the second framework, an optimization problem is established such that the total EE for the whole system, which is again closely related to the uplink and downlink SINRs, will be maximized under transmit power constraints [94]. Considering that a direct use of the uplink and downlink SINR expression, as derived in the previous chapter, in the minimization/maximization problem would lead to a very complicated optimization problem which is extremely difficult to solve. So in this chapter, we will derive the lower bounds of the per-user average SINR for the proposed TDD multi-cell MU-MIMO systems. We will then apply the derived lower bounds in our optimal power allocation problems to facilitate their solution. In the derivation of the average SINR lower bounds, we consider both the conventional linear MRC and ZF detectors for the uplink

together with MRT and ZF precoder for the downlink as employed in our proposed multi-cell MU-MIMO model.

3.2 Lower Bounds of Uplink Average SINR

Based on the derived uplink and downlink SINR expressions in Section 2.3 and 2.4, the lower bounds of the statistic SINRs of MRC and ZF detectors for uplink are derived in this section and MRT and ZF precoder for downlink are derived in the next section.

Proposition 1: When the MRC receiver is employed at BS, the lower bound of the average uplink SINR of the k-th user under MMSE channel estimation can be expressed as

$$\begin{aligned} & E\{\gamma_{lk}^{MRC}\} \geq \gamma_{lk}^{MRC,up} \\ & \triangleq \frac{p_{u,lk}}{\frac{1}{(M-1)\sigma_{llk}^2}\left(\sum\limits_{\kappa=1,\kappa\neq k}^{K} p_{u,l\kappa}\sigma_{lli\kappa}^2+1+\sum\limits_{i=1}^{L}\sum\limits_{\kappa=1}^{K} p_{u,i\kappa}\varepsilon_{li\kappa}^2+\sum\limits_{i\neq l}^{L}\sum\limits_{\kappa=1,\kappa\neq k}^{K}\frac{p_{u,i\kappa}\beta_{li\kappa}^2 p_{p,i\kappa}}{\beta_{ll\kappa}^2 p_{p,l\kappa}}\sigma_{lli\kappa}^2\right)+\sum\limits_{i=1,i\neq l}^{L} p_{u,ik}\frac{\beta_{lik}^2 p_{p,ik}}{\beta_{llk}^2 p_{p,lk}}} \end{aligned} \tag{3.1}$$

Proof: From (2.13), we have

$$\begin{aligned} & E\{\gamma_{lk}^{MRC}\} \\ & = E\{\frac{p_{u,lk}}{\sum\limits_{\kappa=1,\kappa\neq k}^{K} p_{u,l\kappa}\frac{\left|\hat{\boldsymbol{g}}_{llk}^H\hat{\boldsymbol{g}}_{lli\kappa}\right|^2}{\left\|\hat{\boldsymbol{g}}_{llk}\right\|^4}+\frac{1}{\left\|\hat{\boldsymbol{g}}_{llk}\right\|^2}+\sum\limits_{i=1}^{L}\sum\limits_{\kappa=1}^{K} p_{u,i\kappa}\frac{\left|\hat{\boldsymbol{g}}_{llk}^H\Delta\boldsymbol{g}_{li\kappa}\right|^2}{\left\|\hat{\boldsymbol{g}}_{llk}\right\|^4}+\sum\limits_{i=1,i\neq l}^{L}\sum\limits_{\kappa=1,\kappa\neq k}^{K}\frac{p_{u,i\kappa}\beta_{li\kappa}^2 p_{p,i\kappa}}{\beta_{ll\kappa}^2 p_{p,l\kappa}}\frac{\left|\hat{\boldsymbol{g}}_{llk}^H\hat{\boldsymbol{g}}_{lli\kappa}\right|^2}{\left\|\hat{\boldsymbol{g}}_{llk}\right\|^4}+C_1}\} \end{aligned} \tag{3.2}$$

Here,

$$C_1 \triangleq \sum_{i=1,i\neq l}^{L} p_{u,ik}\frac{\beta_{lik}^2 p_{p,ik}}{\beta_{llk}^2 p_{p,lk}} \tag{3.3}$$

From the Jensen's inequality [95], we know that if $f(x)$ is a convex function, and $E[f(x)]$ and $f(E[x])$ are finite, we can write the above inequality as $E[f(x)] \geq f(E[x])$. So based on

the fact that the function $1/x$ is convex when x is positive, we have $E[1/f(x)] \geq 1/E[f(x)]$. Then, we obtain

$$E\{\gamma_{lk}^{MRC}\} \geq \frac{p_{u,lk}}{E\{\sum\limits_{\kappa=1,\kappa\neq k}^{K} p_{u,l\kappa}\frac{\left|\hat{\boldsymbol{g}}_{llk}^H\hat{\boldsymbol{g}}_{ll\kappa}\right|^2}{\|\hat{\boldsymbol{g}}_{llk}\|^4}+\frac{1}{\|\hat{\boldsymbol{g}}_{llk}\|^2}+\sum\limits_{i=1}^{L}\sum\limits_{\kappa=1}^{K} p_{u,i\kappa}\frac{\left|\hat{\boldsymbol{g}}_{llk}^H\Delta\boldsymbol{g}_{li\kappa}\right|^2}{\|\hat{\boldsymbol{g}}_{llk}\|^4}+\sum\limits_{i=1,i\neq l}^{L}\sum\limits_{\kappa=1,\kappa\neq k}^{K}\frac{p_{u,i\kappa}\beta_{li\kappa}^2 p_{p,i\kappa}}{\beta_{ll\kappa}^2 p_{p,l\kappa}}\frac{\left|\hat{\boldsymbol{g}}_{llk}^H\hat{\boldsymbol{g}}_{ll\kappa}\right|^2}{\|\hat{\boldsymbol{g}}_{llk}\|^4}+C_1\}} \tag{3.4}$$

For the denominator of (3.4), it is easy to have

$$\begin{aligned}&\textit{Denominator of } (3.4)\\ &=\sum_{\kappa=1,\kappa\neq k}^{K} p_{u,l\kappa}E\{\frac{\left|\hat{\boldsymbol{g}}_{llk}^H\hat{\boldsymbol{g}}_{ll\kappa}\right|^2}{\|\hat{\boldsymbol{g}}_{llk}\|^4}\}+E\{\frac{1}{\|\hat{\boldsymbol{g}}_{llk}\|^2}\}+\sum_{i=1}^{L}\sum_{\kappa=1}^{K} p_{u,i\kappa}E\{\frac{\left|\hat{\boldsymbol{g}}_{llk}^H\Delta\boldsymbol{g}_{li\kappa}\right|^2}{\|\hat{\boldsymbol{g}}_{llk}\|^4}\}\\ &+\sum_{i=1,i\neq l}^{L}\sum_{\kappa=1,\kappa\neq k}^{K}\frac{p_{u,i\kappa}\beta_{li\kappa}^2 p_{p,i\kappa}}{\beta_{ll\kappa}^2 p_{p,l\kappa}}E\{\frac{\left|\hat{\boldsymbol{g}}_{llk}^H\hat{\boldsymbol{g}}_{ll\kappa}\right|^2}{\|\hat{\boldsymbol{g}}_{llk}\|^4}\}+C_1\end{aligned} \tag{3.5}$$

Since the elements of vectors $\hat{\boldsymbol{g}}_{ll\kappa}$ and $\Delta\boldsymbol{g}_{li\kappa}$ consist of i.i.d. zero-mean Gaussian RVs, these two vectors are rotationally invariant and spherically symmetric. Then, from the property of rotational invariance [96, chapter 4], both $\frac{\hat{\boldsymbol{g}}_{llk}^H\hat{\boldsymbol{g}}_{ll\kappa}}{\|\hat{\boldsymbol{g}}_{llk}\|}$ and $\frac{\hat{\boldsymbol{g}}_{llk}^H\Delta\boldsymbol{g}_{li\kappa}}{\|\hat{\boldsymbol{g}}_{llk}\|}$ are independent of $\|\hat{\boldsymbol{g}}_{llk}\|$ when $\kappa \neq k$, thus the denominator of (3.4) can be rewritten as

$$\begin{aligned}&\textit{Denominator of } (3.4)\\ &=E\{\frac{1}{\|\hat{\boldsymbol{g}}_{llk}\|^2}\}(\sum_{\kappa=1,\kappa\neq k}^{K} p_{u,l\kappa}E\{\frac{\left|\hat{\boldsymbol{g}}_{llk}^H\hat{\boldsymbol{g}}_{ll\kappa}\right|^2}{\|\hat{\boldsymbol{g}}_{llk}\|^2}\}+1+\sum_{i=1}^{L}\sum_{\kappa=1}^{K} p_{u,i\kappa}E\{\frac{\left|\hat{\boldsymbol{g}}_{llk}^H\Delta\boldsymbol{g}_{li\kappa}\right|^2}{\|\hat{\boldsymbol{g}}_{llk}\|^2}\}\\ &+\sum_{i\neq l}^{L}\sum_{\kappa=1,\kappa\neq k}^{K}\frac{p_{u,i\kappa}\beta_{li\kappa}^2 p_{p,i\kappa}}{\beta_{ll\kappa}^2 p_{p,l\kappa}}E\{\frac{\left|\hat{\boldsymbol{g}}_{llk}^H\hat{\boldsymbol{g}}_{ll\kappa}\right|^2}{\|\hat{\boldsymbol{g}}_{llk}\|^2}\})+C_1\end{aligned} \tag{3.6}$$

From the property of spherically symmetric distribution [96], we know that $\frac{\hat{\boldsymbol{g}}_{llk}^H\hat{\boldsymbol{g}}_{ll\kappa}}{\|\hat{\boldsymbol{g}}_{llk}\|}$ and $\frac{\hat{\boldsymbol{g}}_{llk}^H\Delta\boldsymbol{g}_{li\kappa}}{\|\hat{\boldsymbol{g}}_{llk}\|}$ in (3.6) are Gaussian RVs with zero-mean and variance $\sigma_{ll\kappa}^2$ and $\varepsilon_{li\kappa}^2$, respectively.

So we have

$$E\{\frac{\hat{\boldsymbol{g}}_{llk}^H \hat{\boldsymbol{g}}_{ll\kappa}}{\|\hat{\boldsymbol{g}}_{llk}\|}\} = \sigma_{ll\kappa}^2 \tag{3.7}$$

and

$$E\{\frac{\hat{\boldsymbol{g}}_{llk}^H \Delta \boldsymbol{g}_{li\kappa}}{\|\hat{\boldsymbol{g}}_{llk}\|}\} = \varepsilon_{li\kappa}^2 \tag{3.8}$$

Substituting (3.7) and (3.8) into (3.6), we obtain

$$\begin{aligned} &Denominator\ of\ (3.4) \\ &= E\{\tfrac{1}{\|\hat{\boldsymbol{g}}_{llk}\|^2}\}(\sum_{\kappa=1,\kappa\neq k}^{K} p_{u,l\kappa}\sigma_{ll\kappa}^2 + 1 + \sum_{i=1}^{L}\sum_{\kappa=1}^{K} p_{u,i\kappa}\varepsilon_{li\kappa}^2 + \sum_{i\neq l}^{L}\sum_{\kappa=1,\kappa\neq k}^{K} \tfrac{p_{u,i\kappa}\beta_{li\kappa}^2 p_{p,i\kappa}}{\beta_{ll\kappa}^2 p_{p,l\kappa}}\sigma_{ll\kappa}^2) \\ &+ \sum_{i\neq l}^{L} p_{u,ik}\tfrac{\beta_{lik}^2 p_{p,ik}}{\beta_{llk}^2 p_{p,lk}} \end{aligned} \tag{3.9}$$

The term $\frac{1}{\|\hat{\boldsymbol{g}}_{llk}\|^2}$ in (3.9) can be treated as a 1×1 central complex Wishart matrix with M degrees of freedom. From the property of central Wishart matrix [97], we get

$$\begin{aligned} E\{\tfrac{1}{\|\hat{\boldsymbol{g}}_{llk}\|^2}\} &= \tfrac{1}{\sigma_{llk}^2} E\{\left[\left(\tfrac{\hat{\boldsymbol{g}}_{llk}}{\sigma_{llk}}\right)^H \tfrac{\hat{\boldsymbol{g}}_{llk}}{\sigma_{llk}}\right]^{-1}\} \\ &= \tfrac{1}{\sigma_{llk}^2} E\{tr\left\{\left[\left(\tfrac{\hat{\boldsymbol{g}}_{llk}}{\sigma_{llk}}\right)^H \tfrac{\hat{\boldsymbol{g}}_{llk}}{\sigma_{llk}}\right]^{-1}\right\}\} \\ &= \tfrac{1}{(M-1)\sigma_{llk}^2} \end{aligned} \tag{3.10}$$

Substituting (3.10) into (3.9) and (3.4), we obtain the result in (3.1).

Proposition 2: When the ZF receiver is employed at BS, the lower bound of the uplink average SINR of user k under MMSE channel estimation can be expressed as

$$
\begin{aligned}
&E\{\gamma_{lk}^{ZF}\} \geq \gamma_{lk}^{ZF,up} \\
&\triangleq \frac{p_{u,lk}}{\frac{1}{(M-K)\sigma_{llk}^2}(\sum\limits_{i=1}^{L}\sum\limits_{\kappa=1}^{K} p_{u,i\kappa}\varepsilon_{li\kappa}^2+1)+\sum\limits_{i=1,i\neq l}^{L} p_{u,ik}\frac{\beta_{lik}^2 p_{p,ik}}{\beta_{llk}^2 p_{p,lk}}}
\end{aligned} \tag{3.11}
$$

Proof: Similar to the proof of Proposition 1, by using (2.14) and the property $E[1/f(x)] \geq 1/E[f(x)]$ when $f(x) \geq 0$, the lower bound of the average SINR of the user k in cell l can be obtained as

$$
\begin{aligned}
E\{\gamma_{lk}^{ZF}\} &= E\{\frac{p_{u,lk}}{\sum\limits_{i=1}^{L}\sum\limits_{\kappa=1}^{K} p_{u,i\kappa}\left|\hat{\boldsymbol{w}}_{lk}^H \Delta\hat{\boldsymbol{g}}_{li\kappa}\right|^2+\sum\limits_{i=1,i\neq l}^{L} p_{u,ik}\frac{\beta_{lik}^2 p_{p,ik}}{\beta_{llk}^2 p_{p,lk}}+\left\|\hat{\boldsymbol{w}}_{lk}^H\right\|^2}\} \\
&\geq \frac{p_{u,lk}}{E\{\sum\limits_{i=1}^{L}\sum\limits_{\kappa=1}^{K} p_{u,i\kappa}\left|\hat{\boldsymbol{w}}_{lk}^H \Delta\hat{\boldsymbol{g}}_{li\kappa}\right|^2+\sum\limits_{i=1,i\neq l}^{L} p_{u,ik}\frac{\beta_{lik}^2 p_{p,ik}}{\beta_{llk}^2 p_{p,lk}}+\left\|\hat{\boldsymbol{w}}_{lk}^H\right\|^2\}} \\
&= \frac{p_{u,lk}}{\sum\limits_{i=1}^{L}\sum\limits_{\kappa=1}^{K} p_{u,i\kappa}E\{\left|\hat{\boldsymbol{w}}_{lk}^H \Delta\hat{\boldsymbol{g}}_{li\kappa}\right|^2\}+\sum\limits_{i=1,i\neq l}^{L} p_{u,ik}\frac{\beta_{lik}^2 p_{p,ik}}{\beta_{llk}^2 p_{p,lk}}+E\{\left\|\hat{\boldsymbol{w}}_{lk}^H\right\|^2\}}
\end{aligned} \tag{3.12}
$$

Since $\hat{\boldsymbol{w}}_{lk}$ is independent of $\Delta\hat{\boldsymbol{g}}_{li\kappa}$, we obtain

$$
E\{\left|\hat{\boldsymbol{w}}_{lk}^H \Delta\hat{\boldsymbol{g}}_{li\kappa}\right|^2\} = E\{\left\|\hat{\boldsymbol{w}}_{lk}^H\right\|^2\}\varepsilon_{li\kappa}^2 \tag{3.13}
$$

Substituting (3.13) into (3.12), we obtain

$$
E\{\gamma_{lk}^{ZF}\} \geq \frac{p_{u,lk}}{E\{\|\hat{\boldsymbol{w}}_{lk}^H\|^2\}(\sum\limits_{i=1}^{L}\sum\limits_{\kappa=1}^{K} p_{u,i\kappa}\varepsilon_{li\kappa}^2+1)+\sum\limits_{i=1,i\neq l}^{L} p_{u,ik}\frac{\beta_{lik}^2 p_{p,ik}}{\beta_{llk}^2 p_{p,lk}}} \tag{3.14}
$$

As the matrix $\hat{\boldsymbol{G}}_{\boldsymbol{li}}$ consists of i.i.d Gaussian RVs with the same variance for each column elements, it can be written as

$$
\hat{\boldsymbol{G}}_{li} = \boldsymbol{\Lambda}_{li}\boldsymbol{Z} \tag{3.15}
$$

Here, matrix $\boldsymbol{Z}$ has the same size as $\hat{\boldsymbol{G}}_{li}$, whose elements are i.i.d. Gaussian RVs with zero-mean and unit variance, and the $K \times K$ diagonal matrix $\boldsymbol{\Lambda}_l$ is defined as

$$\boldsymbol{\Lambda}_l \triangleq diag\left(\sigma_{ll1}, \sigma_{ll2}, \ldots, \sigma_{llK}\right) \tag{3.16}$$

Based on the property of central Wishart matrix [97], we have

$$\begin{aligned} &E\{\left\|\boldsymbol{w}_{lk}^H\right\|^2\} = E\{\boldsymbol{W}_l^H \boldsymbol{W}_l\}_{kk} = E\{[(\hat{\boldsymbol{G}}_{ll}^H \hat{\boldsymbol{G}}_{ll})^{-1}]_{kk}\} \\ &= E\{[(\boldsymbol{\Lambda}_l)^{-1}(\boldsymbol{Z}^H\boldsymbol{Z})^{-1}(\boldsymbol{\Lambda}_l)^{-1}]_{kk}\} = \tfrac{1}{\sigma_{llk}^2} E\{[(\boldsymbol{Z}^H\boldsymbol{Z})^{-1}]_{kk}\} \\ &= \tfrac{1}{K\sigma_{llk}^2} E\{tr[(\boldsymbol{Z}^H\boldsymbol{Z})^{-1}]\} = \tfrac{1}{(M-K)\sigma_{llk}^2} \end{aligned} \tag{3.17}$$

Substituting (3.17) into (3.14), we get the lower bound of the uplink average SINR for ZF receiver as in (3.11).

3.3 Lower Bounds of Downlink Average SINR

In the previous section, we have derived statistic SINR lower bounds for MRC and ZF receiver. In this section, the lower bounds of average SINR for MRT and ZF precoder are discussed.

Proposition 3: The lower bound of the downlink average SINR of user k in cell l when MRT precoder is employed at BS can be expressed as

$$\begin{aligned} &E\{\tilde{\gamma}_{lk}^{MRT}\} \geq \gamma_{lk}^{MRT,dn} \triangleq \\ &\frac{p_{d,lk}(M-1)\sigma_{llk}^2}{\frac{(M-1)\sigma_{llk}^2}{M} \sum\limits_{\kappa=1,\kappa\neq k}^{K} p_{d,l\kappa} + \sum\limits_{i=1}^{L}\sum\limits_{\kappa=1}^{K} p_{d,i\kappa}\varepsilon_{ilk}^2 + \sum\limits_{i\neq l}^{L}\sum\limits_{\kappa=1}^{K} p_{d,i\kappa}\sigma_{iik}^2 \frac{\beta_{ilk}^2 p_{p,lk}}{\beta_{iik}^2 p_{p,ik}} + 1} \end{aligned} \tag{3.18}$$

Proof: Similar to the proof of Proposition 1, by using (2.16) and the property $E[1/f(x)] \geq 1/E[f(x)]$ when $f(x) \geq 0$, the lower bound of the average SINR of the user k in cell l can be obtained as

$$E\{\tilde{\gamma}_{lk}^{MRT}\} = E\{\frac{p_{d,lk}}{\sum\limits_{\kappa=1,\kappa\neq k}^{K} p_{d,l\kappa}\frac{\left|\hat{\boldsymbol{g}}_{llk}^H\hat{\boldsymbol{g}}_{ll\kappa}\right|^2}{\left\|\hat{\boldsymbol{g}}_{llk}\right\|^2\left\|\hat{\boldsymbol{g}}_{ll\kappa}\right\|^2}+\sum\limits_{i=1}^{L}\sum\limits_{\kappa=1}^{K} p_{d,i\kappa}\frac{\left|\Delta\boldsymbol{g}_{ilk}^H\hat{\boldsymbol{g}}_{ii\kappa}\right|^2}{\left\|\hat{\boldsymbol{g}}_{llk}\right\|^2\left\|\hat{\boldsymbol{g}}_{ii\kappa}\right\|^2}+\sum\limits_{i=1,i\neq l}^{L}\sum\limits_{\kappa=1}^{K} p_{d,i\kappa}\frac{\left|\hat{\boldsymbol{g}}_{iik}^H\hat{\boldsymbol{g}}_{ii\kappa}\right|^2}{\left\|\hat{\boldsymbol{g}}_{llk}\right\|^2\left\|\hat{\boldsymbol{g}}_{ii\kappa}\right\|^2}\frac{\beta_{ilk}^2 p_{p,lk}}{\beta_{iik}^2 p_{p,ik}}+\frac{1}{\left\|\hat{\boldsymbol{g}}_{llk}\right\|^2}}\}$$
$$\geq \frac{p_{d,lk}}{Denominator\ of\ (3.19)} \tag{3.19}$$

where

$$\begin{aligned}
&Denominator\ of\ (3.19)\\
&=\sum_{\kappa=1,\kappa\neq k}^{K} p_{d,l\kappa}E\{\frac{\left|\hat{\boldsymbol{g}}_{llk}^H\hat{\boldsymbol{g}}_{ll\kappa}\right|^2}{\left\|\hat{\boldsymbol{g}}_{llk}\right\|^2\left\|\hat{\boldsymbol{g}}_{ll\kappa}\right\|^2}\}+\sum_{i=1}^{L}\sum_{\kappa=1}^{K} p_{d,i\kappa}E\{\frac{\left|\Delta\boldsymbol{g}_{ilk}^H\hat{\boldsymbol{g}}_{ii\kappa}\right|^2}{\left\|\hat{\boldsymbol{g}}_{llk}\right\|^2\left\|\hat{\boldsymbol{g}}_{ii\kappa}\right\|^2}\}\\
&+\sum_{i\neq l}^{L}\sum_{\kappa=1}^{K} p_{d,i\kappa}E\{\frac{\left|\hat{\boldsymbol{g}}_{iik}^H\hat{\boldsymbol{g}}_{ii\kappa}\right|^2}{\left\|\hat{\boldsymbol{g}}_{llk}\right\|^2\left\|\hat{\boldsymbol{g}}_{ii\kappa}\right\|^2}\}\frac{\beta_{ilk}^2 p_{p,lk}}{\beta_{iik}^2 p_{p,ik}}+E\{\frac{1}{\left\|\hat{\boldsymbol{g}}_{llk}\right\|^2}\}\\
&=\sum_{\kappa=1,\kappa\neq k}^{K} p_{d,l\kappa}E\{\left|\frac{\hat{\boldsymbol{g}}_{llk}^H}{\left\|\hat{\boldsymbol{g}}_{llk}\right\|}\frac{\hat{\boldsymbol{g}}_{ll\kappa}}{\left\|\hat{\boldsymbol{g}}_{ll\kappa}\right\|}\right|^2\}+E\{\frac{1}{\left\|\hat{\boldsymbol{g}}_{llk}\right\|^2}\}(\sum_{i=1}^{L}\sum_{\kappa=1}^{K} p_{d,i\kappa}E\{\frac{\left|\Delta\boldsymbol{g}_{ilk}^H\hat{\boldsymbol{g}}_{ii\kappa}\right|^2}{\left\|\hat{\boldsymbol{g}}_{ii\kappa}\right\|^2}\}\\
&+\sum_{i\neq l}^{L}\sum_{\kappa=1}^{K} p_{d,i\kappa}E\{\frac{\left|\hat{\boldsymbol{g}}_{iik}^H\hat{\boldsymbol{g}}_{ii\kappa}\right|^2}{\left\|\hat{\boldsymbol{g}}_{ii\kappa}\right\|^2}\}\frac{\beta_{ilk}^2 p_{p,lk}}{\beta_{iik}^2 p_{p,ik}}+1)
\end{aligned} \tag{3.20}$$

Similar to the discussion for proposition 1, we have

$$E\{\frac{\left|\Delta\boldsymbol{g}_{ilk}^H\hat{\boldsymbol{g}}_{ii\kappa}\right|^2}{\left\|\hat{\boldsymbol{g}}_{ii\kappa}\right\|^2}\}=\varepsilon_{ilk}^2 \tag{3.21}$$

and

$$E\{\frac{\left|\hat{\boldsymbol{g}}_{iik}^H\hat{\boldsymbol{g}}_{ii\kappa}\right|^2}{\left\|\hat{\boldsymbol{g}}_{ii\kappa}\right\|^2}\}=\sigma_{iik}^2 \tag{3.22}$$

Moreover, the elements of $\frac{\hat{\boldsymbol{g}}_{ll\kappa}}{\left\|\hat{\boldsymbol{g}}_{ll\kappa}\right\|}$ are uncorrelated and dependent RVs following a unit

spherical distribution with zero mean and variance $1/M$, so vector $\frac{\hat{\boldsymbol{g}}_{ll\kappa}}{\|\hat{\boldsymbol{g}}_{ll\kappa}\|}$ is spherical symmetric. Furthermore, the two vectors $\frac{\hat{\boldsymbol{g}}_{ll\kappa}}{\|\hat{\boldsymbol{g}}_{ll\kappa}\|}$ and $\hat{\boldsymbol{g}}_{llk}$ are independent when $\kappa \neq k$. Thus from the property of spherical symmetry [96], $\frac{\hat{\boldsymbol{g}}_{llk}^H}{\|\hat{\boldsymbol{g}}_{llk}\|}\frac{\hat{\boldsymbol{g}}_{ll\kappa}}{\|\hat{\boldsymbol{g}}_{ll\kappa}\|}$ follows a unit spherical distribution with zero mean and variance $1/M$. Therefore, we have

$$E\{\left|\frac{\hat{\boldsymbol{g}}_{llk}^H}{\|\hat{\boldsymbol{g}}_{llk}\|}\frac{\hat{\boldsymbol{g}}_{ll\kappa}}{\|\hat{\boldsymbol{g}}_{ll\kappa}\|}\right|^2\} = \frac{1}{M} \tag{3.23}$$

Substituting (3.21), (3.22) and (3.23) into the last equation of (3.20) and then using (3.20) to (3.19), we get

$$E\{\tilde{\gamma}_{lk}^{MRT}\} \geq \frac{p_{d,lk}}{\frac{1}{M}\sum\limits_{\kappa=1,\kappa\neq k}^{K} p_{d,l\kappa}+E\{\frac{1}{\left\|\hat{\boldsymbol{g}}_{llk}\right\|^2}\}\sum\limits_{i=1}^{L}\sum\limits_{\kappa=1}^{K} p_{d,i\kappa}\varepsilon_{ilk}^2+E\{\frac{1}{\left\|\hat{\boldsymbol{g}}_{llk}\right\|^2}\}\sum\limits_{i\neq l}^{L}\sum\limits_{\kappa=1}^{K} p_{d,i\kappa}\sigma_{iik}^2\frac{\beta_{ilk}^2 p_{p,lk}}{\beta_{iik}^2 p_{p,ik}}+E\{\frac{1}{\left\|\hat{\boldsymbol{g}}_{llk}\right\|^2}\}} \tag{3.24}$$

Finally, substituting (3.10) into (3.24), we get the lower bound of the uplink average SINR for ZF receiver as in (3.18).

Proposition 4: The lower bound of the downlink average SINR of user k in cell l when ZF precoder is employed at BS can be expressed as

$$E\{\tilde{\gamma}_k^{ZF}\} \geq \gamma_{lk}^{ZF,dn} \triangleq \frac{p_{d,lk}}{\frac{1}{(M-K)\sigma_{llk}^2}(\sum\limits_{i=1}^{L}\sum\limits_{\kappa=1}^{K} p_{d,i\kappa}\varepsilon_{ilk}^2+1)+\sum\limits_{i=1,i\neq l}^{L}\frac{p_{d,ik}\beta_{ilk}^2 p_{p,lk}}{\beta_{iik}^2 p_{p,ik}}} \tag{3.25}$$

Proof: By a similar method, we can obtain the lower bound of the average SINR of the

user k in cell l as

$$
\begin{aligned}
E\{\tilde{\gamma}_k^{ZF}\} &= E\{\frac{\frac{p_{d,lk}}{\|\boldsymbol{a}_{lk}\|^2}}{\sum\limits_{i=1}^{L}\sum\limits_{\kappa=1}^{K} p_{d,i\kappa}\frac{\left|\Delta\hat{\boldsymbol{g}}_{ilk}^H\boldsymbol{a}_{i\kappa}\right|^2}{\|\boldsymbol{a}_{i\kappa}\|^2}+\sum\limits_{i=1,i\neq l}^{L}\frac{1}{\|\boldsymbol{a}_{ik}\|^2}\frac{p_{d,ik}\beta_{ilk}^2 p_{p,lk}}{\beta_{iik}^2 p_{p,ik}}+1}\} \\
&\geq \frac{p_{d,lk}}{\sum\limits_{i=1}^{L}\sum\limits_{\kappa=1}^{K} p_{d,i\kappa}E\{\frac{\|\boldsymbol{a}_{lk}\|^2\left|\Delta\hat{\boldsymbol{g}}_{ilk}^H\boldsymbol{a}_{i\kappa}\right|^2}{\|\boldsymbol{a}_{i\kappa}\|^2}\}+\sum\limits_{i=1,i\neq l}^{L}E\{\frac{\|\boldsymbol{a}_{lk}\|^2}{\|\boldsymbol{a}_{ik}\|^2}\}\frac{p_{d,ik}\beta_{ilk}^2 p_{p,lk}}{\beta_{iik}^2 p_{p,ik}}+E\{\|\boldsymbol{a}_{lk}\|^2\}} \\
&= \frac{p_{d,lk}}{\sum\limits_{i=1}^{L}\sum\limits_{\kappa=1}^{K} p_{d,i\kappa}\varepsilon_{ilk}^2 E\{\|\boldsymbol{a}_{lk}\|^2\}+\sum\limits_{i=1,i\neq l}^{L}\frac{p_{d,ik}\beta_{ilk}^2 p_{p,lk}}{\beta_{iik}^2 p_{p,ik}}+E\{\|\boldsymbol{a}_{lk}\|^2\}}
\end{aligned}
\tag{3.26}
$$

Here, the two vectors $\Delta\boldsymbol{g}_{ilk}$ and $\frac{\boldsymbol{a}_{i\kappa}}{\|\boldsymbol{a}_{i\kappa}\|}$ are independent of each other, since $\boldsymbol{A}_l$ only depends on $\hat{\boldsymbol{G}}_{ll}$. Thus, the last equation in (3.26) can be obtained from the property of spherical symmetry.

On the other hand, as $\boldsymbol{A}_l = \boldsymbol{W}_l$, we have

$$
E\{\left\|\boldsymbol{a}_{lk}^H\right\|^2\} = E\{\left\|\boldsymbol{w}_{lk}^H\right\|^2\} = \frac{1}{(M-K)\sigma_{llk}^2} \tag{3.27}
$$

Substituting (3.27) into the last equation of (3.26), we get the final lower bound expression of the average downlink SINR with ZF precoder.

3.4 Conclusion

In this chapter, based on the uplink and downlink average SINRs obtained in chapter 2, we have derived closed-form expressions of the average SINR lower bounds in multi-cell MU-MIMO systems by considering the conventional linear MRC and ZF detectors in the uplink and the MRT and ZF precoder in the downlink. The Jensen's inequality and the properties of central Wishart matrix were used to find the lower bounds of the derived average SINRs.

These lower bounds will be used to replace the true SINR in the energy efficient power allocation optimization problems for TDD MU-MIMO systems in later chapters. As seen from the simulation results of the average SINR lower bounds in the next chapter, the derived SINR lower bounds are very tight, namely, they approach closely the original SINRs yet lead to simplified optimization problems.

Chapter 4

Joint Pilot-Data Power Allocation Based on Total Transmit Power Minimization

4.1 Introduction

In recent years, energy consumption has become a primary concern in the design and operation of MIMO communication systems. Due to economic, operational and environmental reasons, energy efficiency (EE) has been regarded as a new performance metric in the design of 5G wireless networks. One of the most useful approaches for increasing the EE of wireless communication systems is energy efficient power allocation. As discussed in the previous chapters, there are two main energy efficient power control frameworks for MIMO systems, namely, the total transmit power minimization and the EE maximization. In this chapter, we investigate the power control methods in multi-cell MU-MIMO systems based on the first framework.

In the previous power control works such as [11], [57], [58], all users are assumed to have the same pilot power and/or data power. Such equal power allocation strategies may cause squaring effect in low power regime [11] [67], leading to a severe reduction in the system's SE. Moreover, since the users are randomly located in each cell of an MU-MIMO system, the power loss of the received uplink and downlink signals depends on the distance

between the users and BS, which is translated to the large-scale channel fading coefficient. The assumption of equal power allocation among all users is far from accurate and may cause waste of energy. In other words, to keep the same QoS requirement, more power is needed for the users far from BS (with larger large-scale channel fading coefficient), while less power should be allocated for the users close to BS (with lower large-scale channel fading coefficient). Furthermore, most of the previous works, i.e., [48]-[66], considered the EE power control for the uplink and downlink transmissions separately, which limit their use in practical MIMO systems.

On contrary to most previous works, in this chapter we consider a more practical scenario, where the transmit power of pilot or data symbols for different users can be different. Also, based on the MMSE channel estimation, we address the joint pilot-data power control problem for both uplink and downlink transmissions in one optimization problem, so as to achieve a minimum sum power under both per-user SINR and per-user power budget constraints in multi-cell MU-MIMO systems. Besides the joint pilot and data power allocation for conventional MU-MIMO systems, we will then extend our work to massive MU-MIMO case by assuming infinite antennas at BS. The proposed schemes for both conventional and massive MU-MIMO systems take into account the MRC and ZF detectors in the uplink transmission together with MRT and ZF precoder in the downlink transmission. In order to simplify the original optimization problems, the SINR lower bounds derived in the previous chapter are used in the power allocation algorithms instead of the true SINR expressions. Note that such relaxation of the original SINR yields a simplified problem and leads to a suboptimal solution. Finally, numerical results are presented to validate the tightness of the derived SINR lower bounds and the advantages of the proposed energy efficient power

allocation schemes.

4.2 Total Transmit Power Minimization with MRC Receiver and MRT Precoder

Consider the combined use of MRC receiver and MRT precoder in each BS in the multi-cell MU-MIMO system. Let P_{total} be the total transmit power for one transmission frame. By defining

$$\boldsymbol{p}_p \triangleq [p_{p,11}, p_{p,12}, \ldots, p_{p,1K}, \ldots, p_{p,L1}, p_{p,L2}, \ldots, p_{p,LK}], \tag{4.1}$$

$$\boldsymbol{p}_d \triangleq [p_{u,11}, p_{u,12}, \ldots, p_{u,1K}, \ldots, p_{u,L1}, p_{u,L2}, \ldots, p_{u,LK}] \tag{4.2}$$

and

$$\tilde{\boldsymbol{p}}_d \triangleq [p_{d,11}, p_{d,12}, \ldots, p_{d,1K}, \ldots, p_{d,L1}, p_{d,L2}, \ldots, p_{d,LK}], \tag{4.3}$$

the power control problem which minimizes the total transmit power while meeting the per-user SINR and power constraints, as specified by the derived average SINR lower bounds for both MRC receiver and MRT precoder, can be formulated as

$$\min_{\boldsymbol{p}_p, \boldsymbol{p}_d, \tilde{\boldsymbol{p}}_d} P_{total} \triangleq \sum_{l=1}^{L} \sum_{k=1}^{K} (p_{p,lk}\tau + p_{u,lk}T_1 + \zeta_1 p_{d,lk}T_2) \tag{4.4a}$$

$$\text{s.t.} \quad C1 : \gamma_{lk}^{MRC} \geq \gamma_1 \tag{4.4b}$$

$$C2 : \tilde{\gamma}_{lk}^{MRT} \geq \gamma_2 \tag{4.4c}$$

$$C3 : p_{p,lk}\tau + p_{u,lk}T_1 \leq P_1 \tag{4.4d}$$

$$C4 : \sum_{k=1}^{K} p_{u,lk} T_2 \leq P_2 \tag{4.4e}$$

$$C5 : p_{p,lk} \geq 0, p_{u,lk} \geq 0, p_{d,lk} \geq 0 \tag{4.4f}$$

Here, the objective function is the weighted sum of pilot, uplink data and downlink data powers. The first and second constraints represent the uplink and downlink per-user SINR constraints γ_1 and γ_2, respectively. The third and fourth constraints are the power constraint at each user and that at the l-th BS which are given by P_1 and P_2, respectively.

The above optimization problem is very difficult to solve directly, because its first and second constraints are nonconvex. Based on the fact that $\sigma_{lik}^2+\varepsilon_{lik}^2=\beta_{lik}$, by substituting (2.7), (2.8) and (3.1) into (4.4b) and carrying out some derivations, we can rewrite the first constraint C1 as

$$\begin{aligned} C6 : & \tfrac{1}{(M-1)\tau p_{u,lk} p_{p,lk} \beta_{llk}^2} (\sum_{\kappa=1,\kappa\neq k}^{K} p_{u,l\kappa} \beta_{ll\kappa} + 1 + \sum_{j=1}^{L} \tau p_{p,jk} \beta_{ljk} \\ & + \sum_{i=1,i\neq l}^{L} \sum_{\kappa=1,\kappa\neq k}^{K} p_{u,i\kappa} \beta_{li\kappa} + \sum_{j=1}^{L} \tau p_{p,jk} \beta_{ljk} \sum_{\kappa=1,\kappa\neq k}^{K} p_{u,l\kappa} \beta_{ll\kappa} \\ & + \sum_{j=1}^{L} \tau p_{p,jk} \beta_{ljk} \sum_{i=1,i\neq l}^{L} \sum_{\kappa=1,\kappa\neq k}^{K} p_{u,i\kappa} \beta_{li\kappa} + \sum_{i=1}^{L} p_{u,ik} \beta_{lik} \\ & + \tau \sum_{i=1}^{L} p_{u,ik} \beta_{lik} \sum_{j=1,j\neq i}^{L} p_{p,jk} \beta_{ljk}) + \sum_{i=1,i\neq l}^{L} \tfrac{\beta_{lik}^2 p_{u,ik} p_{p,ik}}{\beta_{llk}^2 p_{u,lk} p_{p,lk}} \leq \tfrac{1}{\gamma_1} \end{aligned} \tag{4.5}$$

where the left side of the inequality is posynomial. Similarly, by using (2.7), (2.8) and (3.13) into (4.4c) and conducting some derivations, the second constraint C2 becomes

$$
\begin{aligned}
C7: \frac{(M-1)}{M p_{d,lk}} & \sum_{\kappa=1,\kappa\neq k}^{K} p_{d,l\kappa} + \frac{1}{p_{d,lk}\tau p_{p,lk}\beta_{llk}^2}(\beta_{llk}\sum_{\kappa=1}^{K} p_{d,l\kappa} \\
+\tau\beta_{llk}\sum_{\kappa=1}^{K} p_{d,l\kappa}\sum_{j\neq l}^{L} p_{p,jk}\beta_{ljk} & + \sum_{i\neq l}^{L}\sum_{\kappa=1}^{K} p_{d,i\kappa}\beta_{ilk} + 1 \\
+\tau\sum_{j=1}^{L} p_{p,jk}\beta_{ljk}\sum_{i\neq l}^{L}\sum_{\kappa=1}^{K} p_{d,i\kappa}\beta_{ilk} & + \tau\sum_{j=1}^{L} p_{p,jk}\beta_{ljk}) \leq \frac{(M-1)}{\gamma_1}
\end{aligned}
\tag{4.6}
$$

Then, we can rewrite the minimization problem as

$$
\begin{aligned}
&\min_{\boldsymbol{p}_p,\boldsymbol{p}_d,\tilde{\boldsymbol{p}}_d} \; P_{total} \\
&\text{s.t.} \qquad C3, C4, C5, C6, C7
\end{aligned}
\tag{4.7}
$$

Now, since the objective function and constraints of (4.7) are all posynomials [98] [99] where all the coordinates and coefficients are positive real numbers and the exponents are real numbers, the optimization problem in (4.7) is a standard geometric programming (GP) problem [98]-[100]. It is known that such a GP problem can be solved by using some standard numerical optimization packages, for example, MOSEK [101], TOMLAB [102], YALMIP [103], GPCVX [104] and ConVeX (CVX) [105]. By using these standard packages, we can obtain a globally optimal solution. In our simulation, CVX package is employed to solve the proposed pilot-data power control optimization problems.

4.3 Total Transmit Power Minimization with ZF Receiver/Precoder

Similar to the system with MRC/MRT discussed in the previouse subsection, the pilot-data power allocation problem for ZF receiver and ZF precoder which minimizes the weighted total transmit power subject to the obtained lower bounds on the average SINR and power

constraints can be formulated as

$$\min_{\boldsymbol{p}_p, \boldsymbol{p}_d, \tilde{\boldsymbol{p}}_d} P_{total} \tag{4.8a}$$

$$\text{s.t.} \quad C8 : \gamma_{lk}^{ZF} \geq \gamma_1 \tag{4.8b}$$

$$C9 : \tilde{\gamma}_{lk}^{ZF} \geq \gamma_2 \tag{4.8c}$$

$$C3, C4, C5 \tag{4.8d}$$

By substituting (2.7), (2.8) and (3.8) into (4.8b), we can rewrite (4.8b) as

$$\frac{1+\sum_{j=1}^{L}\tau p_{p,lk}\beta_{llk}}{(M-K)\tau p_{p,lk}p_{u,lk}\beta_{llk}^2}[\sum_{i=1}^{L}\sum_{\kappa=1}^{K}p_{u,i\kappa}\frac{\beta_{li\kappa}(1+\sum_{j\neq i}^{L}\tau p_{p,j\kappa}\beta_{lj\kappa})}{1+\sum_{j=1}^{L}\tau p_{p,j\kappa}\beta_{lj\kappa}}+1]+\sum_{i=1,i\neq l}^{L}\frac{p_{u,ik}}{p_{u,lk}}\frac{\beta_{lik}^2 p_{p,ik}}{\beta_{llk}^2 p_{p,lk}} \leq \frac{1}{\gamma_1} \tag{4.9}$$

By defining $0 \leq t_{l\kappa} \leq 1+\sum_{j=1}^{L}\tau p_{p,j\kappa}\beta_{lj\kappa}$, (4.9) is equivalent to the following three inequalities

$$\begin{aligned} C10 : & \frac{\gamma_1}{(M-K)\tau p_{p,lk}p_{u,lk}\beta_{llk}^2}[\sum_{i=1}^{L}\sum_{\kappa=1}^{K}\frac{\beta_{li\kappa}p_{u,i\kappa}}{t_{l\kappa}}(1+\sum_{j\neq i}^{L}\tau p_{p,j\kappa}\beta_{lj\kappa})(1+\sum_{j=1}^{L}\tau p_{p,jk}\beta_{ljk}) \\ & +1+\sum_{j=1}^{L}\tau p_{p,jk}\beta_{ljk}]+\sum_{i=1,i\neq l}^{L}\frac{\gamma_1\beta_{lik}^2 p_{p,ik}p_{u,ik}}{\beta_{llk}^2 p_{p,lk}p_{u,lk}} \leq 1 \end{aligned} \tag{4.10}$$

$$C11 : t_{l\kappa} \geq 0 \tag{4.11}$$

$$t_{l\kappa} \leq 1+\sum_{j=1}^{L}\tau p_{p,j\kappa}\beta_{lj\kappa} \tag{4.12}$$

It is easy to see that (4.10) and (4.11) are posinomial inequalities [96] [106] but (4.12) is not. Here, we can use a simple approximation as discussed in [106] to convert (4.12) to an posinomial inequality based on the property of geometric inequality that the arithmetic mean is greater than or equal to the geometric mean. Therefore, the right side of (4.12)

becomes

$$1+\sum_{j=1}^{L}\tau p_{p,j\kappa}\beta_{lj\kappa}\geq\prod_{j=1}^{L}(\frac{\tau p_{p,j\kappa}\beta_{lj\kappa}}{\alpha_j})^{\alpha_j}\times(\frac{1}{\alpha_t})^{\alpha_t} \tag{4.13}$$

where $\sum_{j=1}^{L}\alpha_j+\alpha_t=1$. One possibility of computing α_j and α_t is to let

$$\alpha_j=\frac{\tau p_{p,j\kappa}\beta_{lj\kappa}}{1+\sum_{j=1}^{L}\tau p_{p,j\kappa}\beta_{lj\kappa}},\alpha_t=\frac{1}{1+\sum_{j=1}^{L}\tau p_{p,j\kappa}\beta_{lj\kappa}} \tag{4.14}$$

where $p_{p,j\kappa}$ can take any feasible values which satisfy the minimization problem (4.13). Then by replacing the term $1+\sum_{j=1}^{L}\tau p_{p,j\kappa}\beta_{lj\kappa}$ with its lower bound given in (4.13), we can rewrite (4.12) as

$$C12: t_{l\kappa}\prod_{j=1}^{L}(\frac{\tau p_{p,j\kappa}\beta_{lj\kappa}}{\alpha_j})^{-\alpha_j}\times(\alpha_t)^{\alpha_t}\leq 1 \tag{4.15}$$

Similarly, by substituting (2.7), (2.8), (3.19) and using $0\leq t_{l\kappa}\leq 1+\sum_{j=1}^{L}\tau p_{p,j\kappa}\beta_{lj\kappa}$, (4.8c) is equivalent to the following inequality

$$\begin{aligned}C13: &\frac{\gamma_1}{(M-K)\tau p_{p,lk}p_{d,lk}\beta_{llk}^2}[\sum_{i=1}^{L}\sum_{\kappa=1}^{K}\frac{\beta_{ilk}p_{d,i\kappa}}{t_{ik}}(1+\sum_{j\neq l}^{L}\tau p_{p,jk}\beta_{ijk})(1+\sum_{j=1}^{L}\tau p_{p,jk}\beta_{ljk})\\&+1+\sum_{j=1}^{L}\tau p_{p,jk}\beta_{ljk}]+\sum_{i=1,i\neq l}^{L}\frac{\gamma_1\beta_{ilk}^2p_{d,ik}p_{p,lk}}{\beta_{iik}^2p_{d,lk}p_{p,ik}}\leq 1\end{aligned} \tag{4.16}$$

Then, the constraint (4.8b) and (4.8c) can be replaced by (4.10), (4.11), (4.15) and (4.16). We can rewrite the optimization problem (4.8) as

$$\min_{\boldsymbol{p}_p,\boldsymbol{p}_d,\tilde{\boldsymbol{p}}_d,\boldsymbol{t}} P_{total} \tag{4.17a}$$

$$\text{s.t.}\quad C3,C4,C5,C10,C11,C12,C13 \tag{4.17b}$$

where,

$$\boldsymbol{t} \triangleq [t_{11}, t_{12}, \ldots, t_{1K}, \ldots, t_{L1}, t_{L2}, \ldots, t_{LK}] \tag{4.18}$$

Now, the optimization problem (4.17) is a standard GP problem which can be solved by using a standard numerical optimization package as mentioned in the previous subsection.

4.4 Asymptotic Performance under A Very Large Number of BS Antennas

From (3.1), (3.8), (3.13) and (3.19), it can be seen that the SINR lower bounds tend to be infinity for infinite M with fixed pilot and data powers. By following [11, equation (37)], we assume the pilot and data powers of each user are scaled by $\sqrt{M}$, i.e., $E_{p,lk}$=$\sqrt{M}p_{p,lk}$, $E_{u,lk}$=$\sqrt{M}p_{u,lk}$ and $E_{d,lk}$=$\sqrt{M}p_{d,lk}$, for $l = 1, 2, ..., L$ and $k = 1, 2, ..., K$. Then, we have

$$\begin{aligned} &when\ M \to \infty \\ &\gamma_{lk}^{MRC,up}, \gamma_{lk}^{ZF,up} \to \frac{\tau \beta_{llk}^2 E_{p,lk} E_{d,lk}}{1+\tau \sum\limits_{i=1, i\neq l}^{L} \beta_{lik}^2 E_{p,ik} E_{d,ik}} \\ &\gamma_{lk}^{MRC,dn}, \gamma_{lk}^{ZF,dn} \to \frac{\tau \beta_{llk}^2 E_{p,lk} \tilde{E}_{d,lk}}{1+\tau \sum\limits_{i=1, i\neq l}^{L} \beta_{lik}^2 E_{p,ik} \tilde{E}_{d,ik}} \end{aligned} \tag{4.19}$$

which implies that there is nearly no intra-cell interference and uncorrelated noise in massive MU-MIMO systems, leaving only pilot contamination. Moreover, with fixed $E_{p,lk}$, $E_{d,lk}$ and $\tilde{E}_{d,lk}$, the uplink and downlink SINR lower bounds of ZF/ZF and MRC/MRT schemes approach to a constant for a very large value of M.

By using (4.19) into (4.4) and (4.8), respectively, the pilot and data power control problem

with ZF/ZF and that with MRC/MRT have the same formulation as given below,

$$\min_{\boldsymbol{e}_p,\boldsymbol{e}_d,\tilde{\boldsymbol{e}}_d} \sum_{k=1}^{K} (\tau E_{p,lk} + T_1 E_{d,lk} + \zeta_1 T_2 \tilde{E}_{d,lk}) \tag{4.20a}$$

$$\text{s.t.} \quad C14 : \frac{\tau \beta_{llk}^2 E_{p,lk} E_{d,lk}}{1+\tau \sum\limits_{i=1,i\neq l}^{L} \beta_{lik}^2 E_{p,ik} E_{d,ik}} \geq \gamma_1 \tag{4.20b}$$

$$C15 : \frac{\tau \beta_{llk}^2 E_{p,lk} \tilde{E}_{d,lk}}{1+\tau \sum\limits_{i=1,i\neq l}^{L} \beta_{lik}^2 E_{p,ik} \tilde{E}_{d,ik}} \geq \gamma_2 \tag{4.20c}$$

$$C16 : \tau E_{p,lk} + T_1 E_{d,lk} \leq \sqrt{M} P_1 \tag{4.20d}$$

$$C17 : \sum_{k=1}^{K} \tilde{E}_{d,lk} T_2 \leq \sqrt{M} P_2 \tag{4.20e}$$

$$C18 : E_{p,lk} \geq 0, E_{d,lk} \geq 0, \tilde{E}_{d,lk} \geq 0 \tag{4.20f}$$

where

$$\boldsymbol{e}_p \triangleq [E_{p,11}, E_{p,12}, \ldots, E_{p,1K}, \ldots, E_{p,L1}, E_{p,L2}, \ldots, E_{p,LK}] \tag{4.21}$$

$$\boldsymbol{e}_d \triangleq [E_{d,11}, E_{d,12}, \ldots, E_{d,1K}, \ldots, E_{d,L1}, E_{d,L2}, \ldots, E_{d,LK}] \tag{4.22}$$

$$\tilde{\boldsymbol{e}}_d \triangleq [\tilde{E}_{d,11}, \tilde{E}_{d,12}, \ldots, \tilde{E}_{d,1K}, \ldots, \tilde{E}_{d,L1}, \tilde{E}_{d,L2}, \ldots, \tilde{E}_{d,LK}] \tag{4.23}$$

Note that when $M \to \infty$, we have $\sqrt{M} P_1 \to \infty$ and $\sqrt{M} P_2 \to \infty$. Thus the third and forth constraints in (4.20) can be omitted. As a consequence, we can rewrite the optimization problem as

$$\min_{\boldsymbol{e}_p,\boldsymbol{e}_d,\tilde{\boldsymbol{e}}_d} \sum_{k=1}^{K} (\tau E_{p,lk} + T_1 E_{d,lk} + \zeta_1 T_2 \tilde{E}_{d,lk}) \tag{4.24a}$$

$$\text{s.t.} \quad C19 : \frac{1+\tau \sum\limits_{i=1,i\neq l}^{L} \beta_{lik}^2 E_{p,ik} E_{d,ik}}{\tau \beta_{llk}^2 E_{p,lk} E_{d,lk}} \leq \frac{1}{\gamma_1} \tag{4.24b}$$

$$C20 : \frac{1+\tau \sum\limits_{i=1,i\neq l}^{L} \beta_{lik}^2 E_{p,ik} \tilde{E}_{d,ik}}{\tau \beta_{llk}^2 E_{p,lk} \tilde{E}_{d,lk}} \leq \gamma_2 \tag{4.24c}$$

$$C18 \tag{4.24d}$$

It can be seen that (4.24) is a GP problem in which all constraints are posinomial inequalities and can be solved by a standard software package as mentioned earlier.

4.5 Simulation Results and Discussion

Computer simulations are carried out to validate the derived average SINR lower bounds and evaluate the proposed EE power allocation schemes. We consider a two-cell MU-MIMO system ($L = 2$) with a radius of 1000m for each cell. Each BS locates in the cell center serving $K = 3$ users. All users in each cell are distributed uniformly at random with at least a distance of 100m away from the BS. The large-scale channel fading is modeled with $\beta_k = z_k/(r_k/r_h)^v$, where z_k represents a log-normal random variable with standard deviation σ, r_k is the distance between the k-th user and the BS and v means the path loss exponent. Following the parameter setting in [1], we choose σ = 8dB and v=3.8. Throughout the simulation, the normalized additive Gaussian noise with zero mean and unit variance is assumed.

Suppose that the orthogonal frequency-division multiplexing (OFDM) signal is transmitted. According to LTE standard [1], we choose an OFDM symbol interval of $T_s = 71.4\mu s$, a subcarrier spacing of $\Delta f = 15kHz$ and a coherent time interval $T_c = 1ms$. In turn, we

can obtain the useful symbol duration $T_u = 66.7\mu s$, the guard interval length $T_g = 4.7\mu s$ and the total number of symbols in each coherent time interval as $T = (T_c/T_s)T_u/T_g = 196$ symbols. To minimize the overhead of pilot symbols to the minimum level, we choose the smallest amount of training $\tau = K$. The number of symbols for uplink transmission and that of downlink data transmission are assumed to be the same in one coherent time interval, namely $T_1 = T_2 = (T - \tau)/2 = 96$ symbols. In the optimization problem, the weight ζ is assumed to be one. The same target SINR and power constraint are applied for both uplink and downlink transmission. The CVX standard package [105] is used throughout the simulation to solve the GP problem.

To show the tightness of the lower bounds of SINR, Fig. 4.1 compares the simulation results for the original SINR and the derived lower bounds of user 1 in cell 1. Here, equal pilot and data power allocation among all users as in paper [11] is applied with $p_{p,lk} = p_{u,lk} = p_{d,lk}$ for any $k \in K$ and $l \in L$. Then for the fixed scaled pilot-data power we assume $E_{p,lk} = E_{d,lk} = \tilde{E}_{d,lk}$ for any $k \in K$ and $l \in L$. We can see that the derived lower bounds are tight in all cases even for a large number of BS antennas and the uplink and downlink transmission show nearly the same SINR performance in both ZF/ZF and MRC/MRT situations. The MU-MIMO system with ZF/ZF shows a better SINR performance than the system with the MRC/MRT. Moreover, when M becomes large, both uplink and downlink SINRs start to saturate due to the pilot contamination. From the curves with fixed scaled pilot and data powers, it can be observed that the SINR performances of both ZF/ZF and MRC/MRT approach to a constant as M gets very large, which is consistent with the theoretical analysis.

Fig. 4.2 shows the total uplink power, which includes both pilot and uplink data powers,

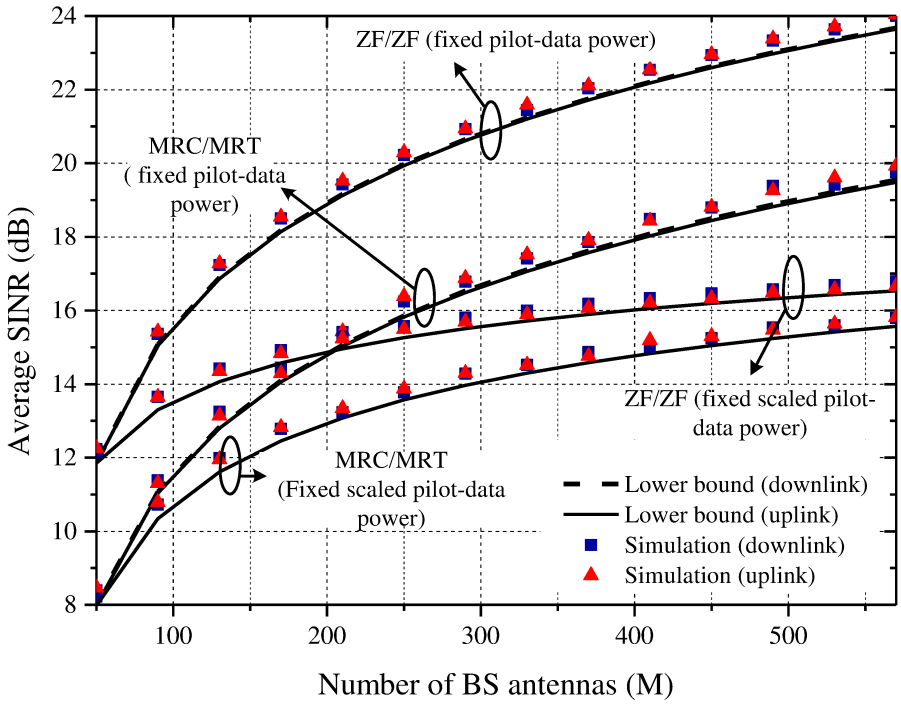

Figure 4.1: Average SINR versus the number of BS antennas

and the downlink power for total transmit power minimization scheme in multi-cell MU-MIMI systems with SINR threshold $\gamma_1 = \gamma_2 = 5dB$ and $\gamma_1 = \gamma_2 = 15dB$. The uplink power includes the power of both pilot and uplink data signal. All the powers are normalized according to the noise power. It can be clearly seen that both uplink and downlink powers decrease as M grows, showing that the use of massive MU-MIMO can save a great deal of transmit power. Note that for the system with MRC/MRT, when the required SINR is chosen as $15dB$, there is no solution when $M \leq 50$ because of the significant crosstalk interference. In low target SINR region, MRC/MRT performs almost as well as the ZF based scheme. For target $15dB$ SINR, ZF/ZF saves about $3dB$ in total uplink and downlink power than MRC/MRT under a large value of M. When M approaches to infinity, from section 4.4 we can calculate the scaled pilot and data powers as $E_{p,k} = 9.04dB, E_{d,k} = \tilde{E}_{d,k} = -10.17dB$

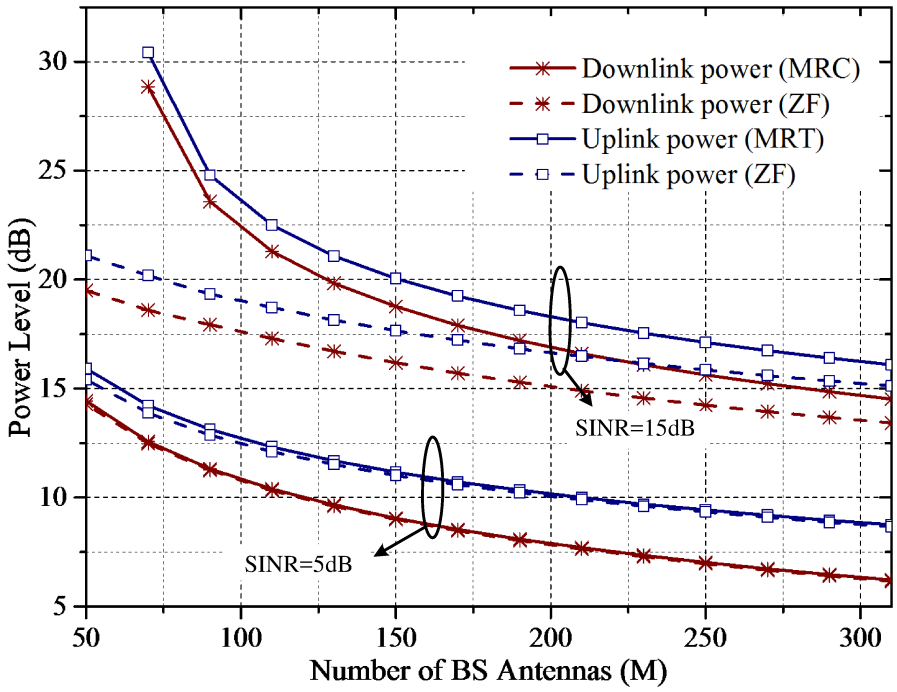

Figure 4.2: Pilot-data power allocation versus number of BS antennas

for $5dB$ target SINR and $E_{p,k} = 18.56dB, E_{d,k} = \tilde{E}_{d,k} = -9.23dB$ for $15dB$ target SINR. Here the pilot and data powers have been scaled by multiplying $\sqrt{M}$.

In order to demonstrate the advantage of our proposed power allocation algorithm as compared with a simple equal pilot-data power allocation where the pilot and data signal have the same power $p_{u,multi}$ for all users as in [11], we define the percentage of the total power saving as

$$\frac{KL(\tau + T_1 + \zeta T_2)p_{u,multi} - \sum_{l=1}^{L}\sum_{k=1}^{K}(p_{p,lk}\tau + p_{u,lk}T_1 + \zeta p_{d,lk}T_2)}{K(\tau + T_1 + \zeta T_2)p_{u,multi}} \tag{4.25}$$

where $p_{u,multi}$ for ZF/ZF and MRC/MRT schemes can be easily found by setting $p_{p,lk} = p_{u,lk} = p_{d,lk} = p_{u,multi}$ in the previous optimization problems (4.7) and (4.17). From Fig. 4.3,

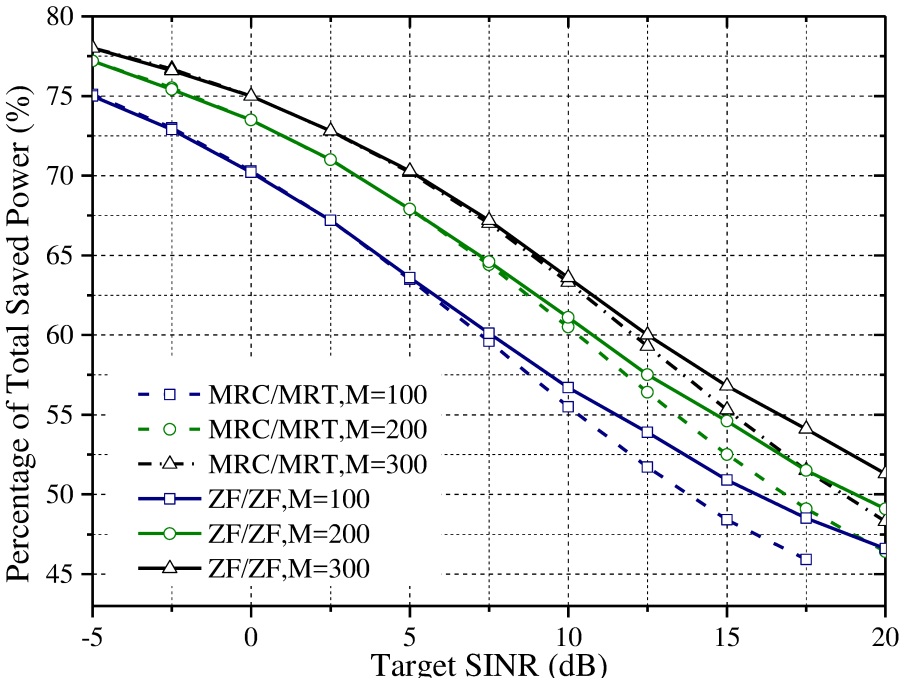

Figure 4.3: Percentage of power saving versus target SINRs

we can see that more than 75% total power can be saved for ZF/ZF and MRC/MRT in low target SINR region, depending on the number of BS antennas and the number of total users. As the required per-user SINR increases, the percentage of power saving decreases. Note that the benefit of deploying a very large number of BS antennas tends to become marginal, since the ultimate SINR performance is limited by the interference, channel estimation error and transmit power constraints. Moreover, for the case of $M = 100$, there is no solution for the equal pilot-data power allocation scheme when the target SINR is larger than $15dB$. From the above discussion, the ZF/ZF scheme always gives a better performance than the MRC/MRT scheme does. However, when M becomes very large which means a huge size of estimated channel coefficient matrix $\hat{\boldsymbol{G}}_{\boldsymbol{li}}$, calculating the inverse of $\hat{\boldsymbol{G}}_{\boldsymbol{li}}$ will be a computational burden which needs complicated processing circuits. Compared with ZF/ZF scheme, the MRC/MRT

scheme with processing matrix equal to the conjugate transpose of $\hat{\boldsymbol{G}}_{\boldsymbol{li}}$ is much easier to implement in the case of a large number of antennas.

4.6 Conclusion

In this chapter, we have investigated the pilot and data power allocation for EE communications in multi-cell MU-MIMO systems with an objective of minimizing the total uplink and downlink transmit power under the per-user SINR requirement and power consumption constraint. The proposed schemes take into account the MRC and ZF detectors in the uplink transmission together with MRT and ZF precoder in the downlink transmission. In order to simplify the original optimization problems, the SINR lower bounds derived in the previous chapter are used in the power allocation algorithms instead of the true SINR expressions. Then, in the MRC/MRT situation, the non-convex optimization problems are converted to a standard GP problem to facilitate their solution based on inequality substitution. For the ZF scheme, geometric inequality is used to approximate the original non-convex optimization to the GP problem. The very large number of BS systems situation is also discussed for multi-cell MU-MIMO systems. Finally, numerical simulation results have confirmed the tightness of the derived per-user average SINR lower bounds and the advantage of the proposed power allocation schemes.

Chapter 5

Joint Pilot-Data Power Allocation Based on Total EE Maximization

5.1 Introduction

Excessive power usage in MIMO networks is a crucial issue for mobile operators since the explosive growth of wireless services contributes largely to the worldwide carbon footprint [106]. As such, significant efforts have been devoted to improving the SE and EE of MIMO communication systems over the past decade, resulting in energy efficient power allocation technologies.

Besides EE based power control methods, the SE based power control in MIMO systems is also very popular and has already been discussed in many papers. For example, the authors of [107] considered the noncooperative multi-cell multicast MIMO network under perfect and imperfect CSI. The authors in [109] studied the joint pilot and data power allocation problems in single cell uplink massive MIMO systems for the case of maximizing the weighted minimum SE and the sum SE. In [110], the authors studied the pilot power allocation with the least squares (LS) and MMSE methods in multi-cell massive MIMO systems. The authors in [111] investigated the pilot and data power allocation based on the lower bound on the uplink capacity for Rayleigh fading channels with maximum ratio

detection. In this thesis, we aim to investigate the energy-efficient power control schemes for MU-MIMO systems. Later in this chapter, we will compare our proposed EE based power allocation schemes with the SE based ones.

As discussed in [11] and [73], the EE of a wireless system is defined as the ratio of the total SE to the total power consumption p_{total}. As such, the total EE of both uplink and downlink of a TDD multi-cell MU-MIMO can be defined as

$$EE = \frac{\sum_{l=1}^{L}\sum_{k=1}^{K}(\frac{T_1+T_2}{T}\frac{T_1}{T_2}E\{R_{lk}\} + \zeta_2\frac{T_1+T_2}{T}\frac{T_2}{T_1}E\{\tilde{R}_{lk}\})}{P_{total}} \tag{5.1}$$

where R_{lk} and $\tilde{R}_{lk}$ denote the uplink and downlink sum rates which are defined as $R_{lk} = \log_2(1+\gamma_{lk})$ and $\tilde{R}_{lk} = \log_2(1+\tilde{\gamma}_{lk})$, respectively, T_1 and T_2 denote the number of uplink data symbols and that of downlink counter parts, respectively, as shown in Fig. 2.2, and ζ_2 is the weighting coefficient.

Based on the SINR lower bounds derived in chapter 3, we can find the lower bounds for uplink and downlink achievable rates, and use such average sum rate lower bounds instead of the true values to construct the optimization problems. Since $f(x) = \log_2(1+x)$ is a monotonically increasing function, the lower bounds of the uplink achievable rate can be obtained as $E\{R_{lk}^{MRC}\} \geq \log_2(1+\gamma_{lk}^{MRC,up})$ and $E\{R_{lk}^{ZF}\} \geq \log_2(1+\gamma_{lk}^{ZF,up})$ when MRC and ZF receivers are used respectively. Similarly, the lower bound on the downlink achievable rate can be found as $E\{\tilde{R}_{lk}^{MRT}\} \geq \log_2(1+\tilde{\gamma}_{lk}^{MRT,dn})$ or $E\{R_{lk}^{ZF}\} \geq \log_2(1+\gamma_{lk}^{ZF,dn})$ when MRT or ZF precoder is used.

In Chapter 4, we have developed joint pilot-data power allocation schemes based on the first optimization framework, namely, the total transmit power minimization. In this

chapter, based on the EE defined in (5.1) and by following the second framework, namely the total EE maximization, we will develop two novel pilot-data power control algorithms for multi-cell MU-MIMO systems with an objective of jointly maximizing the total uplink and downlink EE under BS and per-user power constraints. As discussed in section 4.1, unlike most of the previous works with equal pilot and power allocation schemes i.e. [11] [57] [58], we will consider a more practical scenario, where the transmit power of pilot or data symbols for different users can be different. Moreover, instead of considering uplink and downlink power allocation separately [48]-[66], we will address the joint pilot-data power control problem for both uplink and downlink transmissions in one optimization problem. Besides the joint pilot-data power allocation for conventional MU-MIMO systems, massive MU-MIMO case will also be studied by assuming infinite antennas at BS. The proposed power control methods take into consideration the MRC and ZF detectors in the uplink transmission together with MRT and ZF precoder in the downlink transmission. In order to simplify the original optimization problems, the lower bounds for uplink and downlink achievable rates stated above are used in the power allocation algorithms instead of the true sum rate expressions. In chapter 4, we discussed the first framework for energy-efficient power control in MIMO systems. In the simulation, we will compare the pilot and data power allocation schemes based on the two frameworks, proposed in the previous chapter and this chapter, with the SE maximization scheme in [109].

5.2 Total EE Maximization with MRC Receiver and MRT Precoder

The power allocation problem which maximizes the total EE while meeting the power consumption requirements as specified by the derived average SINR lower bounds for MRC

receiver and MRT precoder can be formulated as

$$\max_{\boldsymbol{p}_p,\boldsymbol{p}_u,\boldsymbol{p}_d} \frac{R_{total}^{MRC/MRT}}{P_{total}} \tag{5.2a}$$

$$\text{s.t.} \quad C3, C4, C5 \tag{5.2b}$$

In the objective function of (5.2), the total weighted sum rate is given by

$$R_{total}^{MRC/MRT} \triangleq \sum_{l=1}^{L}\sum_{k=1}^{K} [a_1 \log_2(1+\gamma_{lk}^{MRC,up}) + \zeta_2 a_2 \log_2(1+\gamma_{lk}^{MRT,dn})] \tag{5.3}$$

where $a_1 \triangleq \frac{T_1+T_2}{T}\frac{T_1}{T_2}$ and $a_2 \triangleq \frac{T_1+T_2}{T}\frac{T_2}{T_1}$. Note that (5.2) is a non-convex fractional optimization problem which is very difficult to solve directly. To overcome this difficulty, we convert (5.2) to an equivalent non-fractional problem by following the Dinkelbach's method as discussed in [112] and [113]. Letting $\eta = \frac{R_{total}^{MRC/MRT}}{P_{total}}$ be the maximum EE in problem (5.2), we have the following equivalent optimization problem when $f(\eta) = 0$.

$$f(\eta) \triangleq \min_{\boldsymbol{p}_p,\boldsymbol{p}_u,\boldsymbol{p}_d} \eta P_{total} - R_{total}^{MRC/MRT} \tag{5.4a}$$

$$\text{s.t.} \quad C3, C4, C5 \tag{5.4b}$$

By following the Dinkelbach's method [112] and [113], the optimal solution to problem (5.4) can be obtained if we can find η such that $f(\eta) = 0$. In order to simplify the above optimization problem, we introduce a new set of variables $x_{u,lk}$ and $x_{d,lk}$ ($l = 1, 2, \ldots, L;\ k = 1, 2, \ldots, K$), with the constraints $0 \leq x_{u,lk} \leq \tilde{\gamma}_{u,lk}^{MRC}$ and $0 \leq x_{d,lk} \leq \tilde{\gamma}_{d,lk}^{MRC}$. Then we can

rewrite the above optimization problem as

$$\min_{\boldsymbol{p}_p,\boldsymbol{p}_u,\boldsymbol{p}_d,\boldsymbol{x_u},\boldsymbol{x_d}} \eta P_{total} - \sum_{l=1}^{L}\sum_{k=1}^{K}[a_1\log_2(1+x_{u,lk}) + \zeta_2 a_2\log_2(1+x_{d,lk})] \tag{5.5a}$$

$$\text{s.t.} \quad C14: x_{u,lk} \leq \tilde{\gamma}_{u,lk}^{MRC} \tag{5.5b}$$

$$C15: x_{d,lk} \leq \tilde{\gamma}_{d,lk}^{MRC} \tag{5.5c}$$

$$C16: x_{u,lk} \geq 0 \tag{5.5d}$$

$$C17: x_{d,lk} \geq 0 \tag{5.5e}$$

$$C3, C4, C5 \tag{5.5f}$$

where

$$\boldsymbol{x}_u \triangleq [x_{u,11}, x_{u,12}, \ldots, x_{u,1K}, \ldots, x_{u,L1}, x_{u,L2}, \ldots, x_{u,LK}] \tag{5.6}$$

$$\boldsymbol{x}_d \triangleq [x_{d,11}, x_{d,12}, \ldots, x_{d,1K}, \ldots, x_{d,L1}, x_{d,L2}, \ldots, x_{d,LK}] \tag{5.7}$$

Similar to the derivation of (4.5), by substituting (2.7), (2.8) and (3.1) into (5.5b), we

can transform the first constraint in problem (5.5) as

$$
\begin{aligned}
C18: \frac{x_{u,lk}}{(M-1)\tau p_{u,lk} p_{p,lk} \beta_{llk}^2} (& \sum_{\kappa=1,\kappa\neq k}^{K} p_{u,l\kappa}\beta_{ll\kappa} + 1 + \sum_{j=1}^{L} \tau p_{p,jk}\beta_{ljk} \\
+ \sum_{i=1,i\neq l}^{L} \sum_{\kappa=1,\kappa\neq k}^{K} & p_{u,i\kappa}\beta_{li\kappa} + \sum_{j=1}^{L} \tau p_{p,jk}\beta_{ljk} \sum_{\kappa=1,\kappa\neq k}^{K} p_{u,l\kappa}\beta_{ll\kappa} \\
+ \sum_{j=1}^{L} \tau p_{p,jk}\beta_{ljk} \sum_{i=1,i\neq l}^{L} \sum_{\kappa=1,\kappa\neq k}^{K} & p_{u,i\kappa}\beta_{li\kappa} + \sum_{i=1}^{L} p_{u,ik}\beta_{lik} \\
+\tau \sum_{i=1}^{L} p_{u,ik}\beta_{lik} \sum_{j=1,j\neq i}^{L} & p_{p,jk}\beta_{ljk}) + x_{u,lk} \sum_{i=1,i\neq l}^{L} \frac{\beta_{lik}^2 p_{u,ik} p_{p,ik}}{\beta_{llk}^2 p_{u,lk} p_{p,lk}} \leq 1
\end{aligned}
\tag{5.8}
$$

Note that the left side of the above inequality is posynomial. Similarly, the second constraint in problem (5.5) can also be converted to a posynomial inequality by substituting (2.7), (2.8) and (3.18) into (5.5c), resulting in

$$
\begin{aligned}
C19: \frac{x_{d,lk}}{M p_{d,lk}} \sum_{\kappa=1,\kappa\neq k}^{K} & p_{d,l\kappa} + \frac{x_{d,lk}}{(M-1) p_{d,lk} \tau p_{p,lk} \beta_{llk}^2} (\beta_{llk} \sum_{\kappa=1}^{K} p_{d,l\kappa} \\
+\tau \beta_{llk} \sum_{\kappa=1}^{K} p_{d,l\kappa} \sum_{j\neq l}^{L} & p_{p,jk}\beta_{ljk} + \sum_{i\neq l}^{L} \sum_{\kappa=1}^{K} p_{d,i\kappa}\beta_{ilk} + 1 \\
+\tau \sum_{j=1}^{L} p_{p,jk}\beta_{ljk} \sum_{i\neq l}^{L} \sum_{\kappa=1}^{K} & p_{d,i\kappa}\beta_{ilk} + \tau \sum_{j=1}^{L} p_{p,jk}\beta_{ljk}) \leq 1
\end{aligned}
\tag{5.9}
$$

After replacing (5.5b) with (5.8), and replacing (5.5c) with (5.9), all the constraints in problem (5.5) are posynomial inequalities, each with the form of a posynomial less than or equal to a constant value. The optimization problem (5.5) can then be treated as a generalized geometric programming (GGP) problem which is a combination of a standard GP and several additive logarithm terms of generalized posynomial [99, section 7.2]. Since all the variables in (5.5) are nonnegative, the constraints can be converted to convex through a logarithmic transform of the variables. We replace the original variables $x_{u,lk}$, $x_{d,lk}$, $p_{p,lk}$, $p_{u,lk}$ and $p_{d,lk}$ with their logarithmic form for all values of $k \in K$ and $l \in L$, then the

variables become $y_{u,lk} = \ln(x_{u,lk})$, $y_{d,lk} = \lg(x_{d,lk})$, $p'_{p,lk} = \ln(p_{p,lk})$, $p'_{u,lk} = \ln(p_{u,lk})$ and $p'_{d,lk} = \ln(p_{d,lk})$. By substituting these new variables into (5.5), all its constraints become convex and the objective function (5.5a) becomes

$$\min_{\boldsymbol{p'}_p, \boldsymbol{p'}_u, \boldsymbol{p'}_d, \boldsymbol{y}_u, \boldsymbol{y}_d} \eta P'_{total} + g(\boldsymbol{y}_u, \boldsymbol{y}_d) \tag{5.10}$$

where

$$\boldsymbol{y}_u \triangleq [y_{u,11}, y_{u,12}, \ldots, y_{u,1K}, \ldots, y_{u,L1}, y_{u,L2}, \ldots, y_{u,lk}] \tag{5.11}$$

$$\boldsymbol{y}_d \triangleq [\tilde{y}_{d,11}, \tilde{y}_{d,12}, \ldots, \tilde{y}_{d,1K}, \ldots, \tilde{y}_{d,L1}, \tilde{y}_{d,L2}, \ldots, y_{d,lk}] \tag{5.12}$$

$$\boldsymbol{p'}_p \triangleq [p'_{p',11}, p'_{p,12}, \ldots, p'_{p,1K}, \ldots, p'_{p,L1}, p'_{p,L2}, \ldots, p'_{p,LK}] \tag{5.13}$$

$$\boldsymbol{p'}_u \triangleq [p'_{u,11}, p'_{u,12}, \ldots, p'_{u,1K}, \ldots, p'_{u,L1}, p'_{u,L2}, \ldots, p'_{u,LK}] \tag{5.14}$$

$$\boldsymbol{p'}_d \triangleq [p'_{d,11}, p'_{d,12}, \ldots, p'_{d,1K}, \ldots, p'_{d,L1}, p'_{d,L2}, \ldots, p'_{d,LK}] \tag{5.15}$$

Moreover, in (5.10) we have

$$P'_{total} \triangleq \sum_{l=1}^{L} \sum_{k=1}^{K} [exp(p'_{p,lk})\tau + exp(p'_{u,lk})T_1 + \zeta_1 exp(p'_{d,lk})T_2] \tag{5.16}$$

$$\begin{aligned} g(\mathbf{y_u}, \mathbf{y_d}) &\triangleq -\sum_{l=1}^{L} \sum_{k=1}^{K} \{[a_1 \log_2[1 + \exp(y_{u,lk})] + \zeta_2 a_2 \log_2[1 + \exp(y_{d,lk})]\} \\ &= \sum_{l=1}^{L} \sum_{k=1}^{K} [a_1 \log_2 \tfrac{1}{1+\exp(y_{u,lk})} + \zeta_2 a_2 \log_2 \tfrac{1}{1+\exp(y_{d,lk})}] \end{aligned} \tag{5.17}$$

Now, we use the FrankWolfe (FW) iterative procedure to solve the above problem. Since $\log_2 \frac{1}{1+\exp(\bullet)}$ is concave, it is easy to see that $g(\boldsymbol{y}_u, \boldsymbol{y}_d)$ is also concave. Then, by following

the first-order Taylor series expansion, we have $f(x,y) \leq f(x_0,y_0) + f_x(x_0,y_0)(x-x_0) + f_y(x_0,y_0)(y-y_0)$. Assuming that $[\boldsymbol{y_u^{(\kappa)}}, \boldsymbol{y_d^{(\kappa)}}]$ is a feasible solution to the problem, we approximate the upper bound of $g(\boldsymbol{x}, \tilde{\boldsymbol{x}})$ by its first-order Taylor series expansion at $[\boldsymbol{y_u^{(\kappa)}}, \boldsymbol{y_d^{(\kappa)}}]$ [114] [115] as

$$g(\boldsymbol{y}_u, \boldsymbol{y}_d) \leq g(\boldsymbol{y}_u^{(\kappa)}, \boldsymbol{y}_d^{(\kappa)}) - \sum_{l=1}^{L}\sum_{k=1}^{K} [a'_1 \frac{y_{u,lk} - y_{u,lk}^{(\kappa)}}{1+\exp(y_{u,lk}^{(\kappa)})} + \zeta_2 a'_2 \frac{y_{d,lk} - y_{d,lk}^{(\kappa)}}{1+\exp(y_{d,lk}^{(\kappa)})}] \tag{5.18}$$

where $a'_1 \triangleq \frac{a_1}{\ln 2}$ and $a'_2 \triangleq \frac{a_2}{\ln 2}$. Based on (5.18), we propose an iterative algorithm to find the optimal solution. After getting the $(\kappa-1)$-th feasible solution $[\boldsymbol{y_u^{(\kappa-1)}}, \boldsymbol{y_d^{(\kappa-1)}}]$, we can obtain the feasible solution at the κ-th iteration by solving the following problem,

$$\begin{aligned} \min_{\boldsymbol{p'}_p, \boldsymbol{p'}_u, \boldsymbol{p'}_d, \boldsymbol{y}_u, \boldsymbol{y}_d} \; & f^{(\kappa)} \triangleq \eta P'_{total} + g(\boldsymbol{y_u^{(\kappa-1)}}, \boldsymbol{y_d^{(\kappa-1)}}) \\ & - \sum_{l=1}^{L}\sum_{k=1}^{K} [a'_1 \frac{y_{u,lk} - y_{u,lk}^{(\kappa-1)}}{1+\exp(y_{u,lk}^{(\kappa-1)})} + \zeta_2 a'_2 \frac{y_{d,lk} - y_{d,lk}^{(\kappa-1)}}{1+\exp(y_{d,lk}^{(\kappa-1)})}] \end{aligned} \tag{5.19a}$$

$$\text{s.t.} \quad C3', C4', C5', C14', C15' \tag{5.19b}$$

Here, C3', C4', C5', C14', C15' represent the constraints of C3, C4, C5, C14, C15, respectively, in the logarithmic transform domain. This iteration continues until no further improvement on the objective function can be achieved. We summarize the algorithm as Algorithm 1 in table 5.1.

The convergence of the inner loop in the above algorithm can be proved as follows.

Proposition 5: Proof of the convergence of inner loop in Algorithm 1

Proof: Let $P'^{(\kappa)}_{total}$ and $P'^{(\kappa-1)}_{total}$ be the value of P'_{total} at iterations κ and $\kappa-1$ for solving

Algorithm 1: The proposed iterative algorithm

Initialization
Set iteration indix $i = 0$, convergence tolerance $\delta > 0$ and EE parameter $\eta^{(0)} = 0$
Choose initial value $[\boldsymbol{y}_u^{(\mathbf{0})}, \boldsymbol{y}_d^{(\mathbf{0})}]$;
Outer loop: **repeat**
  Choose the initial solution $[\boldsymbol{y}_u^{(i)}, \boldsymbol{y}_d^{(i)}] = [\boldsymbol{y}_u^{(i-1)}, \boldsymbol{y}_d^{(i-1)}]$;
  Compute $f^{(i)}$;
  Set $i = i + 1$ and $\kappa = 0$;
  Inner loop: **repeat**
    Set $\kappa = \kappa + 1$;
    Find the optimal solution $[\boldsymbol{y}_u^{(\boldsymbol{\kappa})}, \boldsymbol{y}_d^{(\boldsymbol{\kappa})}], p'_{p,lk}, p'_{u,lk}$ and $p'_{d,lk}$ to problem (5.19) for given $[\boldsymbol{y}_u^{(\boldsymbol{\kappa-1})}, \boldsymbol{y}_d^{(\boldsymbol{\kappa-1})}]$;
    Compute $f^{(\kappa)}$;
  until $\left|f^{(\kappa)} - f^{(\kappa-1)}\right| < \delta$;
  Calculate the corresponding optimal R_{total} and P_{total} based on the obtained solution of inner loop;
  Update $\eta^{(i)} = R_{total}/P_{total}$;
until $\left|\eta^{(i)} - \eta^{(i-1)}\right| < \delta$;
Output optimal solution for $p_{p,lk}$, $p_{u,lk}$ and $p_{d,lk}$.

(5.19), respectively. As $[\boldsymbol{y}_u^{(\kappa)}, \boldsymbol{y}_d^{(\kappa)}]$ is feasible to (5.18), we have the relation as given in (5.20).

$$\begin{aligned}
&\eta P'^{(\kappa)}_{total} + g(\boldsymbol{y}_u^{(\kappa)}, \boldsymbol{y}_d^{(\kappa)}) \\
&\leq \eta P'^{(\kappa)}_{total} + g(\boldsymbol{y}_u^{(\kappa-1)}, \boldsymbol{y}_d^{(\kappa-1)}) - \sum_{l=1}^{L}\sum_{k=1}^{K}\left[a'_1 \frac{y_{u,lk}^{(\kappa)} - y_{u,lk}^{(\kappa-1)}}{1+\exp(y_{u,lk}^{(\kappa-1)})} + \zeta_1 a'_2 \frac{y_{d,lk}^{(\kappa)} - y_{d,lk}^{(\kappa-1)}}{1+\exp(y_{d,lk}^{(\kappa-1)})}\right] \\
&\leq \eta P'^{(\kappa-1)}_{total} + g(\boldsymbol{y}_u^{(\kappa-1)}, \boldsymbol{y}_d^{(\kappa-1)}) - \sum_{l=1}^{L}\sum_{k=1}^{K}\left[a'_1 \frac{y_{u,lk}^{(\kappa-1)} - y_{u,lk}^{(\kappa-1)}}{1+\exp(y_{u,lk}^{(\kappa-1)})} + \zeta_1 a'_2 \frac{y_{d,lk}^{(\kappa-1)} - y_{d,lk}^{(\kappa-1)}}{1+\exp(y_{d,lk}^{(\kappa-1)})}\right] \\
&= \eta P'^{(\kappa-1)}_{total} + g(\boldsymbol{y}_u^{(\kappa-1)}, \boldsymbol{y}_d^{(\kappa-1)})
\end{aligned} \tag{5.20}$$

which proves that the proposed iterative algorithm is monotonically decreasing. Considering that the objective function is lower bounded, the convergence of the inner loop in Algorithm 1 is ensured.

Regarding the proof of the convergence of the outer loop, the readers are referred to [95]. It should be pointed out that despite the guaranteed convergence of Algorithm 1, its solution

may not be the globally optimum because of the non-convex nature of the joint optimization problem.

5.3 Total EE Maximization with ZF Receiver/Precoder

The power allocation problem with ZF used in both receiver and precoder of BS, which maximizes the weighted total EE subject to power constraints, can be formulated as

$$\max_{\boldsymbol{p}_p,\boldsymbol{p}_u,\boldsymbol{p}_d} \frac{R_{total}^{ZF}}{P_{total}} \tag{5.21a}$$

$$\text{s.t.} \qquad C3, C4, C5 \tag{5.21b}$$

with

$$R_{total}^{ZF} \triangleq \sum_{l=1}^{L}\sum_{k=1}^{K}[a_1 \log_2(1+\tilde{\gamma}_{lk}^{ZF,up}) + \zeta_2 a_2 \log_2(1+\gamma_{lk}^{ZF,dn})] \tag{5.22}$$

Similar to the discussion in the previous section, in order to simplify (5.21), we introduce a new set of variables $z_{u,lk}$ and $z_{d,lk}$ $(l = 1, 2, \ldots, L; k = 1, 2, \ldots, L)$, with the constraints $0 \leq z_{u,lk} \leq \tilde{\gamma}_{lk}^{ZF,up}$ and $0 \leq z_{d,lk} \leq \gamma_{lk}^{ZF,dn}$. Then we can rewrite the above maximization problem as the following minimization counterpart,

$$\min_{\boldsymbol{p}_p,\boldsymbol{p}_u,\boldsymbol{p}_d,\boldsymbol{z}_u,\boldsymbol{z}_d} f(\eta) \tag{5.23a}$$

$$\text{s.t.} \qquad C10 : z_{u,lk} \leq \gamma_{lk}^{ZF,up} \tag{5.23b}$$

$$C18 : z_{d,lk} \leq \gamma_{lk}^{ZF,dn} \tag{5.23c}$$

$$C19 : z_{u,lk} \geq 0 \tag{5.23d}$$

$$C20 : z_{d,lk} \geq 0 \tag{5.23e}$$

$$C3, C4, C5 \tag{5.23f}$$

where,

$$\boldsymbol{z}_u \triangleq [z_{u,11}, z_{u,12}, \ldots, z_{u,1K}, \ldots, z_{u,L1}, z_{u,L2}, \ldots, z_{u,LK}], \tag{5.24}$$

$$\boldsymbol{z}_d \triangleq [z_{d,11}, z_{d,12}, \ldots, z_{d,1K}, \ldots, z_{d,L1}, z_{d,L2}, \ldots, z_{d,LK}], \tag{5.25}$$

and $f(\eta)$ is defined in (5.4a).

By substituting (2.7), (2.8) and (3.8) into (5.23b), and performing some derivation, we have

$$\begin{aligned} &\frac{1+\sum_{j=1}^{L} \tau p_{p,lk} \beta_{llk}}{(M-K)\tau p_{p,lk} p_{u,lk} \beta_{llk}^2} [\sum_{i=1}^{L} \sum_{\kappa=1}^{K} p_{u,i\kappa} \frac{\beta_{li\kappa}(1+\sum_{j\neq i}^{L} \tau p_{p,j\kappa} \beta_{lj\kappa})}{1+\sum_{j=1}^{L} \tau p_{p,j\kappa} \beta_{lj\kappa}} + 1] \\ &+ \sum_{i=1, i\neq l}^{L} \frac{p_{u,ik}}{p_{u,lk}} \frac{\beta_{lik}^2 p_{p,ik}}{\beta_{llk}^2 p_{p,lk}} \leq \frac{1}{z_{u,lk}} \end{aligned} \tag{5.26}$$

The left side of (5.26) is the same as that of (4.9). Hence, by following the same method as discussed in chapter 4 and using the property of geometric inequality, it can be verified that (5.26) is equivalent to the three inequalities C11, C12 and C21 below,

$$\begin{aligned} C21 : &\frac{z_{u,lk}}{(M-K)\tau p_{p,lk} p_{u,lk} \beta_{llk}^2} [\sum_{i=1}^{L} \sum_{\kappa=1}^{K} \frac{\beta_{li\kappa} p_{u,i\kappa}}{t_{l\kappa}} (1 + \sum_{j\neq i}^{L} \tau p_{p,j\kappa} \beta_{lj\kappa}) \\ &(1 + \sum_{j=1}^{L} \tau p_{p,jk} \beta_{ljk}) + 1 + \sum_{j=1}^{L} \tau p_{p,jk} \beta_{ljk}] + \sum_{i=1, i\neq l}^{L} \frac{\beta_{lik}^2 p_{p,ik} p_{u,ik} z_{u,lk}}{\beta_{llk}^2 p_{p,lk} p_{u,lk}} \leq 1 \end{aligned} \tag{5.27}$$

Similarly, the second constraint in problem (5.23) can also be converted to a posynomial

inequality by substituting (2.7), (2.8) and (3.25) to (5.23c), resulting in

$$\begin{aligned} C22: \frac{z_{u,lk}}{(M-K)\tau p_{p,lk} p_{d,lk} \beta_{llk}^2} [\sum_{i=1}^{L} \sum_{\kappa=1}^{K} \frac{\beta_{ilk} p_{d,i\kappa}}{t_{ik}} (1 + \sum_{j \neq l}^{L} \tau p_{p,jk} \beta_{ijk}) \\ (1 + \sum_{j=1}^{L} \tau p_{p,jk} \beta_{ljk}) + 1 + \sum_{j=1}^{L} \tau p_{p,jk} \beta_{ljk}] + \sum_{i=1, i \neq l}^{L} \frac{\beta_{ilk}^2 p_{d,ik} p_{p,lk} z_{u,lk}}{\beta_{iik}^2 p_{d,lk} p_{p,ik}} \leq 1 \end{aligned} \tag{5.28}$$

Then we can rewrite the optimization problem (5.23) as

$$\min_{\boldsymbol{p}_p, \boldsymbol{p}_d, \tilde{\boldsymbol{p}}_d, \boldsymbol{z}, \tilde{\boldsymbol{z}}} f(\eta) \tag{5.29a}$$

$$\text{s.t. } C3, C4, C5, C11, C12, C19, C20, C21, C22 \tag{5.29b}$$

It can be seen that (5.29) is a GGP problem with all constraints being posinomial inequalities, which can be converted to a convex problem through a logarithmic transform of the variables. Finally, similar to problem (5.10), we can solve (5.29) by using FW iterative procedure as summarized in Algorithm 1.

5.4 Asymptotic Performance under A Very Large Number of BS Antennas

It has been proved in section 4.3 that with constant pilot and data powers, the SINR lower bounds tend to be infinity for infinite M. By using the SINR lower bounds in (4.19), the joint pilot-data power control optimization problem based on EE maximization scheme with MRC/MRT and that with ZF/ZF can both be written as

$$\begin{aligned} &\max_{\boldsymbol{e}_p, \boldsymbol{e}_d, \tilde{\boldsymbol{e}}_d} \frac{R}{\sum_{k=1}^{K} (\tau E_{p,lk} + T_1 E_{u,lk} + \zeta_1 T_2 \tilde{E}_{d,lk})} \\ &\text{s.t.} \qquad C25, C26, C27 \end{aligned} \tag{5.30}$$

where

$$R \triangleq \sum_{l=1}^{L}\sum_{k=1}^{K}[a_1\log_2(1+\frac{\tau\beta_{llk}^2 E_{p,lk}E_{u,lk}}{1+\tau\sum\limits_{i=1,i\neq l}^{L}\beta_{lik}^2 E_{p,ik}E_{u,ik}}) \\ +\zeta_2 a_2\log_2(1+\frac{\tau\beta_{llk}^2 E_{p,lk}E_{d,lk}}{1+\tau\sum\limits_{i=1,i\neq l}^{L}\beta_{lik}^2 E_{p,ik}E_{d,ik}})] \tag{5.31}$$

The constraints C25 and C26 in (5.30) can be omitted since $\sqrt{M}P_1 \to \infty$ and $\sqrt{M}P_2 \to \infty$ when $M \to \infty$. Then, (5.30) can be simplified as

$$\max_{\boldsymbol{e}_p,\boldsymbol{e}_d,\tilde{\boldsymbol{e}}_d} \frac{R}{\sum\limits_{k=1}^{K}(\tau E_{p,lk}+T_1 E_{u,lk}+\zeta_1 T_2 \tilde{E}_{d,lk})} \\ \text{s.t.} \qquad C27 \tag{5.32}$$

Now, problem (5.32) can be solved by using the same approach as summarized in Algorithm 1.

5.5 Simulation Results and Discussion

In this section, computer simulation is carried out based on the same parameters as discussed in Chapter 4, where a *2*-cell MU-MIMO system is considered with *3* users in each cell. And OFDM signals are transmitted according to the LTE standard and the parameter setting in [1]. The weighted numbers ζ_2 is assumed to be one. Throughout the simulation, a normalized additive Gaussian noise with zero-mean and unit variance is assumed. In addition, the convergence tolerance of the proposed algorithm is set to $\delta = 10^{-3}$. The same average SINR lower bounds are used in EE maximization schemes as that used in total transmit power minimization schemes discussed in Chapter 4. The tightness of the derived lower bounds of average SINR has already been shown in Fig. 4.1.

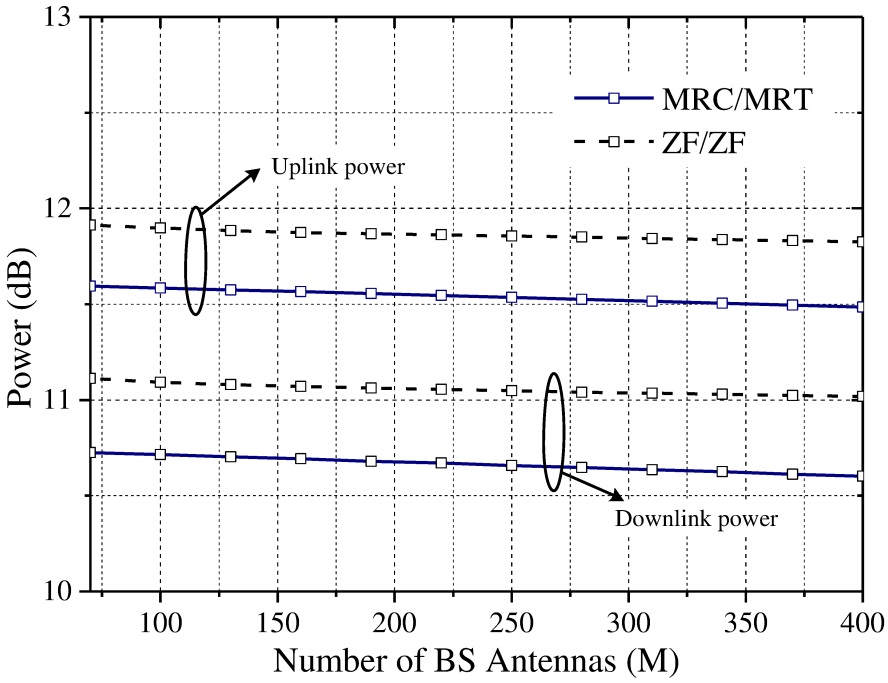

Figure 5.1: Pilot-data power allocation versus number of BS antennas based on EE maximization scheme

Fig. 5.1 and Fig. 5.2 show respectively the total uplink and downlink power and the average SINRs for the EE maximization power allocation schemes versus the number of BS antennas. Here, the uplink power includes the pilot power and uplink data signal power. From these two figures, it is seen that as M grows, the uplink and downlink powers slowly decrease while the corresponding average SINRs increase. To maximize the total EE, the ZF scheme requires approximately 0.5dB more power than the MRC/MRT for both up and downlink transmissions, but meanwhile it provides about 3.5dB higher average SINRs when compared with MRC/MRT. It is worth mentioning that when M grows to infinity, we can calculate the scaled pilot and data powers as $E_{p,11} = 12.32dB$, $E_{u,11} = E_{d,11} = 10.74dB$.

In Fig. 5.3, we compare the EE of the proposed total transmit power minimization scheme in Chapter 4 (with $\gamma_1 = \gamma_2 = 5dB$ threshold), the EE maximization scheme proposed in

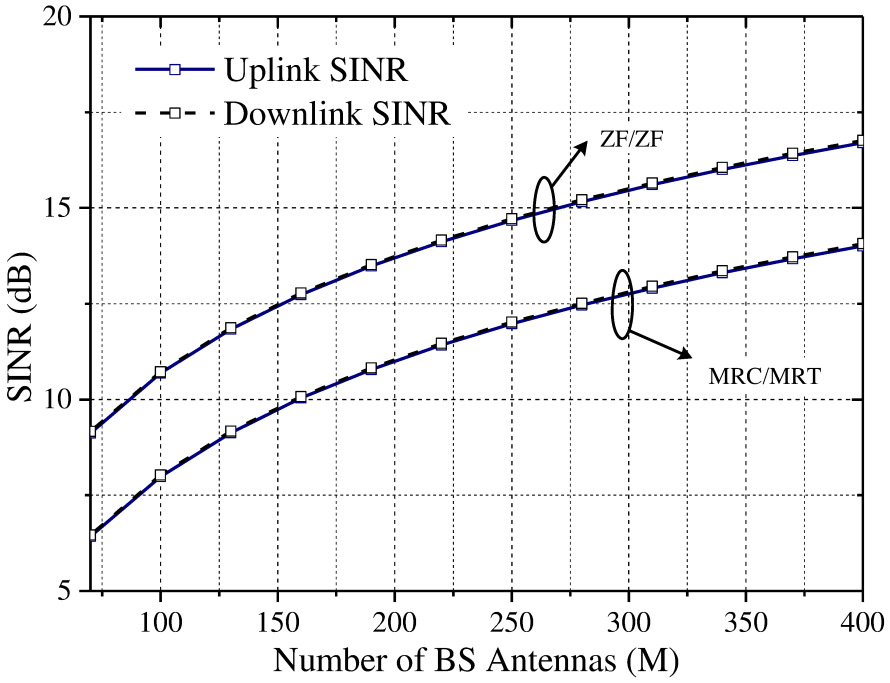

Figure 5.2: Uplink and downlink average SINR versus number of BS antennas based on EE maximization scheme

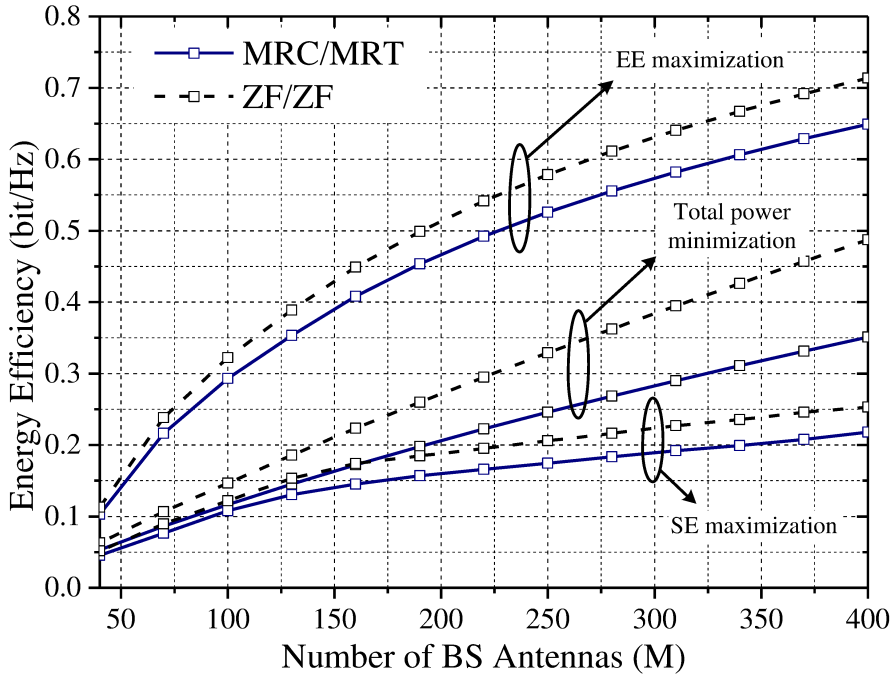

Figure 5.3: Average EE versus number of BS antennas

Chapter 5 and the SE maximization power control scheme discussed in [109]. It is observed that the proposed the EE maximization scheme obtains the best EE performance while SE maximization shows the worst despite the number of BS antennas. This is because the proposed EE maximization scheme decreases the transmit power to avoid sacrificing EE, whereas the SE maximization scheme always uses all of the transmit power. Meanwhile, the total transmit power minimization scheme shows a moderate EE performance, since it always keeps constant uplink and downlink average SINRs. The EE increases as M grows in all the three methods since it has benefited largely from the use of massive MIMO. Even though framework 2 (EE maximization scheme) shows the best EE performance in figure 5.3, it does not mean that framework 2 is better than framework 1, since the purpose of these two frameworks are different in MU-MIMO system design. Framework 1 aims to use the lowest power over a given system performance target, while framework 2 aims to find a balance between system performance and the power cost.

5.6 Conclusion

In this chapter, we have developed novel pilot-data power control algorithms for multi-cell MU-MIMO systems with an objective of jointly maximizing the total uplink and downlink EE under BS and per-user power constraints. The proposed schemes take into account the MRC and ZF detectors in the uplink transmission together with MRT and ZF precoder in the downlink transmission. In order to simplify the original optimization problems, the lower bounds of the average SINR derived in Chapter 3 were used in the proposed power allocation optimization problems in order to facilitate their solution. We have further simplified the optimization problems by converting them to GP problems or recasting the proposed

non-convex problems based on Dinkelbach's method and FrankWolfe iteration to obtain equivalent convex problems which can be easily solved. The very large number of BS systems situation is also discussed for multi-cell MU-MIMO systems. The joint pilot-data power control schemes based on the two frameworks and SE maximization power allocation algorithm are compared and discussed, showing the advantage of the proposed power allocation schemes for massive MIMO systems.

Chapter 6

Joint Pilot-Data Power Allocation with Circuit Power in Consideration

6.1 Introduction

As discussed in Chapter 4 and Chapter 5, very large scale antenna arrays bring substantial improvements in energy and spectral efficiency to wireless systems due to the greatly improved spatial resolution and array gain. Moreover, infinite number of antennas employed at BS, one may achieve in theory an unbounded EE since the user rates grow unboundedly as $M \to \infty$. Even though the power consumption of the radio front-end has not been considered in the previous two chapters, massive MIMO is still a promising candidate for improving the EE of future wireless networks.

In practical systems, however, it is not possible to achieve infinite EE because the power consumed by digital signal processor and analog circuits for baseband processing and radio frequency (RF) grows with M, which means that infinite antennas at BS will introduce infinite circuit power as well. Unfortunately, there are very limited works in open literature that have discussed about how the number of BS antennas M impacts the EE of wireless systems when circuit power is considered. For example, the work in [116] has derived the optimal values of M and K for a given uplink sum rate, but the necessary overhead due to the pilot

signal for channel acquisition was ignored, leading to an unrealistic result, conclusion that a large value of K, even if approaching infinity, would always be beneficial. The authors in [117] analyzed the capacity and estimation accuracy of a TDD massive MIMO systems and discussed how M, K and the transmit power affect the SE and EE of a single-cell MU-MIMO system with different linear processing schemes at the BS.

The main purpose of this chapter is to investigate how the number of BS antennas M impacts the EE of a single-cell massive MU-MIMO system when circuit power consumption is taken into account. Similar to previous chapters, we consider the most commonly used precoder and receiver, namely, ZF, MRT and MRC. It is worth mentioning that our interest in this chapter is to deal with the transmit power minimization based on the first optimization framework of single-cell MU-MIMO systems [118]. If circuit power consumption is considered in multi-cell MU-MIMO systems, the power allocation problem would become very difficult, which will be left as future work.

6.2 Single-cell MU-MIMO Systems with Channel Estimation

6.2.1 Channel Model

Now we simplify the multi-cell MU-MIMO channel model in chapter 2 for single-cell systems. Consider a TDD single-cell MU-MIMO system operating over a bandwidth of BHz with the same frame structure in multi-cell MU-MIMO systems as shown in Fig. 2.2, where we only estimate the uplink CSI at BS and use such estimated uplink CSI for both uplink and downlink data transmission. The system consists of an M-antenna BS serving K ($K<M$) single-antenna mobile users. Let $\boldsymbol{G}$ denote the $M\times K$ channel matrix between the BS and

K MTs with its elements $g_{mk} \triangleq [\boldsymbol{G}]_{mk}$ being the channel coefficients between the k-th user and the m-th antenna of the BS. Then the channel response g_{mk} can be modeled as

$$g_{mk} = h_{mk}\sqrt{\beta_k} \tag{6.1}$$

where $h_{mk} \sim CN(0,1)$ represents the small-scale fading coefficient and $\sqrt{\beta_k}$ models the large-scale fading that incorporates path-loss and shadow fading which is assumed to be constant and known a priori. Then the channel matrix $\boldsymbol{G}$ can be expressed as

$$\boldsymbol{G} = \boldsymbol{H}\boldsymbol{D}^{1/2} \tag{6.2}$$

where $[\boldsymbol{H}]_{mk} = h_{mk}$ and $\boldsymbol{D}$ is a $K \times K$ diagonal matrix with $[\boldsymbol{D}]_{kk} = \beta_k$.

6.2.2 Channel Estimation

In single-cell MU-MIMO systems, during the training phase, the $M \times N_p$ received pilot matrix at the BS can be expressed as

$$\boldsymbol{Y}_p = \boldsymbol{G}\boldsymbol{S}_p + \boldsymbol{N}_p \tag{6.3}$$

where $\boldsymbol{S}_p$ denotes the $K \times N_p$ pilot symbol matrix and $\boldsymbol{N}_p$ is an $M \times N_p$ complex noise matrix whose entries are i.i.d. RVs with zero-mean and unit variance. Assume an orthogonal pilot matrix is used, which means that $\boldsymbol{S}_p$ satisfies

$$\boldsymbol{S}_p\boldsymbol{S}_p^H = diag(\tau p_{p,1}, \tau p_{p,2}, \ldots, \tau p_{p,K}) \tag{6.4}$$

where $p_{p,k}$ $(k = 1, 2, \ldots, K)$ represents the pilot power of the k-th user. Based on the MMSE channel estimation, the estimated channel matrix can be expressed as [22]

$$\hat{\boldsymbol{G}} = \boldsymbol{Y}_p \boldsymbol{S}_p^H (\boldsymbol{D}^{-1} + \boldsymbol{S}_p \boldsymbol{S}_p^H)^{-1} = \boldsymbol{G}\boldsymbol{S}_p \boldsymbol{S}_p^H \Phi + \boldsymbol{N}\boldsymbol{S}_p^H \Phi \tag{6.5}$$

where the $K \times K$ diagonal matrix $\boldsymbol{\Phi}$ is given by

$$\boldsymbol{\Phi} \triangleq (\boldsymbol{D}^{-1} + \boldsymbol{S}_p \boldsymbol{S}_p^H)^{-1} = diag\left(\frac{\beta_1}{1+\beta_1 \tau p_{p,1}}, \ldots, \frac{\beta_K}{1+\beta_K \tau p_{p,K}}\right) \tag{6.6}$$

The estimation error matrix is defined as $\Delta\boldsymbol{G} = \boldsymbol{G} - \hat{\boldsymbol{G}}$. Similar to the Multi-cell MU-MIMO situation, we know that $\hat{\boldsymbol{G}}$ and $\Delta\boldsymbol{G}$ have i.i.d. Gaussian RVs with zero mean. Let $M \times 1$ vectors $\hat{\boldsymbol{g}}_k$ and $\Delta\boldsymbol{g}_k$ denote the k-th column of matrix $\hat{\boldsymbol{G}}$ and that of $\Delta\boldsymbol{G}$, respectively. The elements of $\hat{\boldsymbol{G}}$ are independent of that of $\Delta\boldsymbol{G}$ and the variance of the elements of $\hat{\boldsymbol{g}}_k$ and that of $\Delta\boldsymbol{g}_k$ can be, respectively, calculated as

$$\sigma_k^2 = \frac{\beta_k^2 \tau p_{p,k}}{1 + \beta_k \tau p_{p,k}}, \varepsilon_k^2 = \frac{\beta_k}{1 + \beta_k \tau p_{p,k}} \tag{6.7}$$

6.2.3 Lower Bounds of Average SINR

The derivation of SINR expressions and their lower bounds in single-cell MU-MIMO is very similar to that in multi-cell MU-MIMO systems as discussed in Chapter 3. Here we only give the results for SINR expressions and lower bounds of average SINR for the single-cel MU-MIMO system, without showing the detailed derivation and proof. Similar to the multi-cell MU-MIMO case, we adopt the MRC and ZF detectors in the uplink, and MRT and ZF

precoders in the downlink in the following discussion.

When MRC receiver is employed at BS, the detection matrix is simply given by $\boldsymbol{W} = \hat{\boldsymbol{G}}$. Therefore, we have $\boldsymbol{w}_k^H = \hat{\boldsymbol{g}}_k^H$ (or $\boldsymbol{w}_i^H = \hat{\boldsymbol{g}}_i^H$). The received SINR of user k can be obtained as

$$\gamma_k^{MRC} = \frac{p_{d,k}\left|\hat{\boldsymbol{g}}_k^H \hat{\boldsymbol{g}}_k\right|^2}{\sum\limits_{i=1,i\neq k}^{K} p_{d,i}\left|\hat{\boldsymbol{g}}_k^H \hat{\boldsymbol{g}}_i\right|^2 + \sum\limits_{j=1}^{K} p_{d,j}\left|\hat{\boldsymbol{g}}_k^H \Delta \boldsymbol{g}_i\right|^2 + \left\|\hat{\boldsymbol{g}}_k^H\right\|^2} \tag{6.8}$$

where $p_{d,k}$ $(k = 1, 2, \ldots, K)$ represents the uplink data transmit power for the k-th user.

Proposition 6: When the MRC receiver is employed at BS, the lower bound of the uplink average SINR of user k under MMSE channel estimation can be expressed as

$$E\{\gamma_k^{MRC}\} \geq \gamma_k^{MRC,up} \triangleq \frac{\frac{M\beta_k^2 \tau p_{p,k} p_{d,k}}{1+\beta_k \tau p_{p,k}}}{\sum\limits_{i=1,i\neq k}^{K} \beta_i p_{d,i} + p_{d,k}\frac{\beta_k}{1+\beta_k \tau p_{p,k}} + 1} \tag{6.9}$$

When ZF receiver is used at BS with receiving matrix $\boldsymbol{W} = \hat{\boldsymbol{G}}(\hat{\boldsymbol{G}}^H \hat{\boldsymbol{G}})^{-1}$, we have $\boldsymbol{w}_k^H \hat{\boldsymbol{g}}_k = 1$ and $\boldsymbol{w}_k^H \hat{\boldsymbol{g}}_i = 0$ $(i \neq k)$. Then the received uplink SINR of user k can be obtained as

$$\gamma_k^{ZF} = \frac{p_{d,k}}{\sum\limits_{i=1}^{K} p_{d,i}\left|\boldsymbol{w}_k^H \Delta \boldsymbol{g}_i\right|^2 + \left\|\boldsymbol{w}_k^H\right\|^2} \tag{6.10}$$

where $\boldsymbol{w}_k$ denotes the k-th column of matrix $\boldsymbol{W}$.

Proposition 7: In the case of ZF receiver, the lower bound of the average uplink SINR of user k can be expressed as

$$E\gamma_k^{ZF} \geq \gamma_k^{ZF,up} \triangleq \frac{p_{d,k}}{\frac{1+\beta_k \tau p_{p,k}}{(M-K)\beta_k^2 \tau p_{p,k}}\left(\sum\limits_{i=1}^{K} p_{d,i}\frac{\beta_i}{1+\beta_i \tau p_{p,i}} + 1\right)} \tag{6.11}$$

When MRT precoder is employed at BS with precoding matrix $\boldsymbol{A} = \hat{\boldsymbol{G}}$, we have $\boldsymbol{a}_k^H = \hat{\boldsymbol{g}}_k^H$ (or $\boldsymbol{a}_i^H = \hat{\boldsymbol{g}}_i^H$). Then, the received SINR of user k can be given by

$$\tilde{\gamma}_k^{MRC} = \frac{\tilde{p}_{d,k}\|\hat{\boldsymbol{g}}_k\|^2}{\sum\limits_{i=1,i\neq k}^{K}\tilde{p}_{d,i}\frac{\left|\hat{\boldsymbol{g}}_k^H\hat{\boldsymbol{g}}_i\right|^2}{\|\hat{\boldsymbol{g}}_i\|^2} + \sum\limits_{j=1}^{K}\tilde{p}_{d,j}\frac{\left|\Delta\boldsymbol{g}_k^H\hat{\boldsymbol{g}}_j\right|^2}{\|\hat{\boldsymbol{g}}_j\|^2} + 1} \tag{6.12}$$

where $\tilde{p}_{d,k}$ $(k = 1, 2, \ldots, K)$ represents the downlink data power for the k-th user.

Proposition 8: When MRT precoder is employed at BS, the lower bound of the downlink average SINR of user k can be expressed as

$$\begin{aligned} &E\{\tilde{\gamma}_k^{MRC}\} \geq \gamma_k^{MRC,dn} \\ &\triangleq \frac{\frac{(M-1)\beta_k^2\tau p_{p,k}}{1+\beta_k\tau p_{p,k}}\tilde{p}_{d,k}}{\frac{(M-1)\beta_k^2\tau p_{p,k}}{M(1+\beta_k\tau^{dn}p_{p,k})}\sum\limits_{i=1,i\neq k}^{K}\tilde{p}_{d,i} + \sum\limits_{j=1}^{K}\tilde{p}_{d,j}\frac{\beta_k}{1+\beta_k\tau p_{p,k}} + 1} \end{aligned} \tag{6.13}$$

When ZF precoder [11] is used at BS with precoding matrix $\boldsymbol{A} = \hat{\boldsymbol{G}}(\hat{\boldsymbol{G}}^H\hat{\boldsymbol{G}})^{-1}$, we have $\boldsymbol{g}_k^H\boldsymbol{a}_k = 1$ and $\hat{\boldsymbol{g}}_k^H\boldsymbol{a}_i = 0$ $(i \neq k)$. The downlink SINR of user k can be obtained as

$$\tilde{\gamma}_k^{ZF} = \frac{\frac{\tilde{p}_{d,k}}{\|\boldsymbol{a}_k\|^2}}{\sum\limits_{i=1}^{K}\tilde{p}_{d,i}\frac{\left|\Delta\boldsymbol{g}_k^H\boldsymbol{a}_i\right|^2}{\|\boldsymbol{a}_i\|^2} + 1} \tag{6.14}$$

Proposition 9: In the case of ZF receiver, the lower bound of the average downlink SINR of user k can be expressed as

$$E\{\tilde{\gamma}_k^{ZF}\} \geq \gamma_k^{ZF,dn} \triangleq \frac{\tilde{p}_{d,k}}{\frac{1+\beta_k\tau p_{p,k}}{(M-K)\beta_k^2\tau p_{p,k}}\left(\sum\limits_{i=1}^{K}\tilde{p}_{d,i}\frac{\beta_k}{1+\beta_k\tau p_{p,k}} + 1\right)} \tag{6.15}$$

6.2.4 Circuit Power Consumption Model

The circuit power consumed by different analog components and digital signal processing can be modeled as [33]:

$$P_{CP} = MP_{BS} + KP_U + P_{SYN} + P_{CE} + \sum_{k=1}^{K}(E\{R_k + \tilde{R}_k\})P_{CD} + P_{LP} \tag{6.16}$$

Here, P_{BS} accounts for the power to run the circuit components (such as converters, mixers, and filters) caused by each antenna in BS and P_U by each single-antenna user, respectively. The third term P_{SYN}, which is a constant value, represents the power consumption of the baseband processors, P_{CE} accounts for the power consumption due to channel estimation process in each coherence time interval, P_{CD} is the load/data-rate dependent power consumption, e.g. channel coding, decoding and backhaul processing, and P_{LP} represents the linear processing power consumption at the BS. In (6.16), R_k denotes the uplink achievable rate of user k. Following the definition in [33, equation (6)], R_k is defined as

$$R_k = \frac{T_1}{T_2}(1 - \frac{\tau}{T})B\log(1 + \gamma_k) \tag{6.17}$$

where the factor $\frac{T_1}{T_2}(1 - \frac{\tau}{T})$ accounts for pilot overhead and $\frac{T_1}{T_2}$ represents the ratio of uplink to the downlink transmission. Similarly, the downlink achievable rate of the k-th user $\tilde{R}_k$ can be defined as

$$\tilde{R}_k = \frac{T_2}{T_1}(1 - \frac{\tau}{T})B\log(1 + \tilde{\gamma}_k) \tag{6.18}$$

with pilot overhead $\frac{T_2}{T_1}(1-\frac{\tau}{T})$ and the downlink to uplink transmission ratio $\frac{T_2}{T_1}$. In (6.16), the term P_{CE} can be further expressed as

$$P_{CE} = \frac{2\tau BMK}{TL_{BS}} \tag{6.19}$$

Here L_{BS} is the computational efficiency of processing circuit in BS, which is assumed to be constant in this paper, B/T represents the number of coherence blocks per second, with $T = \tau + T_1 + T_2$. The power cost of transmit precoding and receiving beamforming of MRT/MRC and ZF can be expressed as follows

$$P_{LP}^{MRT/MRC} = B(1-\frac{\tau}{T})\frac{2MK}{L_{BS}} + \frac{3BMK}{TL_{BS}} \tag{6.20}$$

$$P_{LP}^{ZF} = B(1-\frac{\tau}{T})\frac{2MK}{L_{BS}} + \frac{BK^3}{3TL_{BS}} + \frac{3BMK^2+BMK}{TL_{BS}} \tag{6.21}$$

As discussed in [33], (6.20) and (6.21) describe the power cost by the linear processing circuit. By assuming constant B, K, t and T and substituting (6.16), (6.17) and (6.18) into (6.13), we can summarize the total circuit power consumption as

$$P_{CP}^{MRT/MRC} = A^{MRT/MRC}M + \sum_{k=1}^{K}(E\{R_k+\tilde{R}_k\})P_{CD} + B^{MRT/MRC} \tag{6.22}$$

$$P_{CP}^{ZF} = A^{ZF}M + \sum_{k=1}^{K}(E\{R_k+\tilde{R}_k\})P_{CD} + B^{ZF} \tag{6.23}$$

where

$$A^{MRT/MRC} = P_{BS} + \frac{3BK}{TL_{BS}} + \frac{2BK}{L_{BS}} \tag{6.24}$$

$$A^{ZF} = P_{BS} + \frac{2BK}{L_{BS}} + \frac{3BK^2 + BK}{TL_{BS}} \tag{6.25}$$

$$B^{MRT/MRC} = KP_U + P_{SYN} \tag{6.26}$$

$$B^{ZF} = KP_U + P_{SYN} + \frac{BK^3}{3TL_{BS}} \tag{6.27}$$

6.3 Joint Power Allocation with Fixed Number of BS Antennas

In this section, based on the average SINR lower bounds and circuit power model discussed in the previous section, we will develop two algorithms for power allocation between pilot and data symbols to minimize the weighted uplink and downlink transmit power and circuit power consumption while guaranteeing per-user SINR and power constraints.

6.3.1 Power Allocation Based on ZF Receiver/Precoder

We first consider the combined use of the ZF receiver and the ZF precoder. Let P_t be the total transmit power for one transmission frame. In order to determine the best power-consumption trade-off between the uplink and downlink transmission, a weighted sum-power minimization is considered with positive weight parameters ζ_1 and ζ_2. By defining $\boldsymbol{p}_p \triangleq [p_{p,1}, p_{p,2}, \ldots, p_{p,K}]$, $\boldsymbol{p}_d \triangleq [p_{d,1}, p_{d,2}, \ldots, p_{d,K}]$ and $\tilde{\boldsymbol{p}}_d \triangleq [\tilde{p}_{d,1}, \tilde{p}_{d,2}, \ldots, \tilde{p}_{d,K}]$, the power allocation problem which minimizes the total transmit and circuit power while meeting the derived average SINR lower bounds for both ZF receiver and ZF precoder can be formulated as

$$\begin{aligned} \min_{\boldsymbol{p}_p, \boldsymbol{p}_d, \tilde{\boldsymbol{p}}_d} \; & P_c^{ZF} \triangleq \sum_{k=1}^{K} (\tau p_{p,k} + T_1 p_{d,k} + \zeta_1 T_2 \tilde{p}_{d,k}) \\ & + \zeta_2 [A^{ZF} M + C \sum_{k=1}^{K} log(1 + \gamma_k^{ZF,up}) + \tilde{C} \sum_{k=1}^{K} log(1 + \gamma_k^{ZF,dn}) + B^{ZF}] \end{aligned} \tag{6.28a}$$

$$\text{s.t.} \quad \gamma_k^{ZF,up} \geq \gamma_1, \gamma_k^{ZF,dn} \geq \gamma_2 \tag{6.28b}$$

$$\tau p_{p,k} + T_1 p_{d,k} \leq P_1, \sum_{k=1}^{K} \tilde{p}_{d,k} T_2 \leq P_2 \tag{6.28c}$$

$$p_{p,k} > 0, p_{d,k} > 0, \tilde{p}_{d,k} > 0 \tag{6.28d}$$

where $C \triangleq \frac{T_1}{T_2}(1 - \frac{\tau}{T})BP_{CD}$ and $\tilde{C} \triangleq \frac{T_2}{T_1}(1 - \frac{\tau}{T})BP_{CD}$. The above objective function is the weighted sum-power accounting for the uplink pilot power, the uplink and downlink data transmit powers and the circuit power consumption. In optimization problem (6.28), we assume a fixed number of BS antennas, i.e., M is treated as a constant. The first and second constraints represent the uplink and downlink SINR requirement with per-user SINR targets γ_1 and γ_2, respectively. The third and fourth constraints are the power constraints at users and BS with power thresholds P_1 and P_2, respectively.

By comparing (6.28) with the previous minimization problem (4.8) based on the total transmit power minimization, one can see that there are two main differences between the two problems. Firstly, (6.28) is for single-cell MU-MIMO system, while (4.8) is for multi-cell MU-MIMO case. Second, (4.8) only contains the transmit power term in the objective function. In the objective function of (6.28), however, the first term $\sum_{k=1}^{K} (\tau p_{p,k} + T_1 p_{d,k} + \zeta_1 T_2 \tilde{p}_{d,k})$ represents the total transmit power while the second $A^{ZF}M + C \sum_{k=1}^{K} log(1 + \gamma_k^{ZF,up}) + \tilde{C} \sum_{k=1}^{K} log(1 + \gamma_k^{ZF,dn}) + B^{ZF}$ denotes the circuit power consumption which is modelled by following (6.16). In other words, in Chapter 4 we only considered to minimize the total transmit power, while in this chapter we aim to minimize the transmit power and circuit power at the same time.

It is easy to see that this optimization problem is nonconvex and it is very difficult to solve directly. In order to simplify the optimization problem, we introduce a new set of

variables

$$a_k \triangleq \frac{\beta_k}{1+\beta_k \tau p_{p,k}} \tag{6.29}$$

As the range of $p_{p,k}$ is from zero to infinity, from (6.29) we can get the range of a_k as $0 < a_k < \beta_k$. By substituting (6.29) into problem (6.28) and dropping the constant terms, we can rewrite the minimization problem as

$$\min_{\boldsymbol{a},\boldsymbol{p_d},\tilde{\boldsymbol{p}}_{\boldsymbol{d}}} \sum_{k=1}^{K} (\frac{1}{a_k} + T_1 p_{d,k} + \zeta T_2 \tilde{p}_{d,k}) + \zeta_2 [C \sum_{k=1}^{K} log(1+\gamma_k^{ZF,up}) + \tilde{C} \sum_{k=1}^{K} log(1+\gamma_k^{ZF,dn})] \tag{6.30a}$$

$$\text{s.t.} \qquad \frac{(M-K)p_{d,k}(\beta_k - a_k)}{\sum_{i=1}^{K} p_{d,i} a_i + 1} \geq \gamma_1 \tag{6.30b}$$

$$\frac{(M-K)\tilde{p}_{d,k}(\beta_k - a_k)}{a_k \sum_{i=1}^{K} \tilde{p}_{d,i} + 1} \geq \gamma_2 \tag{6.30c}$$

$$a_k^{-1} + T_1 p_{d,k} \leq P_1 + \frac{1}{\beta_k} \tag{6.30d}$$

$$\sum_{k=1}^{K} \tilde{p}_{d,k} T_2 \leq P_2 \tag{6.30e}$$

$$0 < a_k < \beta_k, p_{d,k} > 0, \tilde{p}_{d,k} > 0 \tag{6.30f}$$

where

$$\boldsymbol{a} \triangleq [a_1, a_2, \ldots, a_K]. \tag{6.31}$$

In order to simplify the concave logarithmic terms, we define

$$x_k = \frac{p_{d,k}(\beta_k - a_k)}{\sum_{i=1}^{K} p_{d,i} a_i + 1} \tag{6.32}$$

By multiplying $\frac{a_k}{(\beta_k - a_k)}$ at both sides of the equation and then taking summation of x_k for all $k \in K$, we get

$$\sum_{k=1}^{K} \frac{a_k x_k}{(\beta_k - a_k)} = \frac{\sum_{k=1}^{K} p_{d,k} a_k}{\sum_{i=1}^{K} p_{d,i} a_i + 1} \tag{6.33}$$

After some derivation, we have

$$\sum_{i=1}^{K} p_{d,i} a_i = \frac{\sum_{k=1}^{K} \frac{a_k x_k}{(\beta_k - a_k)}}{1 - \sum_{k=1}^{K} \frac{a_k x_k}{(\beta_k - a_k)}} \tag{6.34}$$

Using (6.34) into the denominator of (6.32), we can get the expression of $p_{d,k}$ as

$$p_{d,k} = \frac{\frac{x_k}{(\beta_k - a_k)}}{1 - \sum_{i=1}^{K} \frac{a_i x_i}{(\beta_i - a_i)}} \tag{6.35}$$

For downlink data power $\tilde{p}_{d,k}$, we define

$$\tilde{x}_k = \frac{(\beta_k - a_k)\tilde{p}_{d,k}}{a_k \sum_{i=1}^{K} \tilde{p}_{d,i} + 1} \tag{6.36}$$

In a similar manner, we get

$$\sum_{k=1}^{K} \tilde{p}_{d,k} = \frac{\sum_{i=1}^{K} \frac{\tilde{x}_i}{(\beta_i - a_i)}}{1 - \sum_{i=1}^{K} \frac{a_i \tilde{x}_i}{(\beta_i - a_i)}} \tag{6.37}$$

and

$$\tilde{p}_{d,k} = \frac{\frac{\tilde{x}_k}{(\beta_k - a_k)} \left[\sum_{i=1, i \neq k}^{K} \frac{a_k \tilde{x}_i}{(\beta_i - a_i)} - \sum_{i=1, i \neq k}^{K} \frac{a_i \tilde{x}_i}{(\beta_i - a_i)} + 1 \right]}{1 - \sum_{i=1}^{K} \frac{a_i \tilde{x}_i}{(\beta_i - a_i)}} \tag{6.38}$$

Using the range $0 < \alpha_k < \beta_k, p_{d,k} > 0, \tilde{p}_{d,k} > 0$ from (6.30f) to (6.32), (6.35), (6.36) and (6.38), we have the following constraints for x_k and $\tilde{x}_k$

$$x_k > 0, \tilde{x}_k > 0, \sum_{k=1}^{K} \frac{a_k x_k}{(\beta_k - a_k)} < 1, \sum_{k=1}^{K} \frac{a_k \tilde{x}_k}{(\beta_k - a_k)} < 1 \tag{6.39}$$

In order to further simplify the objective function (6.30), we define

$$p_{d,k} \leq y_k, \sum_{k=1}^{K} \tilde{p}_{d,k} \leq \tilde{y} \tag{6.40}$$

For $p_{d,k}$ and $\tilde{p}_{d,k}$ are all positive values, we know the ranges for y_k and $\tilde{y}$, i.e., $y_k > 0$ and $\tilde{y} > 0$. Then substituting (6.32), (6.35), (6.41), (6.38), (6.39) and (6.40) into problem (6.30) and dropping the redundant constraints, the minimization problem is equivalent to

$$\begin{aligned} &\min_{\boldsymbol{a},\boldsymbol{x},\tilde{\boldsymbol{x}},\boldsymbol{y},\tilde{y}} \sum_{k=1}^{K} (\tfrac{1}{a_k} + T_1 y_k) + \zeta_1 T_2 \tilde{y} \\ &+ \zeta_2 \{ C \sum_{k=1}^{K} log[1 + (M-K)x_k] + \tilde{C} \sum_{k=1}^{K} log[1 + (M-K)\tilde{x}_k] \} \end{aligned} \tag{6.41a}$$

$$\text{s.t.} \quad x_k \geq \frac{\gamma_1}{M-K} \tag{6.41b}$$

$$\tilde{x}_k \geq \frac{\gamma_2}{M-K} \tag{6.41c}$$

$$\frac{x_k}{y_k(\beta_k - a_k)} + \sum_{i=1}^{K} \frac{a_i x_i}{(\beta_i - a_i)} \leq 1 \tag{6.41d}$$

$$\sum_{i=1}^{K} \frac{\tilde{x}_i}{\tilde{y}(\beta_i - a_i)} + \sum_{i=1}^{K} \frac{a_i \tilde{x}_i}{(\beta_i - a_i)} \leq 1 \tag{6.41e}$$

$$\frac{1}{a_k} + T_1 y_k \leq P_1 + \frac{1}{\beta_k}, T_2 \tilde{y} \leq P_2 \tag{6.41f}$$

$$0 < a_k < \beta_k, y_k > 0, \tilde{y} > 0 \tag{6.41g}$$

where

$$\boldsymbol{x} \triangleq [x_1, x_2, \ldots, x_K] \tag{6.42}$$

$$\tilde{\boldsymbol{x}} \triangleq [\tilde{x}_1, \tilde{x}_2, \ldots, \tilde{x}_K] \tag{6.43}$$

$$\boldsymbol{y} \triangleq [y_1, y_2, \ldots, y_K] \tag{6.44}$$

The above optimization problem is still not convex. Note that the left-side of the two constraints (6.41d) and (6.41e) are a monotonically decreasing function of $\frac{1}{(\beta_k - a_k)}$, while these two constraints contain the linear combination of $\frac{1}{(\beta_k - a_k)}$, so we can use the property as described in [98, section 7.1] to simplify the above optimization problem. We define a new variable b_k such that $\frac{1}{(\beta_k - a_k)} \leq b_k$, which can be further expressed as the generalized posynomial inequality $\frac{1}{b_k} + a_k \leq \beta_k$. As the range a_k is $0 < a_k < \beta_k$, we have $b_k > 0$. Then after some derivations, the above problem becomes

$$\begin{aligned} &\min_{\boldsymbol{a},\boldsymbol{x},\tilde{\boldsymbol{x}},\boldsymbol{y},\tilde{y},\boldsymbol{b}} \sum_{k=1}^{K} (\tfrac{1}{a_k} + T_1 y_k) + \zeta_1 T_2 \tilde{y} \\ &+\zeta_2 \{C \sum_{k=1}^{K} log[1 + (M-K)x_k] + \tilde{C} \sum_{k=1}^{K} log[1 + (M-K)\tilde{x}_k]\} \end{aligned} \tag{6.45a}$$

$$\text{s.t.} \quad \frac{x_k b_k}{y_k} + \sum_{i=1}^{K} a_i x_i b_i \leq 1 \tag{6.45b}$$

$$\sum_{i=1}^{K} \frac{\tilde{x}_i b_i}{\tilde{y}} + \sum_{i=1}^{K} a_i \tilde{x}_i b_i \leq 1 \tag{6.45c}$$

$$\frac{1}{b_k} + a_k \leq \beta_k, b_k > 0 \tag{6.45d}$$

$$\frac{1}{a_k} + T_1 y_k \leq P_1 + \frac{1}{\beta_k}, T_2 \tilde{y} \leq P_2 \tag{6.45e}$$

$$0 < a_k < \beta_k, y_k > 0, \tilde{y} > 0 \tag{6.45f}$$

where

$$\boldsymbol{b} \triangleq [b_1, b_2, \ldots, b_K] \tag{6.46}$$

Now, the constraints in the above optimization problem are all posynomial inequalities, each with the form of a posynomial less than a constant value. The problem (6.45) can be treated as a generalized geometric programming (GGP) problem which can be considered as a combination of a standard GP and several additive logarithm terms of generalized posynomial [99, section 7.2]. Since all the variables in (6.45) are nonnegative, the optimization problem (6.45) can be converted to a convex problem through a logarithmic change of the variables as discussed in [99, section 7.2]. We replace original variables a_k, x_k, $\tilde{x}_k$, y_k, $\tilde{y}$ and b_k with their logarithmic form for all values of $k \in K$. Then, the variables become $a'_k = \log(a_k)$, $x'_k = \log(x_k)$, $\tilde{x}'_k = \log(\tilde{x}'_k)$, $y'_k = \log(y_k)$, $\tilde{y}' = \log(\tilde{y}')$ and $b'_k = \log(b_k)$. After substituting these new variables in (6.45), the minimization problem becomes a convex optimization problem and can be solved very efficiently by employing the augmented Lagrangian method or by using a standard numerical optimization packages, for example, ConVeX (CVX) [105]. Then, we can calculate the values for $p_{p,k}$, $p_{d,k}$ and $\tilde{p}_{d,k}$ by substituting the solution of problem (6.45) to (6.29), (6.35) and (6.38).

6.3.2 Power Allocation Based on MRC Receiver and MRT Precoder

Similar to the previous subsection, the power allocation problem which minimizes the weighted transmit and circuit power subject to the obtained lower bounds on the average SINR for MRC receiver and MRT precoder can be formulated as

$$\min_{\boldsymbol{p}_p,\boldsymbol{p}_d,\tilde{\boldsymbol{p}}_d} P_c^{MRC/MRT} \triangleq \sum_{k=1}^{K} (\tau p_{p,k} + T_1 p_{d,k} + \zeta_1 T_2 \tilde{p}_{d,k}) \\ +\zeta_2[A^{MRC/MRT} M + C \sum_{k=1}^{K} log(1+\gamma_k^{MRC,up}) + \tilde{C} \sum_{k=1}^{K} log(1+\gamma_k^{MRT,dn}) + B^{MRC/MRT}] \tag{6.47a}$$

$$\text{s.t.} \quad \gamma_k^{MRC,up} \geq \gamma_1, \gamma_k^{MRT,dn} \geq \gamma_2 \tag{6.47b}$$

$$\tau p_{p,k} + T_1 p_{d,k} \leq P_1, \sum_{k=1}^{K} \tilde{p}_{d,k} T_2 \leq P_2 \tag{6.47c}$$

$$p_{p,k} > 0, p_{d,k} > 0, \tilde{p}_{d,k} > 0 \tag{6.47d}$$

Due to the concave logarithmic terms in the objective function, the above problem is very difficult to solve. In order to simplify this problem, we define

$$z_k = \frac{\sum_{i=1,i\neq k}^{K} \beta_i p_{d,i} + p_{d,k} a_k + 1}{(\beta_k - a_k) p_{d,k}} + 1 \tag{6.48}$$

and

$$\tilde{z}_k = \frac{[\frac{(M-1)\beta_k}{M} + \frac{1}{M} a_k] \sum_{i=1,i\neq k}^{K} \tilde{p}_{d,i} + \tilde{p}_{d,k} a_k + 1}{(\beta_k - a_k)(M-1)\tilde{p}_{d,k}} + \frac{1}{M}. \tag{6.49}$$

Using (6.48), (6.49) and a similar approach as in the previous subsection, we can get

$$p_{d,k} = \frac{1}{(\beta_k - a_k)z_k[1 - \sum_{i=1}^{K} \frac{\beta_i}{(\beta_i - a_i)z_i}]}, \tag{6.50}$$

$$\tilde{p}_{d,k} = \frac{[\frac{(M-1)\beta_k}{M} + \frac{1}{M}a_k]}{(M-1)(\beta_k - a_k)\tilde{z}_k} \frac{\sum_{i=1}^{K} \frac{1}{(M-1)(\beta_i - a_i)\tilde{z}_i}}{1 - \sum_{i=1}^{K} \frac{[\frac{(M-1)\beta_i}{M} + \frac{1}{M}a_i]}{(M-1)(\beta_i - a_i)\tilde{z}_i}} + \frac{1}{(M-1)(\beta_k - a_k)\tilde{z}_k}, \tag{6.51}$$

and

$$\sum_{k=1}^{K} \tilde{p}_{d,k} = \frac{\sum_{i=1}^{K} \frac{1}{(M-1)(\beta_i - a_i)\tilde{z}_i}}{1 - \sum_{i=1}^{K} \frac{[\frac{(M-1)\beta_i}{M} + \frac{1}{M}a_i]}{(M-1)(\beta_i - a_i)\tilde{z}_i}}. \tag{6.52}$$

Substituting the range of a_k, $p_{d,k}$ and $\tilde{p}_{d,k}$ into equations (6.48) to (6.51), we get

$$z_k > 1, \sum_{k=1}^{K} \frac{\beta_k}{(\beta_k - a_k)z_k} < 1, \tilde{z}_k > \frac{1}{M}, \sum_{k=1}^{K} \frac{[\frac{(M-1)\beta_k}{M} + \frac{1}{M}a_k]}{(M-1)(\beta_k - a_k)\tilde{z}_k} < 1 \tag{6.53}$$

By substituting (6.29), (6.51), (6.50), (6.52) and (6.53) into problem (6.47) and dropping the constant value in the objective function and redundant constraints, then the optimization problem becomes

$$\min_{\boldsymbol{a},\boldsymbol{z},\tilde{\boldsymbol{z}},\boldsymbol{y},\tilde{y}} \sum_{k=1}^{K} (\tfrac{1}{a_k} + y_k T_1) + \zeta_1 T_2 \tilde{y} + \zeta_2 [C \sum_{k=1}^{K} log(1 + \tfrac{M}{z_k - 1}) + \tilde{C} \sum_{k=1}^{K} log(1 + \tfrac{1}{\tilde{z}_k - \frac{1}{M}})] \tag{6.54a}$$

$$\text{s.t.} \quad z_k \leq \frac{M}{\gamma_1} + 1 \tag{6.54b}$$

$$\tilde{z}_k \leq \frac{1}{\gamma_2} + \frac{1}{M} \tag{6.54c}$$

$$\frac{1}{(\beta_k - a_k)z_k y_k} + \sum_{i=1}^{K} \frac{\beta_i}{(\beta_i - a_i)z_i} \leq 1 \tag{6.54d}$$

$$\sum_{k=1}^{K} \frac{1}{\tilde{y}(\beta_k - a_k)(M-1)\tilde{z}_k} + \sum_{k=1}^{K} \frac{\frac{(M-1)\beta_k}{M} + \frac{1}{M}a_k}{(\beta_k - a_k)(M-1)\tilde{z}_k} \leq 1 \tag{6.54e}$$

$$z_k > 1, \tilde{z}_k > \frac{1}{M} \tag{6.54f}$$

$$\frac{1}{a_k} + T_1 y_k \leq P_1 + \frac{1}{\beta_k}, T_2 \tilde{y} \leq P_2 \tag{6.54g}$$

$$0 < a_k < \beta_k, y_k > 0, \tilde{y} > 0 \tag{6.54h}$$

Here

$$\boldsymbol{z} \triangleq [z_1, z_2, \ldots, z_K] \tag{6.55}$$

and

$$\tilde{\boldsymbol{z}} \triangleq [\tilde{z}_1, \tilde{z}_2, \ldots, \tilde{z}_K]. \tag{6.56}$$

Similar to the optimization problem (6.41), here we use the property as described in [98,section 7.1] to convert (6.54) into a GGP problem. We define a set of new variables t_k and $\tilde{t}_k$, such that $\frac{M}{z_k - 1} \leq t_k$ and $\frac{1}{\tilde{z}_k - \frac{1}{M}} \leq \tilde{t}_k$ which can be further expressed as the generalized posynomial inequality $\frac{M}{t_k} + 1 \leq z_k$ and $\frac{1}{\tilde{t}_k} + \frac{1}{M} \leq \tilde{z}_k$. From (6.54f), we can find the range for t_k and $\tilde{t}_k$ as $t_k > \gamma_1$ and $\tilde{t}_k > \gamma_2$. We also replace the term $\frac{1}{(\beta_k - a_k)}$ with b_k, along with the constraint $\frac{1}{b_k} + a_k \leq \beta_k$ and $b_k > 0$. After derivations, the previous problem becomes

$$\begin{aligned} \min_{\boldsymbol{a},\boldsymbol{z},\tilde{\boldsymbol{z}},\boldsymbol{y},\tilde{y},\boldsymbol{b},\boldsymbol{t},\tilde{\boldsymbol{t}}} & \sum_{k=1}^{K} (\tfrac{1}{a_k} + y_k T_1) + \zeta_1 T_2 \tilde{y} \\ & + \zeta_2 [P_{CD} \sum_{k=1}^{K} log(1 + t_k) + P_{CD} \sum_{k=1}^{K} log(1 + \tilde{t}_k)] \end{aligned} \tag{6.57a}$$

$$\text{s.t.} \frac{b_k}{z_k y_k} + \sum_{i=1}^{K} \frac{b_i \beta_i}{z_i} \leq 1 \tag{6.57b}$$

$$\sum_{k=1}^{K} \frac{b_k}{(M-1)\tilde{y}\tilde{z}_k} + \sum_{k=1}^{K} \frac{b_k[\frac{(M-1)\beta_k}{M} + \frac{1}{M}a_k]}{(M-1)\tilde{z}_k} \leq 1 \tag{6.57c}$$

$$\frac{1}{b_k} + a_k \leq \beta_k, \frac{M}{t_k} + 1 \leq z_k, \frac{1}{\tilde{t}_k} + \frac{1}{M} \leq \tilde{z}_k \tag{6.57d}$$

$$z_k \leq \frac{M}{\gamma_1} + 1, \tilde{z}_k \leq \frac{1}{\gamma_2} + \frac{1}{M} \tag{6.57e}$$

$$b_k > 0, t_k > \gamma_1, \tilde{t}_k > \gamma_2 \tag{6.57f}$$

$$\frac{1}{a_k} + T_1 y_k \leq P_1 + \frac{1}{\beta_k}, T_2 \tilde{y} \leq P_2 \tag{6.57g}$$

$$0 < a_k < \beta_k, y_k > 0, \tilde{y} > 0 \tag{6.57h}$$

Here

$$\boldsymbol{t} \triangleq [t_1, t_2, \ldots, t_K] \tag{6.58}$$

and

$$\tilde{\boldsymbol{t}} \triangleq [\tilde{t}_1, \tilde{t}_2, \ldots, \tilde{t}_K]. \tag{6.59}$$

Similar to the previous problem (6.45), (6.57) is also a GGP problem with a combination of a standard GP and several additive logarithmic terms of generalized posynomial as described in [99, section 7.2]. Since all variables in (6.57) are nonnegative, similar to the optimization problem (6.45), (6.57) can also be converted to a convex optimization problem through a logarithmic change of the variables and then be solved by standard numerical optimization packages, i.e., CVX [105].

6.4 Joint Power Allocation with Variable Number of BS Antennas

As discussed in [22], with the assumption of infinite number of BS antennas, uncorrelated noise and intra-cell interference can be completely averaged out, leading to "favorable propagation" and unbounded achievable uplink and downlink rate. However, power consumed by digital signal processing and analog circuits also grows with the number of BS antennas. So the number of BS antennas plays an important role in the performance of MU-MIMO communication systems. In this section, we develop two EE power control algorithms with consideration of variable number of BS antennas.

6.4.1 Power Allocation Based on ZF Receiver/Precoder

Similar to the previous fixed number of BS antennas case, the power allocation problem can be formulated as

$$\begin{aligned} &\min_{\boldsymbol{p}_p,\boldsymbol{p}_d,\tilde{\boldsymbol{p}}_d,M} P_c^{ZF} \\ &\text{s.t.} M \geq K \\ &(6.28b),(6.28c),(6.28d) \end{aligned} \tag{6.60}$$

Then, by substituting (6.32), (6.35), (6.36), (6.38) and (6.39) into problem (6.60), after some derivation, we get

$$\begin{aligned} &\min_{\boldsymbol{a},\boldsymbol{x},\tilde{\boldsymbol{x}},\boldsymbol{y},\tilde{y},\boldsymbol{b},M'} \sum_{k=1}^{K} (\tfrac{1}{a_k} + T_1 y_k) + \zeta_1 T_2 \tilde{y} \\ &+\zeta_2 [A^{ZF} M' + C \sum_{k=1}^{K} log(1 + M' x_k) + \tilde{C} \sum_{k=1}^{K} log(1 + M' \tilde{x}_k)] \end{aligned} \tag{6.61a}$$

$$\text{s.t.} \tfrac{x_k b_k}{y_k} + \sum_{i=1}^{K} a_i x_i b_i \leq 1 \tag{6.61b}$$

$$\sum_{i=1}^{K} \frac{\tilde{x}_i b_i}{\tilde{y}} + \sum_{i=1}^{K} a_i \tilde{x}_i b_i \leq 1, \frac{1}{b_k} + a_k \leq \beta_k, b_k > 0, M' > 0 \tag{6.61c}$$

$$(6.46b), (6.46c), (6.46f, (6.46g)$$

Here $M' \triangleq M - K$. Now, (6.61)is a GGP problem with a combination of a standard GP and several additive logarithmic terms of generalized posynomial as described in [99]. Since all variables in (6.61) are nonnegative, (6.61) can also be converted to a convex optimization problem through a logarithmic change of the variables as discussed in [99, section 7.2] and then be solved by standard numerical optimization packages, i.e., CVX [105].

6.4.2 Power Allocation Based on MRT Precoder and MRC Receiver

The EE power control problem with consideration of variable number of BS antennas based on MRT precoder and MRC receiver can be formulated as

$$\begin{aligned} &\min_{\boldsymbol{p}_p, \boldsymbol{p}_d, \tilde{\boldsymbol{p}}_d, M} P_c^{MRC/MRT} \\ &\text{s.t.} M \geq K \\ &(6.47b), (6.47c), (6.47d) \end{aligned} \tag{6.62}$$

We follow a similar method in section 6.4 to simplify problem (6.57). By substituting (6.29), (6.50), (6.51), (6.52) and (6.53) into problem (6.62) and performing some derivation, we get

$$\begin{aligned} &\min_{\boldsymbol{a}, \boldsymbol{z}, \tilde{\boldsymbol{z}}, \boldsymbol{y}, \tilde{y}, \boldsymbol{b}, \boldsymbol{t}, \tilde{\boldsymbol{t}}, M} \sum_{k=1}^{K} (\frac{1}{a_k} + y_k T_1) + \zeta_1 T_2 \tilde{y} \\ &+ \zeta_2 [A^{MRC/MRT} M + C \sum_{k=1}^{K} log(1 + t_k) + \tilde{C} \sum_{k=1}^{K} log(1 + \tilde{t}_k)] \end{aligned} \tag{6.63}$$

$$\text{s.t.} (6.62b), (6.62c), (6.62d), (6.62e), (6.62f), (6.62g), (6.62h)$$

It is worth-mentioning that if the number of BS antennas M is fixed, then the optimization problem (6.63) would degrade to (6.57) which is a GGP problem as discussed in subsection 6.4. When the pilot and data power are fixed, which means $\boldsymbol{a}, \boldsymbol{z}, \tilde{\boldsymbol{z}}, \boldsymbol{y}, \tilde{y}, \boldsymbol{b}$ all have fixed values, (6.63) becomes

$$\min_{\tilde{\boldsymbol{t}}, M} A^{MRC/MRT} M + C \sum_{k=1}^{K} log(1 + \tfrac{M}{z_k - 1}) + \tilde{C} \sum_{k=1}^{K} log(1 + \tilde{t}_k) \tag{6.64a}$$

$$\text{s.t.} \tfrac{1}{M-1} \sum_{k=1}^{K} \tfrac{b_k}{\tilde{y}\tilde{z}_k} + \tfrac{1}{M} \sum_{k=1}^{K} \tfrac{\beta_k b_k}{\tilde{z}_k} + \tfrac{1}{M(M-1)} \sum_{k=1}^{K} \tfrac{a_k b_k}{\tilde{z}_k} \leq 1 \tag{6.64b}$$

$$\max\{\gamma_1(z_k - 1), K\} \leq M \leq \tfrac{1}{\tilde{z}_k - \frac{1}{\gamma_2}} \tag{6.64c}$$

$$\tfrac{1}{\tilde{t}_k} + \tfrac{1}{M} \leq \tilde{z}_k \tag{6.64d}$$

$$\tilde{t}_k \geq \gamma_2 \tag{6.64e}$$

By replacing the term $\frac{1}{M-1}$ with a new variable $\tilde{M}$, and using the constraint $\frac{1}{M-1} \leq \tilde{M}$ and $\tilde{M} > 0$, (6.64) becomes

$$\min_{\tilde{\boldsymbol{t}}, M, \tilde{M}} A^{MRC/MRT} M + C \sum_{k=1}^{K} log(1 + \tfrac{M}{z_k - 1}) + \tilde{C} \sum_{k=1}^{K} log(1 + \tilde{t}_k) \tag{6.65a}$$

$$\text{s.t.} \tilde{M} \sum_{k=1}^{K} \tfrac{b_k}{\tilde{y}\tilde{z}_k} + \tfrac{1}{M} \sum_{k=1}^{K} \tfrac{\beta_k b_k}{\tilde{z}_k} + \tfrac{\tilde{M}}{M} \sum_{k=1}^{K} \tfrac{a_k b_k}{\tilde{z}_k} \leq 1 \tag{6.65b}$$

$$\max\{\gamma_1(z_k - 1), K\} \leq M \leq \tfrac{1}{\tilde{z}_k - \frac{1}{\gamma_2}} \tag{6.65c}$$

$$\tfrac{1}{\tilde{t}_k} + \tfrac{1}{M} \leq \tilde{z}_k \tag{6.65d}$$

$$\tilde{t}_k \geq \gamma_2 \tag{6.65e}$$

$$\tfrac{1}{\tilde{M}} + 1 \leq M \tag{6.65f}$$

$$\tilde{M} > 0 \tag{6.65g}$$

Similar to the previous problem (6.45) and (6.61), (6.65) is also a GGP problem with a combination of a standard GP and several additive logarithm terms of generalized posynomial. As a result, (6.65) can be converted to a convex optimization problem through a logarithmic change of the variables and then be solved by standard numerical optimization packages.

Based on the discussion above, we give an iterative algorithm to find out the suboptimal pilot and data power as well as the number of antennas at BS for optimization problem (6.63). It can be seen that when the pilot and data powers or M is fixed, (6.65) can be converted to a convex optimization problem which is easy to solve. Hence, the minimization problem can be divided into two parts: at the iteration k, with the fixed $M(k)$, we can obtain three sets of new pilot-data allocation vector $P_{p,k}(k+1)$, $P_{d,k}(k+1)$ and $\tilde{P}_{d,k}(k+1)$, to minimize the total power while satisfying all constraints; then after updating $P_{p,k}(k)$, $P_{d,k}(k)$ and $\tilde{P}_{d,k}(k)$ to $P_{p,k}(k+1)$, $P_{d,k}(k+1)$ and $\tilde{P}_{d,k}(k+1)$, by fixing the pilot and data power obtained in the previous step, we calculate the optimal number of antennas at BS, $M(k+1)$, by solving (6.65). Such an alternating optimization procedure continues until the error tolerance is satisfied. The proposed iteration is summarized as follow.

Algorithm 2:

1. Initialization: initialize $M(0)$, $P_{p,k}(0)$, $P_{d,k}(0)$ and $\tilde{P}_{d,k}(0)$; set iteration number $k = 0$; set the error tolerance Δ.

2. With the fixed $M(k)$, calculate the optimal pilot and data powers $P_{p,k}(k+1)$, $P_{d,k}(k+1)$ and $\tilde{P}_{d,k}(k+1)$ based on (6.63);

3. With the fixed $P_{p,k}(k+1)$, $P_{d,k}(k+1)$ and $\tilde{P}_{d,k}(k+1)$, calculate the optimal number of antennas $M(k+1)$. Then calculate the objective function in (6.65) by using $M(k+1)$, $P_{p,k}(k+1)$, $P_{d,k}(k+1)$ and $\tilde{P}_{d,k}(k+1)$ to obtain the total power $P(k+1)$;

4. Terminate the loop if $|P(k+1) - P(k)| \leq \Delta$. Otherwise, let $k = k+1$ and go to Step 2.

It is worth mentioning that the convergence of the algorithm above is guaranteed because the total transmitted power is minimized at each iterative step. However, it should be pointed out that the proposed algorithm is not guaranteed to give the global optimal solution due to the nonconvex nature of the original problem.

6.5 Simulation Results and Discussion

In this section, numerical simulations are carried out to validate the derived average SINR lower bounds for single-cell MU-MIMO systems and evaluate the proposed EE power allocation methods. We consider a single cell MU-MIMO system with a radius of 1000m. All $K = 4$ users are assumed to be located uniformly over the cell at random with a minimum distance of $r_h = 100$m away from the BS. The large-scale channel fading is modeled with $\beta_k = z_k/(r_k/r_h)^v$, where z_k represents a log-normal random variable with standard deviation σ, r_k is the distance between the k-th user and the BS and v means the path loss exponent. Following the parameter setting in [1], we choose $\sigma = 8$dB and v=3.8. Throughout the simulation, the normalized additive Gaussian noise with zero mean and unit variance is assumed.

Same as the multi-cell MU-MIMO cases discussed in Chapter 4 and Chapter 5, we suppose that the OFDM signal is transmitted according to LTE standard [1]. The simulation parameters are summarized in Table 6.1. The parameters in circuit power consumption model are chosen according to paper [33, table II]. In the optimization problem, the weight ζ_1 and ζ_2 are assumed to be 1 and 0.01, respectively. The same target SINR and power constraint are applied for both uplink and downlink transmission. In the following simulation, all powers are normalized according to noise power.

Table 6.1 Simulation Paremeters

Parameter	Value
Cell Radius	1000 m
Minimum distance	100 m
Transmission bandwidth	10MHz
Channel coherence time	1 ms
Subcarrier spacing	15 kHz
OFDM symbol interval	71.4 μs
Symbol duration	66.7 μs
Guard interval length	4.7 μs
Relative pilot length	4
Power required to run the circuit components at BS, P_{BS}	1W
Power required to run the circuit components at user, P_U	0.1W
Power consumed by baseband processor, P_{SYN}	2W
Power consumed by linear processing at BS, P_{SYN}	0.5W
Computational efficiency at BS, L_{BS}	12.8 Gflops/W
Computational efficiency at user, L_U	5 Gflops/W

In order to validate the tightness of average SINR lower bounds in single-cell MU-MIMO systems, we give the simulation results for the original average SINR and the derived lower bounds for comparison in Fig. 6.1. Here, we have initially assumed that equal pilot and data power allocation among all users is applied with $p_{p,k} = p_{d,k} = \tilde{p}_{d,k} = 10$ for any $k \in K$ as in paper [22]. It is clearly seen that the derived lower bounds are tight in all cases despite the number of BS antennas. In both ZF receiver/precoder and MRC receiver/MRT precoder

situations, the uplink and downlink transmission show nearly the same SINR performance. The MU-MIMO system with ZF receiver/precoder shows a better SINR performance than the system with the MRC receiver/MRT precoder used at BS.

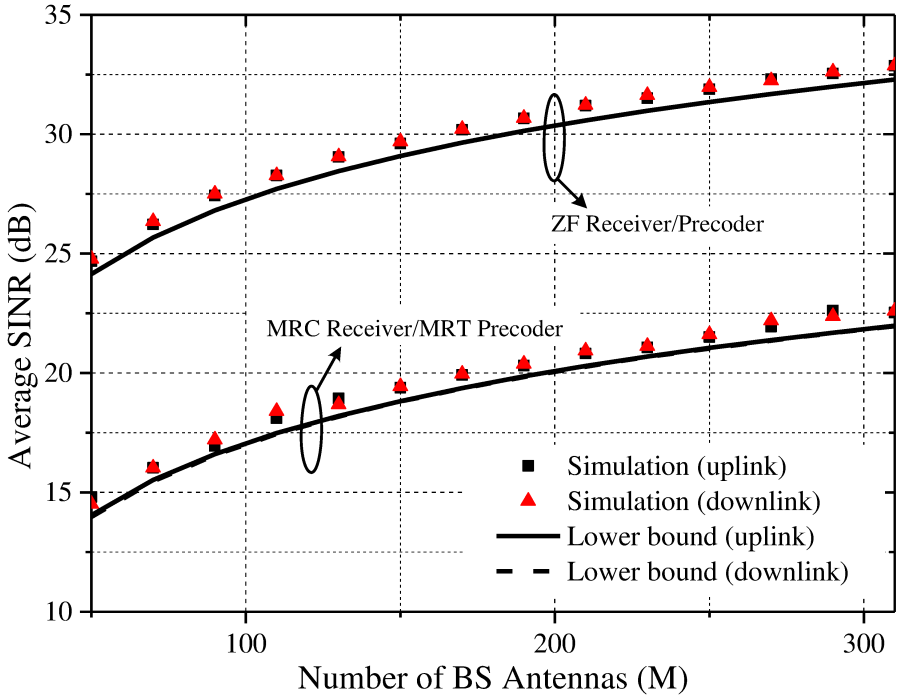

Figure 6.1: Average SINR versus the number of BS antennas

Fig. 6.2 shows the uplink, downlink and the processing circuit power versus the number of BS antennas with $\gamma_1 = \gamma_2 = 5dB$ and $\gamma_1 = \gamma_2 = 15dB$, respectively, for the fixed number of BS antennas schemes discussed in section 6.3. The uplink power includes the power of both pilot and uplink data signal. Note that for the system with MRC receiver and MRT precoder, when the required SINR is chosen as $15dB$, there is no solution for $M \leq 70$ because of the significant crosstalk interference. When M becomes large, the total uplink or downlink power required to achieve the $15dB$ SINR target between ZF/ZF and MRC/MRT schemes is less than $5dB$. In low target SINR region, MRC/MRT performs almost as well

as the ZF based scheme. Moreover, the circuit power cost of ZF/ZF is always higher than that of MRC/MRT, this is because the processing circuit for ZF/ZF is more complicated than that of MRC/MRT. It can be seen that as M grows, both uplink and downlink powers decrease, showing that the use of massive MU-MIMO can save a great deal of transmit power. However, when M grows, the the corresponding circuit power increases severely. It means that even the system spectral and energy efficiency can be beneficial with very large or even infinite M because the user rates grow unboundedly as M goes to infinity [22], leading to infinite but unrealistic spectral or energy efficiency because infinity M will also cause infinity power consumed by digital signal processing and analog circuits.

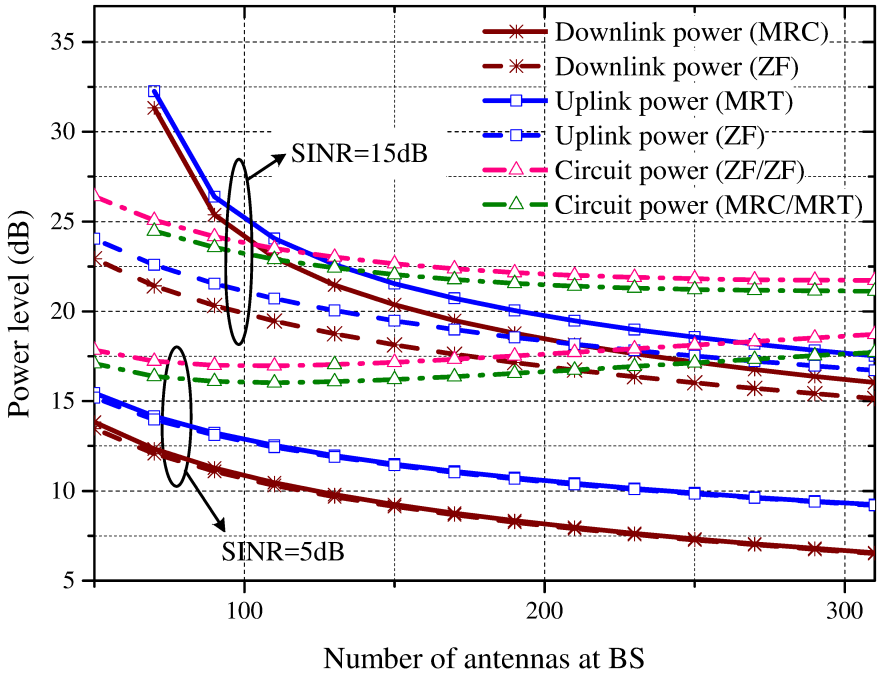

Figure 6.2: Pilot-data power allocation with fixed number of BS antennas versus number of BS antennas

Fig. 6.3 and Fig. 6.4 show the transmit and weighted total power versus the target SINR thresholds. Here, the transmit power includes the power of pilot, uplink and downlink

signals, and the weighted total power means the weighted sum of transmit power and circuit power cost. The results in these two figures are based on the algorithm in section 6.4 for variable number of BS antennas. It can be seen ZF/ZF requires lower transmit and weighted total power then MRC/MRT under the same SINR target. However, MRC/MRT requires less number of BS antennas than ZF/ZF under low SINR requirement. This is because the circuit power cost in MRC/MRT system is lower than that in ZF/ZF system under equal pilot and data power allocation. It is worth mentioning that ZF/ZF scheme gives a better transmit power performance than the MRC/MRT scheme does. However, ZF/ZF scheme also has more circuit power cost when compared to MRC/MRT which leads to a larger M requirement in low target SINR region.

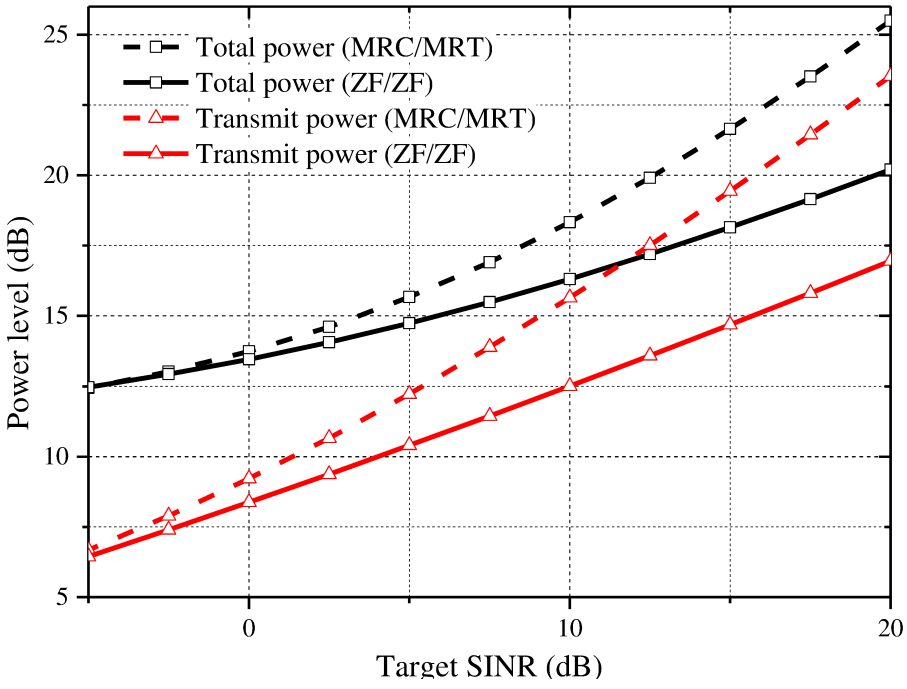

Figure 6.3: Total power versus target SINRs with variable number of BS antennas

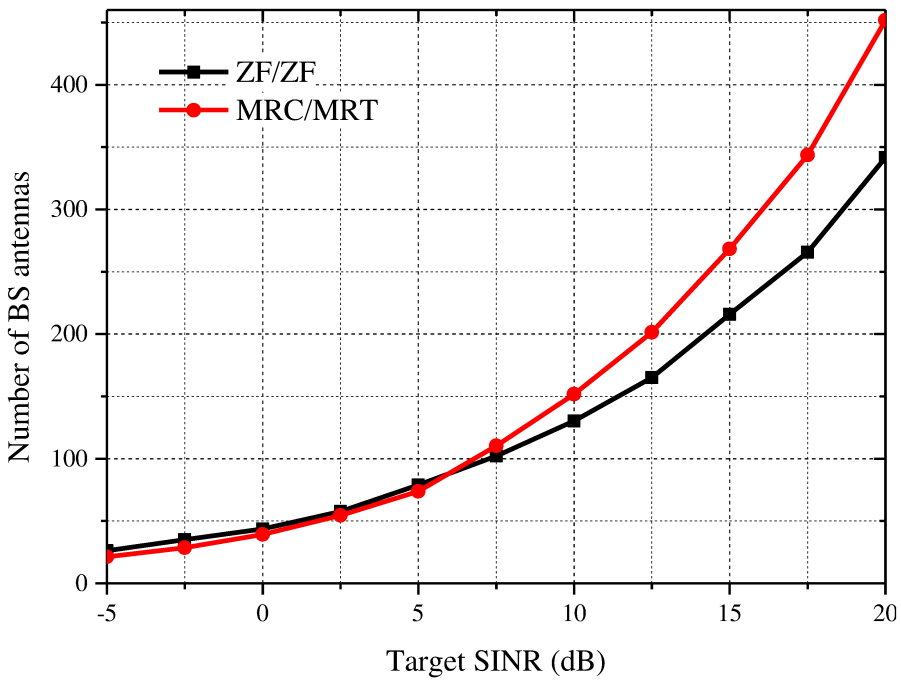

Figure 6.4: Pilot-data power allocation with variable number of BS antennas versus number of BS antennas

In Fig. 6.5, we compare the weighted total power of the proposed fixed number of BS antennas schemes discussed in section 6.3, the variable number of BS antennas schemes in section 6.4 and the pilot-data power allocation schemes proposed in Chapter 4. However, as the pilot-data power control scheme in Chapter 4 is based on multi-cell case, we degrade it to single-cell case for comparison which is the same as the (6.28) and (6.47) but removing the second term in their objective functions. Here, the weighted total power of schemes proposed in Chapter 4 also includes circuit power consumption which is calculated by using the same equations discussed in section 6.2.4 based on the pilot and data powers. In simulation, we choose $M = 200$ to calculate the corresponding pilot and data powers in the fixed number of BS antennas schemes and schemes proposed in Chapter 4. It is obviously that the two variable number of BS antennas scheme obtains the best power saving performance while

the schemes proposed in Chapter 4 without taking consideration of circuit power shows the worst, showing that with suitable number of BS antennas, the power saving performance can be further improved.

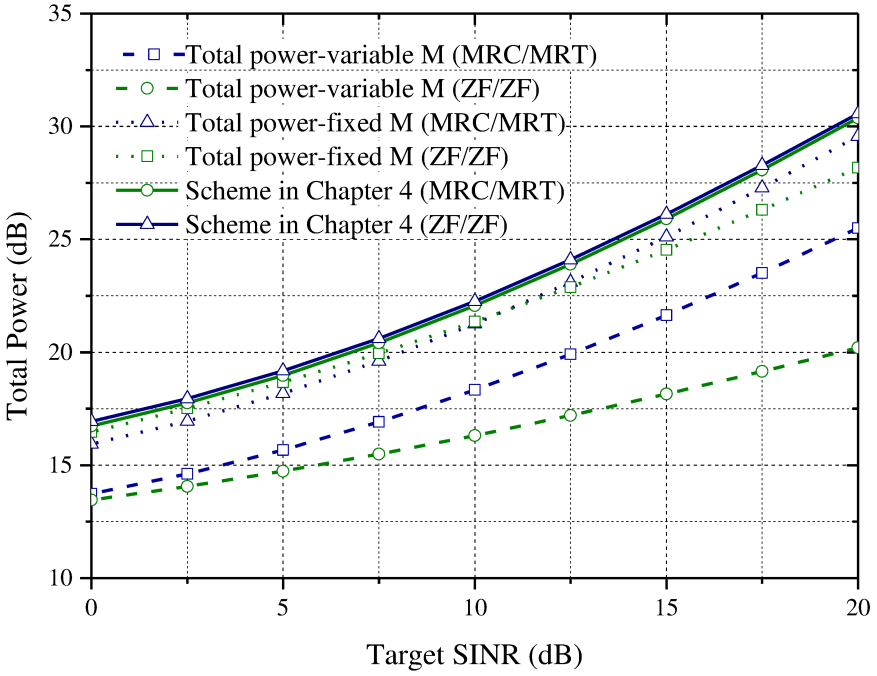

Figure 6.5: Total power versus target SINRs

Similar to Chapter 4, here, we also compare our proposed schemes with a simple equal pilot-data power allocation where the pilot and data signal have the same power p_u for all users as in [22]. We define the percentage of the total power saving for the algorithm as

$$\frac{K(\tau + T_1 + \zeta_1 T_2)p_u - \sum_{k=1}^{K} (\tau p_{p,k} + T_1 p_{d,k} + \zeta_1 T_2 \tilde{p}_{d,k})}{K(\tau + T_1 + \zeta_1 T_2)p_u} \tag{6.66}$$

where p_u for ZF/ZF and MRC/MRT schemes can be easily found by setting $p_{p,k} = p_{d,k} = \tilde{p}_{d,k} = p_u$ in the previous optimization problems in section 6.3. For the algorithm in section

6.4, we define the percentage of the total power saving as $\frac{P_c^{ZF}(p_u)-P_c^{ZF}}{P_c^{ZF}(p_u)}$ and $\frac{P_c^{MRC/MRT}(p_u)-P_c^{MRC/MRT}}{P_c^{MRC/MRT}(p_u)}$, respectively. Here, $P_c^{ZF}(p_u)$ and $P_c^{MRC/MRT}(p_u)$ denote the circuit power cost for ZF/ZF scheme and that for MRC/MRT scheme when equal power allocation is used, namely, by setting $p_{p,k} = p_{d,k} = \tilde{p}_{d,k} = p_u$ in the previous optimization problems (6.60) and (6.62), respectively. From Fig. 6.6, it can be seen that about 75% to 79% total power has been saved for ZF/ZF and MRC/MRT in low target SINR region, depending on the number of BS antennas. The percentage of power saving decreases as the required per-user SINR increases. It should be mentioned that the benefit of deploying a large number of BS antennas tends to become marginal, since the ultimate SINR performance is limited by the interference and channel estimation error.

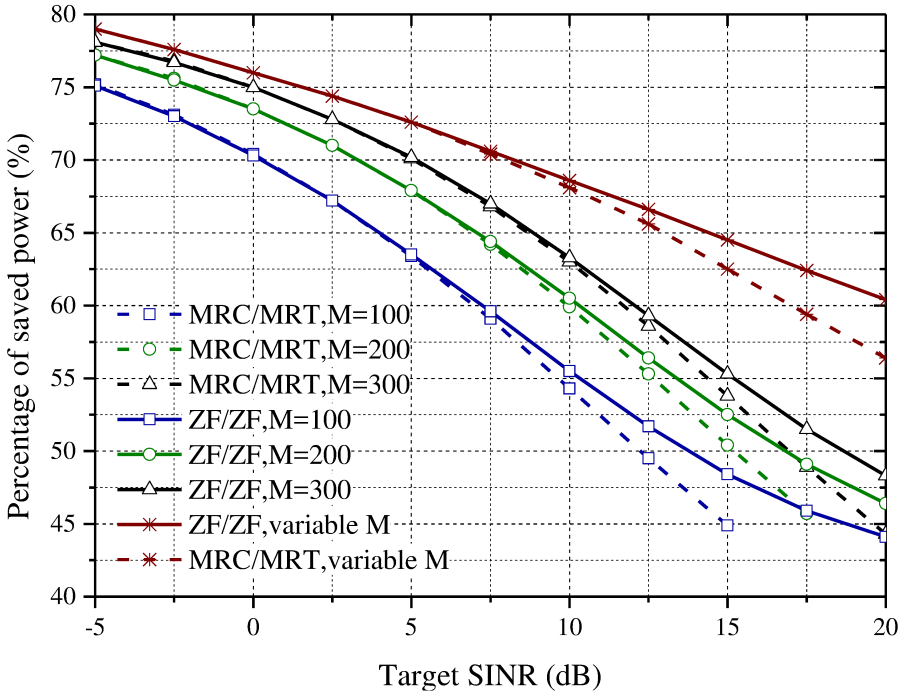

Figure 6.6: Percentage of power saving versus target SINR

6.6 Conclusion

In this chapter, we have investigated the pilot-data power allocation for EE communications in single-cell MU-MIMO systems with an objective of minimizing the pilot power as well as the total uplink and downlink data power and processing circuit power consumption. We have first analysed the uplink and downlink SINRs and then derived their lower bounds, based on which two EE power allocation optimization problems are formulated under the per-user SINR requirement and power constraint. For the fixed number of BS antennas case, the non-convex optimization problems are then converted to standard GP and general GP problems to facilitate the solutions. For the variable number of BS antennas case, an iterative algorithm is proposed to solve the optimization problem. Numerical simulation results have demonstrated the tightness of the SINR lower bounds for single-cell MU-MIMO systems and the impacts of number of BS antennas on EE.

Chapter 7

Summary and Further Research Directions

7.1 Concluding Remarks

In this thesis, several joint pilot and data power allocation algorithms for both conventional and massive MU-MIMO systems have been developed based on two energy efficient power allocation frameworks, in order to pursue high energy efficiency of next-generation green communication.

First, the close-form expressions of the average SINR lower bounds under MMSE channel estimation for both uplink and downlink transmissions in multi-cell MU-MIMO systems have been derived, by considering the conventional linear MRC and ZF detectors in the uplink and the MRT and ZF precoder in the downlink. Based on the derived uplink and downlink average SINRs, the Jensen's inequality and the properties of central Wishart matrix were applied to find the lower bounds of the derived SINRs. These lower bounds of the per-user average SINR are used to replace the true SINR to simplify the power allocation optimization problem. It has been shown that such relaxation of the original average SINR yields a simplified problem and leads to a suboptimal solution.

Second, based on the first EE power allocation framework, we have investigated the pilot and data power allocation for EE communications in multi-cell MU-MIMO systems with an objective of minimizing the total uplink and downlink transmit power under the per-user

SINR requirement and power constraint. The proposed schemes take into account the MRC and ZF detectors in the uplink transmission together with MRT and ZF precoders in the downlink transmission. In order to simplify the original optimization problems, the derived SINR lower bounds instead of the true values were used in the power allocation algorithms. Then, the non-convex optimization problems are converted to a standard GP problem to facilitate their solution based on inequality substitution. For the pilot-data power control scheme with ZF precoder and ZF detector, geometric inequality is used to approximate the original non-convex optimization to GP problem. The case of very large number of BS antennas has also been discussed by assuming infinite number of antennas at BS.

Third, two pilot and data power control schemes have been proposed and investigated based on the second EE power allocation framework to jointly maximize the total EE for both uplink and downlink transmission under per-user and BS power constraints for multi-cell TDD MU-MIMO systems. The original non-convex power allocation problems have been simplified by using the derived SINR lower bounds and Dinkelbach's method and FrankWolfe (FW) iteration to obtain an equivalent convex problem. The pilot-data power allocation schemes based on the two frameworks are compared with the SE maximization scheme. From the simulation results, the second framework shows a better EE performance than the first framework.

Finally, we have investigated the pilot-data power allocation for EE communications in single-cell MU-MIMO systems with an objective of minimizing the total uplink and downlink transmit power and processing circuit power consumption. Based on the discussion

in chapters 2 and 3, the system models and SINR lower bounds are degraded from multi-cell to single-cell MU-MIMO. The model of processing circuit power consumption is discussed. Then, pilot and data power allocation schemes are proposed which minimize the total weighted uplink and downlink transmit power while meeting the per-user SINR and BS power constraints with circuit power consumption under consideration. In our proposed power control schemes, both fixed and variable numbers of BS antennas have been investigated. For the fixed number of BS antennas case, the non-convex optimization problems are converted to a general GP problem to facilitate their solution. For the variable number of BS antennas case, an iterative algorithm is proposed to solve the optimization problem.

7.2 Future Work

During my study of green communication technology, some original ideas have been proposed on designing power control algorithm to improve the energy efficiency of the MU-MIMO systems. Nevertheless, there are still some issues that require further investigation.

1. The pilot-data power allocation algorithm in single-cell massvie MIMO systems with the consideration of circuit power consumption based on the second framework can be investigated.

2. In this thesis, we only discussed the pilot-data power allocation schemes in multi-cell massive MU-MIMO systems without considering the circuit power consumption. Our work in chapters 4 and 5 can be further extended with the consideration of both transmit power and circuit power cost. To the best of our knowledge, there is no such power control technique yet that exploits the energy efficiency in multi-cell massive MU-MIMO systems among pilot and data symbols and circuit power. Also, the circuit power consumption model

for multi-cell situation is worth-studying.

3. The proposed power allocation algorithms are based on the assumption that there is no correlation between BS antennas. In practice, the antennas at BS are not perfectly independent, where correlation may cause some noise in SINR. Therefore, it is desirable to establish a more effective and robust channel model to estimate the SINRs.

References

[1] T. L. Marzetta, "Noncooperative cellular wireless with unlimited numbers of BS antennas," IEEE Trans. Wireless Commun., vol. 9, no. 11, pp. 3590-3600, Nov. 2010.

[2] G. Li, J. Niu, D. Lee, J. Fan, and Y. Fu, "Multi-cell coordinated scheduling and MIMO in LTE," IEEE Commun. Surveys Tuts., vol. 16, no. 2, pp. 761-775, 2014.

[3] F. Boccardi, R. Heath, A. Lozano, T. Marzetta, and P. Popovski, "Five disruptive technology directions for 5G," IEEE Commun. Mag., vol. 52, no. 2, pp. 74-80, Feb. 2014.

[4] G. L. Stuber, J. Barry, S. McLaughlin, Y. G. Li, M. A. Ingram, and T. Pratt, "Broadband MIMO-OFDM wireless communications," Proc. IEEE, vol. 92, no. 2, pp. 271-294, Feb. 2004.

[5] E. G. Larsson, F. Tufvesson, O. Edfors, and T. L. Marzetta, "Massive MIMO for next generation wireless systems," IEEE Commun. Mag., vol. 52, no. 2, pp. 186-195, Feb. 2014.

[6] F. Rusek, D. Persson, B. K. Lau, E. G. Larsson, T. L. Marzetta, O. Edfors, and F. Tufvesson, "Scaling up MIMO: opportunities and challenges with very large arrays," IEEE Sign. Process. Mag., vol. 30, pp. 40-60, Jan. 2013.

[7] H. Huh, G. Caire, H. C. Papadopoulos, and S. A. Ramprashad, "Achieving 'massive MIMO' spectral efficiency with a not-so-large number of antennas," IEEE Trans. Wireless Commun., vol. 11, no. 9, pp. 3226-3239, Sep. 2012.

[8] X. Gao, O. Edfors, F. Rusek, and F. Tufvesson, "Massive MIMO performance evaluation based on measured propagation data," IEEE Trans. Wireless Commun., vol. 14, no. 7, pp. 3899-3911, July 2015.

[9] J. Zhu, R. Schober, and V. K. Bhargava, "Secure transmission in multi-cell massive MIMO systems," IEEE Trans. Wireless Commun., vol. 13, no. 9, pp. 4766-4781, Sep. 2014.

[10] L. Lu, G. Li, A. Swindlehurst, A. Ashikhmin, and R. Zhang, "An overview of massive MIMO: Benefits and challenges," IEEE J. Sel. Topics Signal Process., vol. 8, no. 5, pp. 742-758, Oct. 2014.

[11] H. Q. Ngo, E. G. Larsson, and T. L. Marzetta, "Energy and spectral efficiency of very large multiuser MIMO systems," IEEE Trans. Commun., vol. 61, no. 4, pp. 1436-1449, Apr. 2013.

[12] Qi Zhang, Shi Jin, Kai-KitWong, Hongbo Zhu, and Michail Matthaiou, "Power scaling of uplink massive MIMO Systems with arbitrary-rank channel means", IEEE J. Sel. Top. Sign. Proces., vol. 8, no. 5, Oct. 2014.

[13] A. Fehske, G. Fettweis, J. Malmodin, and G. Biczok, "The global footprint of mobile Communications: the ecological and economic perspective," IEEE Commun. Mag., pp. 55-62, Aug. 2011.

[14] O. Eunsung, B. Krishnamachari, L. Xin, and Z. Niu, “Toward dynamic energy-efficiency operation of cellular network infrastructure,” IEEE Commun. Mag., vol. 49, no. 6, pp. 56-61, Jun. 2011.

[15] D. Feng et al., “A survey of energy-efficient wireless Communications,” IEEE Commun. Surveys Tuts., vol. pp, no. 99, pp. 1-12, Feb. 2012.

[16] G. Y. Li, Z. Xu, C. Xiong, C. Yang, S. Zhang, Y. Chen, and S. Xu, “Energy-efficient wireless communications: tutorial, survey, and open issues,” IEEE Wireless Commun. Mag., vol. 18, no. 6, pp. 28-35, Dec. 2011.

[17] X. Xiao, X. Tao, and J. Lu, “Energy-efficient resource allocation in LTE-based MIMO-OFDMA systems with user rate constraints,” IEEE Trans. Veh. Communun., vol. 64, no. 1, pp. 125-197, Jan. 2015

[18] Z. Hasan, H. Boostanimehr, and V. K. Bhargava, “Green cellular networks: A survey, some research issues and challenges,” IEEE Commun. Surveys Tuts., vol. 13, no. 4, pp. 524-540, Fourth Quart., 2011.

[19] M. A. Marsan, L. Chiaraviglio, D. Ciullo, and M. Meo, “Optimal energy savings in cellular access networks,” Proc. IEEE ICC Workshops, Jun. 2009, pp. 1-5.

[20] Y. Chen, S. Zhang, S. Xu, and G. Y. Li, “Fundamental tradeoffs on green wireless networks,” IEEE Commun. Mag., vol. 49, no. 6, pp. 30-37, June 2011.

[21] G. Miao, N. Himayat, G. Y. Li, and A. Swami, “Cross-layer optimization for energy-efficient wireless communications: a survey,” Wireless Commun. and Mobile Comput. vol. 9, no. 4. pp. 529–542, 2009.

[22] Y. Kim, G. Miao and T. Hwang, “Energy efficient pilot and link adaptation for mobile users in TDD multi-user MIMO systems,” IEEE Trans. Wireless Commun., vol. 13, no. 1, pp. 382-393, Jan. 2014.

[23] Kim and B. Daneshrad, “Energy-constrained link adaptation for MIMO OFDM wireless communication systems,” IEEE Trans. Wireless Commun., vol. 9, no. 9, pp. 2820–2832, Sep. 2010.

[24] S. Cui, A. J. Goldsmith, and A. Bahai, “Energy-efficiency of MIMO and cooperative MIMO techniques in sensor networks,” IEEE J. Sel. Areas Commun., vol. 22, no. 6, pp. 1089–1098, Aug. 2004.

[25] Z. Xu et al., “Energy-efficient power allocation for pilots in training-based downlink OFDMA systems,” IEEE Trans. Commun., vol. 60, no. 10, pp. 3047–3058, Oct. 2012.

[26] M. Biguesh and A. B. Gershman, “Training based MIMO channel estimation: a study of estimator tradeoffs and optimal training signals,” IEEE Trans. Signal Process., vol. 54, no.3, pp. 884-893, Mar. 2006.

[27] D. Samardzija and N. Mandayam, ``Pilot-assisted estimation of MIMO fading channel response and achievable data rates'', IEEE Trans, on Signal Processing, vol. 51, no. 11, pp. 2882-2890, Nov 2003.

[28] M. Medard, "The effect upon channel capacity in wireless communications of perfect and imperfect knowledge of the channel," IEEE Trans. Inf. Theory, vol. 46, no. 3, pp. 933–946, May 2000.

[29] A. Soysal and S. Ulukus, "Joint channel estimation and resource allocation for MIMO systems–part I: single-user analysis," IEEE Trans. Wireless Commun., vol. 9, no. 2, pp. 624–631, Feb. 2009.

[30] J. H. Kotecha and A. M. Sayeed, "Transmit signal design for optimal estimation of correlated MIMO channels," IEEE Trans. Inf. Theory, vol. 49, no. 10, pp. 2562–2579, Oct. 2003.

[31] E. Baccarelli and M. Biagi, "Power-allocation policy and optimized design of multiple-antenna systems with imperfect channel estimation," IEEE Trans. Veh. Technol., vol. 53, no. 1, pp. 136-145, Jan. 2004.

[32] H. Yin, D. Gesbert, M. Filippou, and Y. Liu, "A coordinated approach to channel estimation in large-scale multiple-antenna systems," IEEE J. Sel. Areas Commun., vol. 31, no. 2, pp. 264–273, Feb. 2013.

[33] E. Bjornson, L. Sanguinetti, J. Hoydis, and M. Debbah, "Optimal design of energy-efficient multi-user MIMO systems: Is massive MIMO the answer?" IEEE Trans. Wireless Commun., vol. 14, no. 6, pp. 3059-3075, Jun. 2015.

[34] H. Huh, G. Caire, H. C. Papadopoulos, and S. A. Ramprashad, "Achieving 'massive MIMO' spectral efficiency with a not-so-large number of antennas,'' IEEE Trans. Wireless Commun., vol. 11, no. 9, pp. 3226-3239, Sep. 2012.

[35] X. Gao, O. Edfors, F. Rusek, and F. Tufvesson, "Massive MIMO performance evaluation based on measured propagation data," IEEE Trans. Wireless Commun., vol. 14, no. 7, pp. 3899–3911, July 2015.

[36] J. Hoydis, S. ten Brink, and M. Debbah, "Massive MIMO in the UL/DL of cellular networks: How many antennas do we need?" IEEE J. Sel. Areas Commun., vol. 31, no. 2, pp. 160-171, Feb. 2013.

[37] H. Kim and B. Daneshrad, "Energy-constrained link adaptation for MIMO OFDM wireless communication systems," IEEE Trans. Wireless Commun., vol. 9, no. 9, pp. 2820–2832, Sep. 2010.

[38] M. Gursoy, "On the capacity and energy efficiency of training-based transmissions over fading channels", IEEE Trans. Inf. Theory, pp. 4543–4567, 2009.

[39] J. Xu, L. Qiu, and S. Zhang, "Energy-efficient iterative water-filling for the MIMO broadcasting channels," 2012 IEEE Wireless Communications and Networking Conference (WCNC), pp. 1-5, Apr. 2012.

[40] C. Hellings, N. Damak, and W. Utschick, "Energy-efficient zero-forcing with user selection in parallel vector broadcast channels," in Proc. 2012 International ITG Workshop on Smart Antennas (WSA), pp. 168-175, Mar. 2012.

[41] Y. Rui, Q. T. Zhang, L. Deng, P. Cheng, and M. Li, "Mode selection and power optimization for energy efficiency in uplink virtual MIMO systems," IEEE J. Sel. Areas Commun., vol. 31, no. 5, pp. 926-936, May 2013.

[42] B. Yang, K. B. Letaief, R. Cheng, Z. Cao, "Channel estimation for OFDM transmission in multipath fading channels based on parametric channel modeling", IEEE Trans. Commun., vol. 49, no. 3, pp. 467-479, Aug. 2001.

[43] Z. Wang, H. Zhu, and K. J. R. Liu, "A MIMO-OFDM channel estimation approach using time of arrivals", IEEE Trans. Wireless Commun., vol. 4, no. 3, pp. 1207-1213, May 2005.

[44] I. Barhumi, G. Leus, and M. Moonen, "Optimal training design for MIMO OFDM systems in mobile wireless channels", IEEE Trans. Sign. Proces., vol. 51, no. 6, pp. 1615-1624, May 2003.

[45] Y. Wang, C. Li, Y. Huang, D.Wang, T. Ban, and L. Yang, "Energy-efficient optimization for downlink massive MIMO FDD systems with transmit-side channel correlation," IEEE Trans. Veh. Technol., vol. 65, no. 9, pp. 7228-7243, Sep. 2016.

[46] M. Jang, Y. Kwon, H. Park, and T. Hwang, "Energy-efficient power control for TDD MISO systems," IEEE Trans. Veh. Technol., vol. 64, no. 10, pp. 4815-4856, Oct. 2015.

[47] C. Xiong, G. Y. Li, S. Zhang, Y. Chen, and S. Xu, "Energy- and spectral-efficiency tradeoff in downlink OFDMA networks," IEEE Trans. Wireless Commun., vol. 10, no. 11, pp. 3874–3886, Nov. 2011.

[48] H. Q. Ngo, E. G. Larsson, and T. L. Marzetta, "Massive MU-MIMO downlink TDD systems with linear precoding and downlink pilots," in Proc. IEEE Allerton Conf. Commun., Control, Comput., Monticello, IL, USA, Oct. 2013, pp. 293–298.

[49] J. Chen, K. Wong, "Improving energy efficiency for multi user MIMO systems with effective capacity constraints," IEEE 69th Vehicular Technology Conference (VTC) spring, pp. 1-5, May 2009.

[50] P. Rayi1 and M.V.S. Prasad, "Optimization of energy and spectral efficiency of massive MIMO small cell system," 2015 International Conference on Smart Technologies and Management for Computing, Communication, Controls, Energy and Materials (ICSTM), pp.233-238, May 2015.

[51] K. Guo, Y. Guo, G. Fodor and G. Ascheid, "Uplink power control with MMSE receiver in multi-Cell MU-Massive-MIMO systems," IEEE ICC 2014 Wireless Commun. Symp., pp. 5184-5190, Jun. 2014.

[52] Y.-K. Song, D. Kim, and J. Zander, “Pilot power adjustment for saving transmit power in pilot channel assisted DS-CDMA mobile systems,” IEEE Trans. Wireless Commun., vol. 9, no. 2, pp. 488–493, Feb. 2010.

[53] H. Pennanen, A. Tolli, J. Kaleva, P. Komulainen, and M. Latva-aho, “Decentralized linear transceiver design and signaling strategies for sum power minimization in multi-cell MIMO systems,” IEEE Trans. Signal Process, vol. 64, no. 7, pp. 1729-1743, Apr. 2016.

[54] Z. Wang, C. He, and A. He, “Robust AM-MIMO based on minimized transmission power,” IEEE Commun. Lett., vol. 10, no. 6, pp. 432–434, Jun. 2006.

[55] A. He, S. Srikanteswara, K. Bae, R. Newman, J. H. Reed, W. H. Tranter, M. Sajadieh, and M. Verhelst, “Power consumption minimization for MIMO systems-a cognitive radio approach,” IEEE J. Sel. Areas Commun., vol. 29, no. 2, pp. 469–479, Feb. 2011.

[56] L. Fu, M. Johansson and M. Bengtsson, “Energy efficient transmissions in cognitive MIMO systems with multiple data streams,” IEEE Trans. Wireless Commun., vol. 14, no. 9, pp. 5171 - 5184, May 2015.

[57] L. Chen, G. Wei, “Energy-efficient power allocation for training-based multiple-input multiple-output system with and without feedback,” IET Commun., vol. 7, no. 15, pp. 1697-1707, 2013.

[58] X. Zhou, T. A. Lamahewa, P. Sadeghi, and S. Durrani, “Two-way training: optimal power allocation for pilot and data transmission,” IEEE Trans. Wireless Commun., vol. 9, no. 2, pp. 564-569, Feb. 2010.

[59] Y. Wang, C. Li, Y. Huang, D.Wang, T. Ban, and L. Yang, “Energy-efficient optimization for downlink massive MIMO FDD systems with transmit-side channel correlation,” IEEE Trans. Veh. Technol., vol. 65, no. 9, pp. 7228-7243, Sep. 2016.

[60] Y. Kim, G. Miao and T. Hwang, “Energy efficient pilot and link adaptation for mobile users in TDD multi-user MIMO systems,“ IEEE Trans. Wireless Commun., vol. 13, no. 1, pp. 382-393, Jan. 2014.

[61] G. Miao, “Energy-efficient uplink multi-user MIMO,” IEEE Trans. Wireless Commun., vol. 12, no. 5, pp. 2302-2313, May 2013.

[62] A. Helmy, L. Musavian, and T. Le-Ngoc, “Energy-efficient power adaptation over a frequency selective fading channel with delay and power constraints,” IEEE Trans. Wireless Commun., vol. 12, no. 9, pp. 4529-4541, Sep. 2013.

[63] L. Musavian and T. Le-Ngoc, “Energy-efficient power allocation over Nakagamim fading channels under delay-outage constraints,” IEEE Trans. Wireless Commun., vol. 13, no. 8, pp. 4081-4091, Aug. 2014.

[64] C. Xiong, G. Y. Li, Y. Liu, Y. Chen, and S. Xu, "Energy-efficient design for downlink OFDMA with delay-sensitive traffic," IEEE Trans. Wireless Commun., vol. 12, no. 6, pp. 3085-3095, Jun. 2013.

[65] C. She, C. Yang and L. Liu, "Energy-efficient resource allocation for MIMO-OFDM systems serving random sources with statistical QoS requirement," IEEE Trans. Commun., vol. 63, no. 11, pp. 4125-4141, Nov. 2015.

[66] Y. Kwon, T. Hwang, and X.Wang, "Energy-efficient transmit power control for multi-tier MIMO HetNets," IEEE J. Sel. Topics Signal, vol. 33, no. 10, pp. 2070-2086, Oct. 2015.

[67] B. Hassibi and B.M. Hochwald, "How much training is needed in multiple antenna wireless links?" IEEE Trans. Inf. Theory, vol. 49, no. 4, pp. 951-963, Apr. 2003.

[68] A. Khansefid, and H. Minn, "Asymptotically optimal power allocation for massive MIMO uplink," IEEE Global Conference on Signal and Information Processing, pp. 627–631, 2014.

[69] H. Q. Ngo, M. Matthaiou, and E. G. Larsson, ''Massive MIMO with optimal power and training duration allocation,'' IEEE Wireless Commun. Lett., vol. 3, no. 6, pp. 605–608, Dec. 2014.

[70] Q. Zhang, S. Jin, M. McKay, D. Morales-Jimenez, and H. Zhu, "Power allocation schemes for multicell massive MIMO systems," IEEE Trans. Wireless communication, vol. 14, no. 11, pp. 5941–5955, Nov. 2015

[71] E. Björnson, P. Zetterberg, M. Bengtsson, and B. Ottersten, "Capacity limits and multiplexing gains of MIMO channels with transceiver impairments," IEEE Commun. Lett., vol. 17, no. 1, pp. 91–94, Jan. 2013.

[72] T. Koch, A. Lapidoth, and P. P. Sotiriadis, "Channels that heat up," IEEE Trans. Inf. Theory, vol. 55, no. 8, pp. 3594–3612, Aug. 2009.

[73] E. Bjornson, J. Hoydis, M. Kountouris, and M. Debbah, "Massive MIMO systems with non-ideal hardware: Energy efficiency, estimation, and capacity limits," IEEE Trans. Inf. Theory, vol. 60, no. 11, pp. 7112-7139, Nov. 2014.

[74] A. Pitarokoilis, S. K. Mohammed, and E. G. Larsson, "Uplink performance of time-reversal MRC in massive MIMO systems subject to phase noise," IEEE Trans. Wireless Commun., to be published. [Online]. Available: http://arxiv.org/abs/1306.4495

[75] C. Studer and E. G. Larsson, "PAR-aware large-scale multi-user MIMO OFDM downlink," IEEE J. Sel. Areas Commun., vol. 31, no. 2, pp. 303–313, Feb. 2013.

[76] S. J. Lee, "On the training of MIMO-OFDM channels with least square channel estimation and linear interpolation", IEEE Communications Letters, vol. 12, no. 2, pp. 100-102, February 2008.

[77] D. Samardzija and N. Mandayam, "Pilot-assisted estimation of MIMO fading channel response and achievable data rates", IEEE Trans. on Signal Processing, vol. 51, no. 11, pp. 2882-2890, Nov 2003.

[78] M. Biguesh and A. B. Gershman, “MIMO channel estimation: optimal training and tradeo®s between estimation techniques”, in Proc. IEEE International Conference on Communications, 2004, vol. 5, pp. 2658-2662.

[79] V. Barroso and J. Xavier, “Blind identification of MIMO channels: a closed form solution based on second order statistics”, in Thirty-Third Asilomar Conference on Signals, Systems, and Computers, 1999, vol. 1, pp. 70-74.

[80] J. K. Tugnait, “Blind estimation and equalization of MIMO channels via multi delay whitening”, IEEE Journal on Selected Areas in Communications, vol. 19, no. 8, pp. 1507-1519, 2001.

[81] Z. Ding and L. Qiu, “Blind MIMO channel identi¯cation from second order statistics using rank deficient channel convolution matrix”, IEEE Trans. on Signal Processing, vol. 51, no. 2, pp. 535-544, 2003.

[82] Z. Ding and D. B. Ward, “Subspace approach to blind and semi-blind channel estimation for space-time block codes”, IEEE Trans. on Wireless Communications, vol. 4, no. 2, pp. 357-362, 2005.

[83] A. Medles, D. T. M. Slock, and E. De Carvalho, “Linear prediction based semi-blind estimation of MIMO FIR channels”, in Proc. IEEE Third Workshop on Signal Processing Advances in Wireless Communications, 2001, pp. 58-61, 2001.

[84] Y. Zeng and T. Ng, “A semi-blind channel estimation method for multiuser multi-antenna OFDM systems”, IEEE Trans. on Signal Processing, vol. 52, no. 5, pp. 1419-1429, 2004.

[85] C.R. Murthy, A. K. Jagannatham, and B. D. Rao, “Training-based and semi-blind channel estimation for MIMO systems with maximum ratio transmission”, IEEE Trans. on Signal Processing, vol. 54, no. 7, pp. 2546-2558, 2006.

[86] Y. H. Zeng, S. D. Ma, and T. S. Ng, “Semi-blind estimation of channels and symbols for asynchronous MIMO systems”, IEE Proceedings-Communications, vol. 152, no. 6, pp. 883-889, 2005.

[87] S. M. Kay, Fundamentals of Statistical Signal Processing: Estimation Theory. Upper Saddle River, NJ, USA: Prentice-Hall, Inc., 1993.

[88] Y. Zhang and W.P. Zhu, “Energy-efficient pilot and data power allocation in massive multi-user multiple-input multiple-output communication systems,” IET Commun., pp. 1-9, Jun. 2016.

[89] Y. Zhang and Wei-Ping Zhu, “Energy-efficient pilot and data power allocation in massive MIMO communication systems based on MMSE channel estimation”, 41st IEEE International Conference on Acoustics, Speech and Signal Processing (ICASSP 2016), May 2016.

[90] G. Y. Li, Z. Xu, C. Xiong, C. Yang, S. Zhang, Y. Chen, and S. Xu, “Energy efficient wireless communications: tutorial, survey, and open issues,” IEEE Wireless Communications, vol. 18, no. 6, pp. 28–35, Dec. 2011.

[91] Y. Chen, S. Zhang, S. Xu, and G. Y. Li, "Fundamental trade-offs on green wireless networks," IEEE Communications Magazine, vol. 49, no. 6, pp. 30–37, 2011.

[92] J. Wu, S. Rangan, and H. Zhang, Green communications: theoretical fundamentals, algorithms and applications. CRC Press, 2012.

[93] Y. Zhang and Wei-Ping Zhu, "Energy efficient pilot and data power allocation in multi-cell multi-user massive MIMO communication systems", 2016 IEEE 84th Vehicular Technology Conference (VTC-Fall), Sep. 2016.

[94] Y. Zhang and Wei-Ping Zhu, "Energy Efficient Joint Pilot and Data Power Allocation in Multi-Cell Multi-User Massive MIMO Systems", submitted to IEEE Trans. Veh. Technol..

[95] K. G. Derpanis, "Jensen's Inequality", 2005, Online Available: http://www.cse.yorku.ca/~kosta/CompVis_Notes/jensen.pdf

[96] W. Bryc, "Rotation invariant distributions," Lecture Notes in Statist., vol. 100, pp. 51-69, 1995.

[97] A. M. Tulino and S. Verd, "Random matrix theory and wireless communications," Foundations Trends Commun. Inf. Theory, vol. 1, no. 1, pp. 1-182, June 2004.

[98] M. Chiang, "Geometric programming for communication systems," Foundations Trends Commun. Inf. Theory, vol. 2, no. 1-2, pp 1-154, Jul. 2005.

[99] S. Boyd, S. J. Kim, L. Vandenberghe, and A. Hassibi, "A tutorial on geometric programming," Optimization and Engineering, vol. 8, no. 1, pp. 67-127, 2007.

[100] L. Zhao and W. Z. Song, "A new multi-objective microgrid restoration via semi-definite programming," 2014 IEEE International Performance Computing and Communications Conference (IPCCC), pp. 1-8, 2014.

[101] "The MOSEK Optimization Tools Version 2.5. Users Manual and Reference," MOSEK ApS, 2002. Online Available: http://www.mosek.com.

[102] "Users Guide for TOMLABGP," TOMLAB, 2005. Online Available: http://www.tomlab.biz/docs/TOMLABGP.pdf

[103] J. Lofberg, YALMIP. Yet Another LMI Parser. Version 2.4, LinkpingUniv., Linkping, Sweden, 2003. Online Available: http://www.control.ee.ethz.ch/ joloef/yalmip.php

[104] gpcvx, A MATLAB Solver for Geometric Programs in Convex Form, Stanford Univ., Stanford, CA, 2006. Online Available: http://www.stanford.edu/ boyd/ggplab/gpcvx.pdf

[105] M. Grant, S. Boyd, and Y. Ye, CVX: Matlab Software for Disciplined Convex Programming, ver. 1.1, Nov. 2007. Online Available: www.stanford.edu./ boyd/cvx

[106] D. Feng et al., "A survey of energy-efficient wireless Communications," IEEE Commun. Surveys Tuts., vol. pp, no. 99, pp. 1-12, Feb. 2012.

[107] Z. Xiang, M. Tao, and X. Wang, "Massive MIMO multicasting in non-cooperative cellular networks," IEEE J. Sel. Areas Commun., vol. 32, no. 6, pp. 1180-1193, Jun. 2014.

[108] H. V. Cheng, E. Bjrnson, and E. G. Larsson, "Optimal pilot and payload power control in single-cell massive MIMO systems," IEEE Trans. Signal Process., vol. 65, no. 9, pp. 2363-2378, May 2017.

[109] P. Liu, S. Jin, T. Jiang, Q. Zhang, and M. Matthaiou, "Pilot power allocation through user grouping in multi-cell massive MIMO systems," IEEE Trans. Commun., vol. 65, no. 4, pp. 1561-1574, Apr. 2017.

[110] T. V. Chien, E. Bjrnson, E. G. Larsson, "Joint pilot design and uplink power allocation in multi-cell massive MIMO systems," IEEE Trans. Wireless Commun., 2017, submitted. [Online]. Available: https://arxiv.org/abs/1707.03072

[111] Y. Shen, E.Y. Lam and N. Wong,"A Signomial Programming Approach for Binary Image Restoration by Penalized Least Squares," IEEE Trans. Circuits Syst. Express Briefs, vol. 55, no. 1, pp. 41-45, Jan. 2008.

[112] X. Xiao, X. Tao, and J. Lu, "Energy-efficient resource allocation in LTE-based MIMO-OFDMA systems with user rate constraints," IEEE Trans. Veh. Tech., vol. 64, no. 1, pp. 125-197, Jan. 2015.

[113] W. Dinkelbach, "On nonlinear fractional programming," Management Science, vol. 13, pp. 492498, Mar. 1967.

[114] X. Zhang and H. Li, "Energy efficiency optimization for MIMO cognitive radio network," 2015 IEEE International Conference on Communications (ICC), pp. 7713- 7718, Jun. 2015.

[115] H.H. Kha, H.D. Tuan and H.H. Nguyen, "Fast global optimal power allocation in wireless networks by local DC programming," IEEE Trans. Wireless Commun., vol. 11, no.2, pp. 510-515, Feb. 2012.

[116] S. Mohammed, "Impact of transceiver power consumption on the energy efficiency spectral efficiency tradeoff of zero-forcing detector in massive MIMO systems," 2014, submitted. [Online]. Available: http://arxiv.org/abs/1401.4907v1

[117] E. Bjornson, L. Sanguinetti, J. Hoydi, and M. Debbah, "optimal design of energy-efficient multi-user MIMO systems: is massive MIMO the answer?," IEEE Trans. Wireless Commun., vol. 14, no. 6, pp. 3059-3075, Jun. 2015.

[118] Y. Zhang and Wei-Ping Zhu, "Energy Efficient Pilot and Data Power Allocation in Massive MIMO Communication Systems under Consideration of Circuit Power", 2018 IEEE 84th Vehicular Technology Conference (VTC-Fall), Aug. 2018.